Cotecmar

SHIP

SCIENCE & TECHNOLOGY

CIENCIA & TECNOLOGÍA DE BUQUES

ISSN 1909-8642

COTECMAR
COLOMBIA

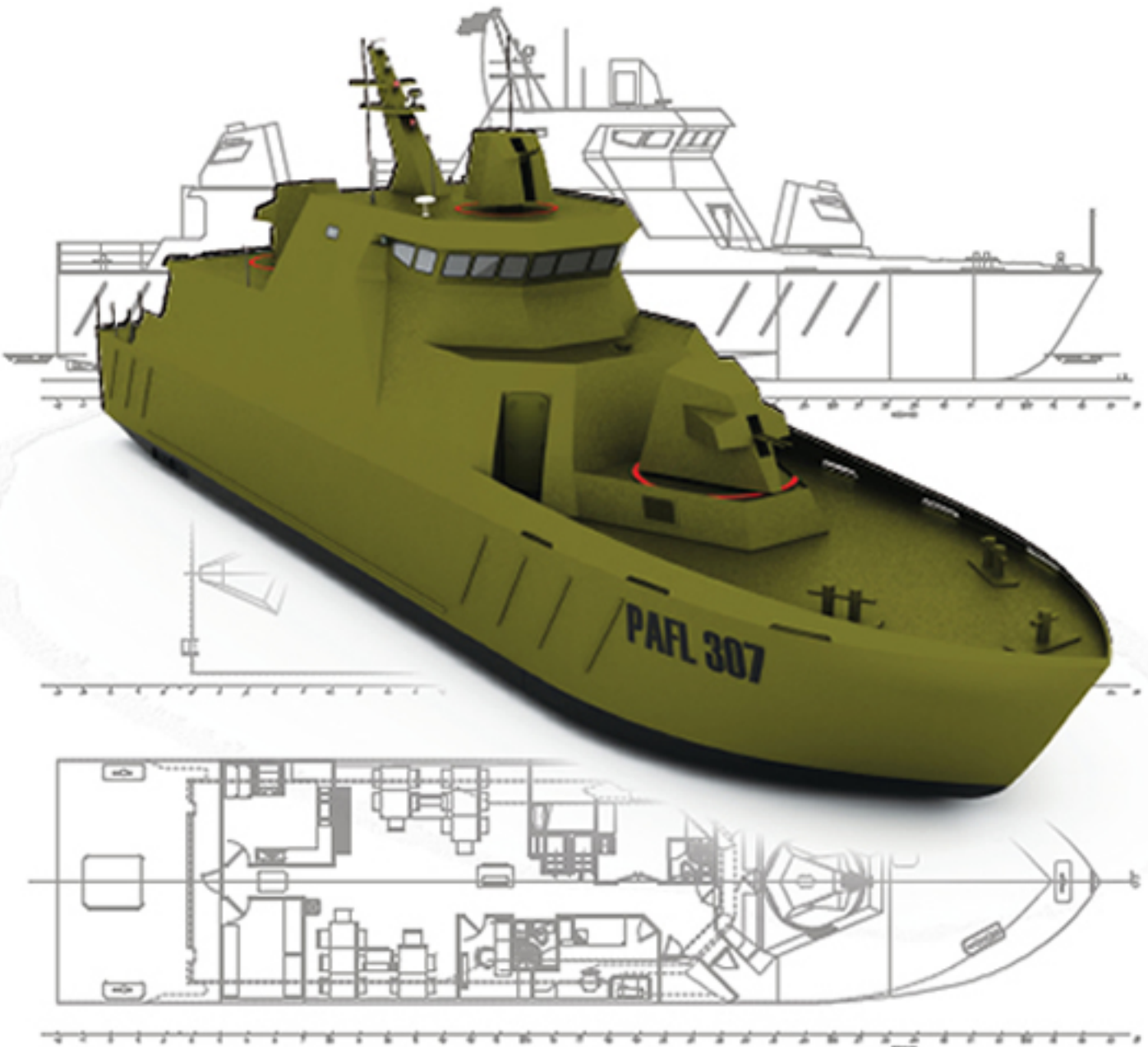

Vol. 5 - n.° 9
(1 - 120) July 2011

Ship Science & Technology ISSN 1909-8642 Vol. 4 - No. 9 - July 2011

SHIP
SCIENCE & TECHNOLOGY
CIENCIA & TECNOLOGÍA DE BUQUES

Volume 5, Number 9 July 2011 ISSN 1909-8642

The *Ship Science & Technology* specializes in topics related to naval architecture and naval, marine, and ocean engineering. Every six months, the journal publishes scientific papers that constitute original contributions in the development of the areas mentioned, resulting from research projects of the Science and Technology Corporation for the Naval, Maritime, and Riverine Industries and other institutions and researchers. It is distributed nationally and internationally by exchange or subscription.

A publication of

Corporación de Ciencia y Tecnología para el Desarrollo de la Industria Naval, Marítima y Fluvial - Cotecmar
Electronic version: www.shipjournal.co

Editorial Coordinator
Karen Domínguez Martínez. MMSc. (c)
Jimmy Saravia Arenas. MMSc. (c)

Layout and design
Mauricio Sarmiento Barreto

Printed by
C&D Publicidad & Marketing. Bogotá, D.C.

SHIP
SCIENCE & TECHNOLOGY
CIENCIA & TECNOLOGÍA DE BUQUES

Volume 5, Number 9 July 2011 ISSN 1909-8642

SHIP
SCIENCE & TECHNOLOGY
CIENCIA & TECNOLOGÍA DE BUQUES

Editorial Note

Cartagena de Indias, 21 July 2011.

In this opportunity,the Ship Science & Technology Journalstarts the seriesof special publicationswith the best works presented during the 2nd International Ship Design and Naval Engineering Congress - ISDNEC held in the city of Cartagena de Indias on the 16, 17 and 18 of March, 2011 and whose objective was that of *"Consolidating a dissemination scenario supported on the process, exchange, development, and appropriation of knowledge related to the research, technological development, and innovation of the naval, maritime, riverine, and ports industries"*.

With an academic program conformed by three plenary lectures, 22 scientific papers, 16 technical papers, and two forums, the 2nd International Ship Design and Naval Engineering Congress – ISDNEC 2011 had attendees from Germany, Brazil, Ecuador, the United States, Spain, Panama, and Paraguay, again demonstrating COTECMAR's commitment and leadership in the generation of synergy between the scientific community and naval technology. Likewise, we managed to position the Congress as the first event of this specialization at the national level and as one of the main scenarios for scientific dissemination for the naval, maritime, and riverine industry within the international context.

This edition is dedicated to works from the topic *"Design of maritime and riverine vessels"* specifically in areas of ship design and optimization, ship dynamics, hydrodynamic sand ergonomics, whose opening was given by the keynote speakers: Dr. Apóstolos Papanikolaou, Professor of the National Technical University (NTUA) of Athens, Greece; Dr. Andres Cura, Professor of "Dynamics of Maritime Systems" at the Technical University of Berlin in Germany, and Dr. Jonathan Ross, Naval Architect, expert and consultant of the United States Navy on themes of integration of ergonomic factors in vessel design.

Lastly, I wish to share with our readers, authors, editorial committee, scientific committee, and editorial team the indexation in category "C"of the Ship Science & Technology Journal granted in March 2011 by Colombia's COLCIENCIAS Publindex National Bibliographic Index, recognizing that our publication has scientific and editorial quality standards, stability, visibility, and national and international recognition, success key factors that permit us to offer our target audience up-to-date and specialized knowledge on themes related to naval engineering and architecture, as well as to marine engineering and oceanic engineering.

I thank all of you for this accomplishment.

Commander, OSCAR DARÍO TASCÓN MUÑOZ

SHIP
SCIENCE & TECHNOLOGY
CIENCIA & TECNOLOGÍA DE BUQUES

Nota Editorial

Cartagena de Indias, 21 de Julio de 2011.

En esta oportunidad la Revista *Ship Science & Technology* inicia la serie de publicaciones especiales con los mejores trabajos presentados en el Segundo Congreso Internacional de Diseño e Ingeniería Naval realizado en la ciudad de Cartagena de Indias los días 16, 17 y 18 de Marzo de 2011 y cuyo objetivo fue el de *"Consolidar un espacio de divulgación apoyado en el proceso, intercambio, desarrollo y apropiación de conocimientos relacionados con la investigación, desarrollo tecnológico e innovación de la industria naval, marítima, fluvial y portuaria"*.

Con un programa académico conformado por tres conferencias magistrales, veintidós ponencias científicas, dieciséis ponencias técnicas y dos foros, el Segundo Congreso Internacional de Diseño e Ingeniería Naval – CIDIN 2011 contó con asistentes de Alemania, Brasil, Ecuador, EEUU, España, Panamá y Paraguay, demostrando nuevamente el compromiso y liderazgo de Cotecmar para la generación de sinergia entre la comunidad científica y tecnológica naval. Asimismo, se logra posicionar al Congreso como el primer evento de esta especialidad a nivel nacional y como uno de los principales espacios de divulgación científica para la industria naval, marítima y fluvial en el contexto internacional.

Esta edición está dedicada a los trabajos del eje temático *"Diseño de embarcaciones marítimas y fluviales"* específicamente en las áreas de diseño de buques y optimización, dinámica del buque, hidrodinámica y ergonomía, cuya apertura se da con los tres conferencistas principales: Dr. Apóstolos Papanikolaou, Profesor de la National Technical University of Athens (NTUA) de Grecia; Dr. Andres Cura, Profesor de "Dynamics of Maritime Systems" en la Technical University Berlin de Alemania y el Dr. Jonathan Ross Arquitecto Naval, experto y consultor de la Armada de los EEUU en temas de integración de los factores ergonómicos en el diseño de embarcaciones.

Por último, quiero compartir con nuestros Lectores, Autores, Comité Editorial, Comité Científico y Equipo Editorial, la indexación en la categoría "C" de la Revista *Ship Science & Technology* realizada en Marzo de 2011 por parte del Índice Bibliográfico Nacional Publindex de Colciencias, Colombia, acreditando que nuestra publicación cuenta con estándares de calidad científica y editorial, estabilidad, visibilidad y reconocimiento nacional e internacional, factores claves de éxito que nos permiten ofrecer al público objetivo conocimiento actualizado y especializado en temas relacionados con ingeniería naval, arquitectura naval, ingeniería marina e ingeniería oceánica.

A todos ustedes mil gracias por este logro.

Capitán de Fragata OSCAR DARÍO TASCÓN MUÑOZ

Holistic Ship Design Optimization: Merchant and Naval Ships

Optimización del diseño holístico de buques: Embarcaciones Mercantes y Navales

Apostolos D. Papanikolaou [1]

Abstract

The present paper provides a brief introduction to a *holistic* approach to ship design optimization, defines the generic ship design optimization problem, and demonstrates its solution by using advanced optimization techniques for the computer-aided generation, exploration, and selection of optimal designs. It discusses proposed methods on the basis of some typical ship design optimization problems of cargo and naval ships related to multiple objectives, leading to improved and partly innovative design features with respect to ships' economy, cargo carrying capacity, safety, survivability, comfort, required powering, environmental protection, or combat strength, as applicable.

Key words: holistic ship design, parametric design, multi-criteria optimization, naval ships.

Resumen

Este documento brinda una breve introducción a un enfoque *holístico* a la optimización del diseño de embarcaciones, define el problema genérico de la optimización del diseño de embarcaciones y demuestra su solución mediante el uso de técnicas avanzadas de optimización asistidas por computador para la generación, exploración y selección de diseños óptimos. Discute los métodos propuestos sobre la base de algunos problemas típicos de optimización de diseño de embarcación de buques de carga y navales relacionados a los objetivos múltiples, conllevando a características de diseño mejoradas y parcialmente innovadoras con respecto a la economía de la embarcación, capacidad de carga, seguridad, supervivencia, comodidad, potencia requerida, protección ambiental o fortaleza de combate, como sea aplicable.

Palabras claves: diseño holístico de buques, diseño paramétrico, optimización de múltiples criterios, buques navales.

Date Received: December 7th, 2010 - *Fecha de recepción: 7 de Diciembre de 2010*
Date Accepted: January 21th, 2011 - *Fecha de aceptación: 21 de Enero de 2011*

[1] National Technical University of Athens, Ship Design Laboratory. Athens-Zografou, Greece. e-mail: papa@deslab.ntua.gr

Introduction

Ships are built to cover needs of society through the provision of specific services. These services may be on a commercial or non-commercial basis; whereas, in the first case (commercial ships) the objective is to generate profit for the ship owner, the latter case is related to a public service of some kind, the cost of which is generally assumed by a governmental authority. The main bulk of commercial ships are cargo ships, which carry all types of cargo (solid and liquid cargo or passengers) and provide in fact the largest (by volume of cargo and transport distance, [ton-miles]) worldwide transportation work, compared to other modes of transport.

The design of ships is a complex endeavor requiring the successful coordination of many disciplines, of both technical and non-technical nature, and of individual experts to arrive at valuable design solutions. Inherently coupled with the design process is design optimization, namely the selection of the best solution out of many feasible ones on the basis of a criterion, or rather a set of criteria. Such evaluation criteria are the shipbuilding cost or the required freight rate for merchant ships or more complex ones that include, besides economy, ship performance in terms of safety, comfort, survivability in intact and damage condition and environmental friendliness. A systemic approach to ship design may consider the ship as a complex system integrating a variety of subsystems and their components, e.g., for merchant ships subsystems for cargo storage and handling, energy/power generation and ship propulsion, accommodation of crew/passengers and ship navigation, whereas for naval ships combat systems are added.

Considering that ship design should actually address the whole ship's life cycle, it may be split into various stages that are traditionally composed of the concept/preliminary design, the contractual and detailed design, the ship construction/fabrication process, and ship operation for an economic life and scrapping/recycling. It is evident that an optimal ship is the outcome of a *holistic* optimization of the entire, above defined, ship system over its whole life cycle. But even the simplest component of the above-defined optimization problem, namely the 1st loop (conceptual/preliminary design), is complex enough to be simplified (*reduced*) in practice. Inherent to ship design optimization are the conflicting requirements resulting from the design constraints and optimization criteria (merit or objective functions), reflecting the competing interests of the various ship design stake holders (ship-owner, shipbuilder, cargo owner and cargo forwarder, flag and class authorities, etc.).

The present paper provides a brief introduction to a *holistic* approach to ship design optimization, defines the generic ship design optimization problem, and demonstrates its solution by use of advanced optimization techniques for the computer-aided generation, exploration, and selection of optimal designs. It discusses proposed methods on the basis of some typical ship design problems of cargo and naval ships related to optimizations with multiple objectives and leading to improved and partly innovative design features with respect to ship economy, cargo carrying capacity, safety, survivability, comfort, required powering, environmental protection or combat strength (naval ships), as applicable.

Holistic Ship Design Optimization

Inherently coupled with the design process is design optimization, namely the selection of the best solution out of many feasible ones on the basis of a criterion, or rather a set of criteria. A systemic approach to ship design may consider the ship as a complex system, integrating a variety of subsystems and their components, e.g., subsystems for cargo storage and handling, energy/power generation and ship propulsion, accommodation of crew/passengers, and ship navigation. They are all serving well-defined ship functions.

Ship functions may be divided into two main categories, namely *payload* functions and *inherent* ship functions.For example, for Ro-Ro passenger ships, the payload functions are all those related to the provision of public and private accommodation spaces for the passengers and spaces/handling and access equipment for the cargo (Ro-Ro decks, ramps, ventilation, etc.); inherent ship functions

Fig. 1. Payload and Ship functions of Cargo Ships (Levander, 2003)

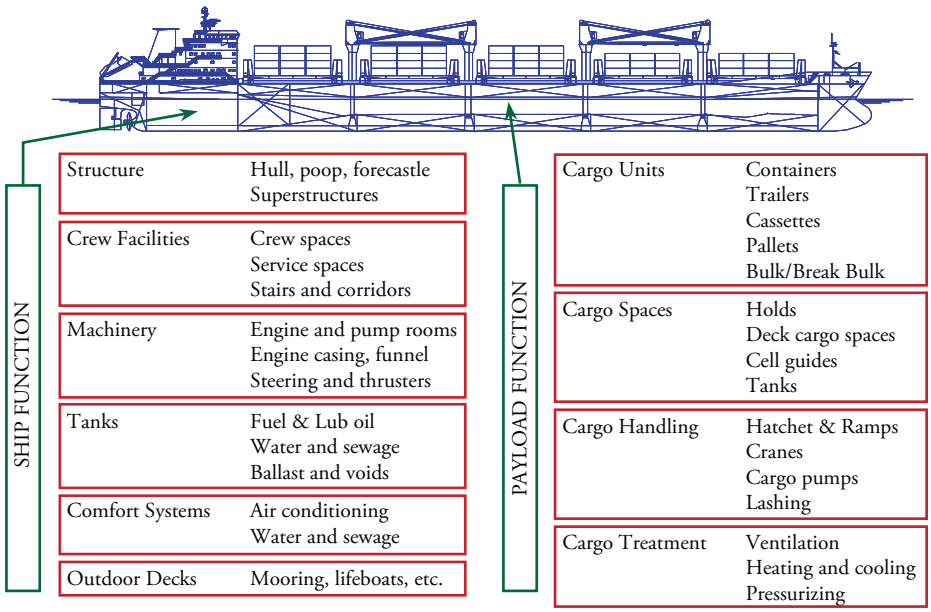

are those related to the transport of passengers and cargo safely from port to port with certain speed, namely the ship as a system, consisting of ship's hull (main and superstructure), facilities of crew, navigation control (bridge), machinery, tanks (fuel and lubrication oil, water and sewage, ballast and voids), comfort systems (air conditioning, water and sewage, electrical), mooring and life-saving equipment, etc. (Fig. 1).

Independently, considering that ship design should actually address the whole ship's life cycle, it may be split into various stages that are traditionally composed of the concept/preliminary design, the contractual and detailed design, the ship construction/fabrication process, and ship operation for an economic life and scrapping/recycling. It is evident that the optimal ship with respect to her whole life cycle is the outcome of a *holistic*[1] optimization of the entire, above defined ship system for its life-cycle. It is noted that mathematically, every constituent of the above defined life-cycle ship system forms evidently itself a complex nonlinear optimization problem for the design variables, with a variety of constraints and criteria/objective functions to be jointly optimized. Even the simplest component of the ship design process, namely the 1st loop (conceptual/preliminary design), is complex enough to be simplified (reduced[2]) in practice. Also, inherent to ship design optimization are the conflicting requirements resulting from the design constraints and optimization criteria (merit or objective functions), reflecting the interests of the various ship design stake holders: ship owners/operators, ship builders, classification society/coast guard, regulators, insurers, cargo owners/forwarders, port operators etc.

Assuming a specific set of requirements (usually the *shipowner's requirements for merchant ships* or *mission statement for naval ships*), a ship needs to be optimized for lowest construction cost, for highest operational efficiency or lowest Required Freight Rate (RFR), for highest safety and comfort of passengers/crew, for satisfactory protection of cargo and the ship herself as hardware and last but not least, for minimum environmental impact, particularly for oil carriers with respect to marine pollution in case of accidents and for high-speed vessels with respect to generated wave wash. Recently, even aspects of ship engine emissions

[1] Principle of holism according to Aristotle (*Metaphysics*): "The whole is more than the sum of the parts"

[2] Principle of *reductionism* may be seen as the opposite of *holism*, implying that a complex system can be approached by *reduction* to its fundamental parts. However, *holism* and *reductionism* should be regarded as complementary approaches, as they are both needed to satisfactorily address complex systems in practice.

and air pollution need to be considered (see current discussions about the Energy Efficiency Design Index (EEDI), International Maritime Organization-MEPC, 2008). Many of these requirements are clearly conflicting and a decision regarding the optimal ship design needs to be rationally made.

To make things more complex but coming closer to reality, even the specification of a set of design requirements with respect to ship type, cargo capacity, speed, range, etc. is complex enough to require another optimization procedure that satisfactorily considers the interests of all shareholders of the ship as an industrial product and service vehicle of international markets or others. Actually, the initial set of ship design requirements is the outcome of a compromise of intensive discussions between highly experienced decision makers, mainly on the shipbuilder's side and end users who attempt to articulate their desires and tradeoffs they are willing to allow. A way to undertake and rationally consolidate this kind of discussion has been advanced by the EU-funded project LOGBASED (*Brett et al., 2006*).

Since the mid 60s with the advance of computer hard- and software more and more parts of the design process were taken over by computers, particularly the heavy algorithmic and drafting elements of ship design. Simultaneously, the first computer-aided preliminary design software systems were introduced, dealing with the mathematical parametric exploration of the design space on the basis of empirical/simplified ship models for specific ship types or the optimization of design variables for specific economic criteria by gradient based search techniques. With the further and faster advance of computer hard- and software tools, along with their integration into powerful hard- and software design systems, the time has come to look ahead in ship design optimization in a *holistic* way, namely by addressing and optimizing several and gradually all aspects of ship life (or all elements of the entire ship life-cycle system), at least the stages of design, construction and operation; within a *holistic* ship design optimization we should herein also understand exhaustive multi-objective and multi-constrained ship design optimization procedures even for individual stages of ship life (e.g., conceptual design) with *least reduction* of the entire real problem (*Nowacki, 2009, Andrews et al., 2009, Papanikolaou et al., 2009a, and Papanikolaou, 2009b*).

The use of Genetic Algorithms (GA), combined with gradient-based search techniques in micro-scale exploration and with a utility functions technique for the design evaluation, is advanced in the present paper as a generic-type optimization technique to generate and identify optimized designs through effective exploration of the large-scale, nonlinear design space and a multitude of evaluation criteria. Several applications of this generic, multi-objective ship design optimization approach by using the design software platform of the Ship Design Laboratory of NTUA, integrating well-established naval architectural and optimization software packages with various application methods and software tools, as necessary to evaluate stability, resistance, seakeeping, structural integrity, etc., may be found in the listed references. The following examples, deduced from past projects of NTUA-SDL, may be highlighted.

- Hydrodynamic hull form optimization of high-speed, twin-hull vessels (*Papanikolaou, 1991, Papanikolaou et al., 1996*).
- Hull form optimization of high-speed mono- and twin-hull vessels for least wave resistance and wave wash (*EU project FLOWMART, Zaraphonitis and Papanikolaou, 2003*).
- Multi-objective optimization of naval ships (Boulougouris and Papanikolaou, 2004).
- Hull form optimization of a wave piercing, high-speed, mono-hull vessel for least resistance and best seakeeping (*EU project VRSHIP-ROPAX2000, Boulougouris and Papanikolaou, 2006*).
- Parametric design and multi-objective optimization of conventional and high-speed ROPAX ships (*Zaraphonitis and Papanikolaou, 2003, Skoupas et al., 2009*).
- Risk-based ship design (see a series of examples of application by various research teams, *Papanikolaou* (ed), 2009c).
- Logistics-based optimization of ship design (*Gkohari and Papanikolaou, 2010*).

- Multi-objective tanker optimization (*Papanikolaou et al., 2010*).

The Generic Ship Design Optimization Problem

Within a *holistic* ship design optimization, we should herein mathematically understand exhaustive multi-objective and multi-constrained optimization procedures with *least reduction* of the entire real design problem. The generic ship design optimization problem and its basic elements may be defined as follows (Fig. 2).

- **Optimisation Criteria (Merit Functions, Goals):** This refers to a list of mathematically defined performance/efficiency indicators that may be eventually reduced to an economic criterion, namely the profit of the initial investment. Independently, there may be optimization criteria (merit functions or goals) that may be formulated without direct reference to economic indicators, see, e.g., optimization studies for a specific X ship function, like ship performance in calm water and in seaways, ship safety, ship strength including fatigue, etc. The ship design optimization criteria are generally complex nonlinear functions of the design parameters (vector of design variables) and are often defined by algorithmic routines in a computer-aided design procedure. According to Levander (2003), the most important performance indicators for cargo vessels are summarized in Fig. 3.
- **Constraints:** It mainly refers to a list of mathematically defined criteria (in the form of mathematical inequalities or equalities) resulting from regulatory frameworks pertaining to safety (for ships, mainly the international SOLAS and MARPOL regulations). This list may be extended by a second set of criteria characterized by uncertainty with respect to their actual values and being determined by the market conditions (demand and supply data for merchant ships), by the cost of major materials (for ships: cost of steel, fuel, workmanship), by the anticipated financial conditions (cost of money, interest rates), and other case-specific constraints. It should be noted that the latter set of criteria is often regarded as a set of input data with uncertainty to the optimization problem and may be assessed on the basis of probabilistic assessment models.
- **Design Parameters:** It refers to a list of parameters (vector of design variables)

Fig. 2. Generic Ship Design Optimization Problem

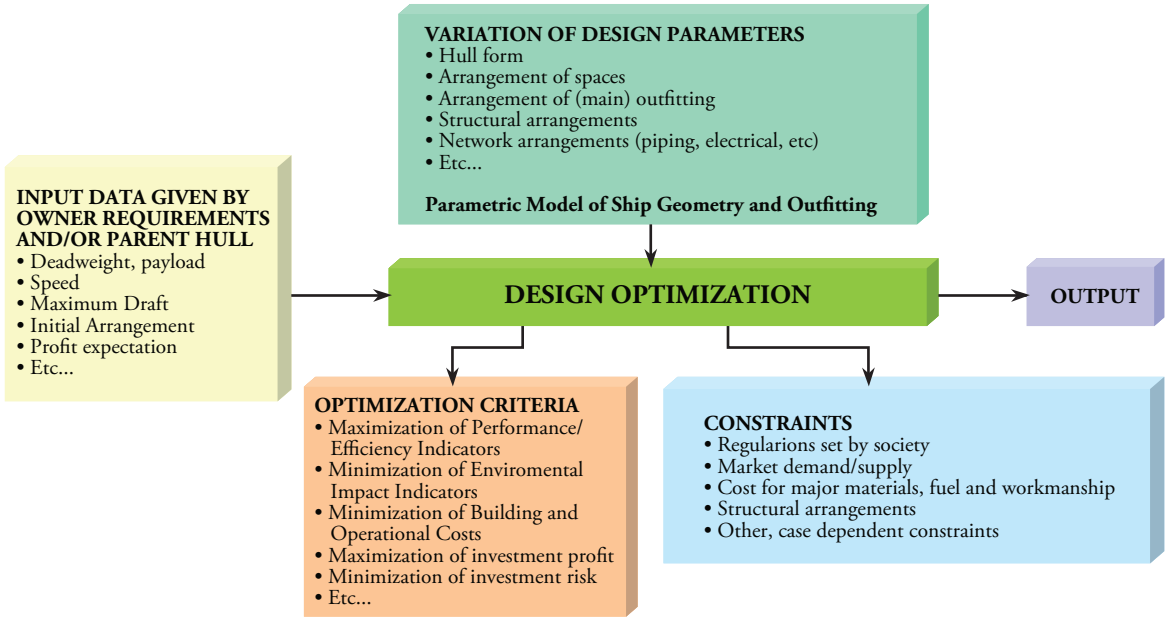

Fig. 3. Key Performance Indicators for Cargo Ships (Levander, 2003)

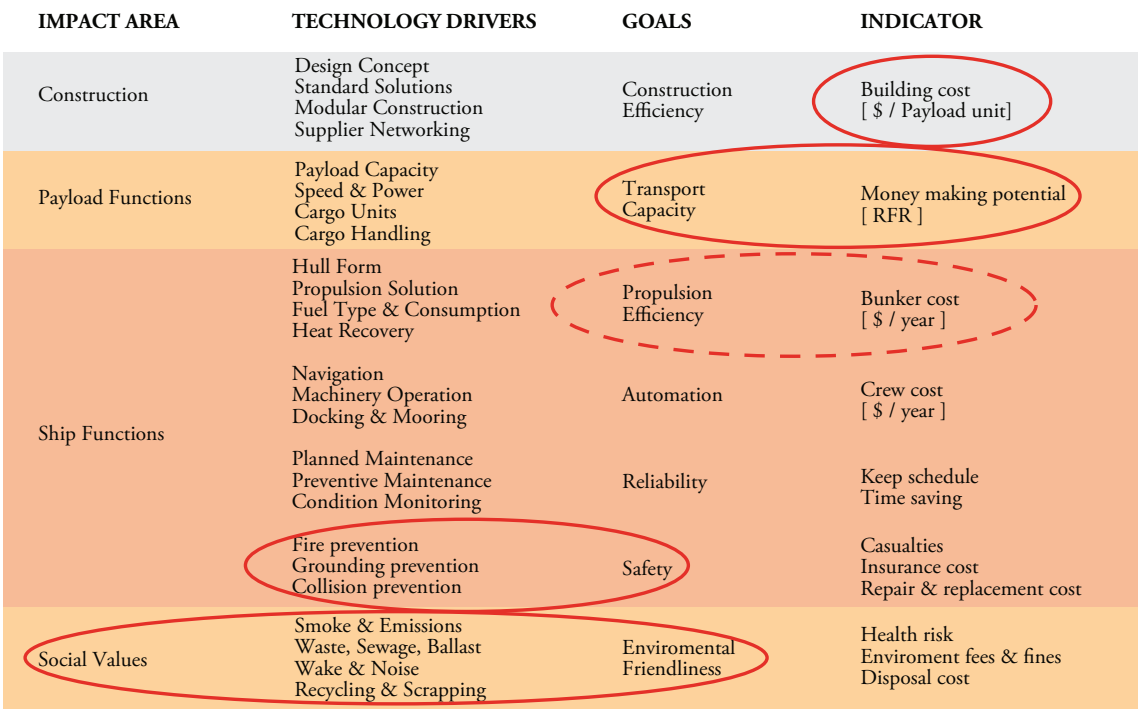

IMPACT AREA	TECHNOLOGY DRIVERS	GOALS	INDICATOR
Construction	Design Concept Standard Solutions Modular Construction Supplier Networking	Construction Efficiency	Building cost [$ / Payload unit]
Payload Functions	Payload Capacity Speed & Power Cargo Units Cargo Handling	Transport Capacity	Money making potential [RFR]
Ship Functions	Hull Form Propulsion Solution Fuel Type & Consumption Heat Recovery	Propulsion Efficiency	Bunker cost [$ / year]
	Navigation Machinery Operation Docking & Mooring	Automation	Crew cost [$ / year]
	Planned Maintenance Preventive Maintenance Condition Monitoring	Reliability	Keep schedule Time saving
	Fire prevention Grounding prevention Collision prevention	Safety	Casualties Insurance cost Repair & replacement cost
Social Values	Smoke & Emissions Waste, Sewage, Ballast Wake & Noise Recycling & Scrapping	Enviromental Friendliness	Health risk Enviroment fees & fines Disposal cost

characterizing the design under optimization; for ship design, this includes the ship's main dimensions, unless specified by the ship owner's requirements (length, beam, side depth, draft) and may be extended to include the ship's hull form, arrangement of spaces and of (main) outfitting, of (main) structural elements and of (main) networking elements (piping, electrical, etc), depending on the availability of topological-geometry models relating the ship's design parameters to a generic ship model to be optimized.

- **Input Data:** This initially includes the traditional owner's specifications/ requirements, which for a merchant ship are the required cargo capacity (deadweight and payload), service speed, range, etc., and may be complemented by a variety of further data affecting ship design and its economic life, like financial data (profit expectations, interest rates), market conditions (demand and supply data), costs for major materials (steel and fuel), etc. The input data set may include, besides numerals of quantities, more general type of knowledge data, like drawings (of ship general arrangements) and qualitative information that needs to be properly translated for inclusion in a computer-aided optimization procedure.
- **Output:** It includes the entire set of design parameters (vector of design variables) for which the specified optimization criteria/merit functions obtain mathematically extreme values (minima or maxima); for multi-criteria optimization problems, optimal design solutions are on the so-called Pareto front and may be selected on the basis of tradeoffs by the decision maker/designer. For the exploration and final selection of Pareto design solutions, a variety of strategies and techniques may be employed.

In mathematical terms, the multi-objective optimization problem may be formulated as:

$$\min\ [\mu_1(x), \mu_2(x), \ldots, \mu_n(x)]^T, \quad \text{subject to } g(x) \le 0 \text{ and } h(x) = 0 \text{ and } x_l \le x \le x_u \tag{1}$$

where μ_i is the i-th objective function, g and h are a set of inequality and equality constraints, respectively, and x is the vector of optimization or vector of design variables. The solution to the above problem is a set of Pareto solutions, namely

solutions for which improvement in one objective cannot be achieved without worsening of at least one other objective. Thus, instead of a unique solution, a multi-objective optimization problem has (theoretically) infinite solutions, namely the Pareto set of solutions.

The use of Multi-Objective Genetic Algorithms (MOGA), combined with gradient based search techniques in micro-scale exploration and with a utility functions technique for the design evaluation, is advanced in the present paper as a generic type optimization technique for generating and identifying optimized designs through effective exploration of the large-scale, nonlinear design space and a multitude of evaluation criteria occurring in ship design. Several applications of this generic, multi-objective ship design optimization approach by use of NTUA-SDL[3]'s design software system, integrating the naval architectural software package *NAPA*[4], the optimization software *modeFRONTIER*[5] and various application software tools, as necessary for the evaluation of stability, resistance, seakeeping etc. may be found in the listed references.

Two typical application examples of the introduced generic ship design optimization procedure of NTUA-SDL are presented and briefly commented in the following.

Examples of Optimization of Merchant and Naval Ships

Multi-objective Optimization of Tanker Ships

This application gives an overview of research studies undertaken at the Ship Design Laboratory of NTUA within the framework of the EU-funded project SAFEDOR (2005-2009) and, thereafter, in collaboration with Germanischer Lloyd (*Papanikolaou et al., 2010*). The studies introduce a risk-based parametric optimization of double-hull tankers to achieve innovative designs with increased cargo carrying capacity and improved environmental protection, while challenging

[3] National Technical University of Athens – Ship Design Laboratory, NTUA-SDL, http://www.naval.ntua.gr/sdl
[4] NAPA Oy (2005), NAPA software, http://www.NAPA.fi/
[5] E.STE.CO (2003), "modeFrontier software v.2.5.x", http://www.esteco.it/

Fig. 4. Generic Procedure for the Ship Design Optimization Problem – NTUA-SDL

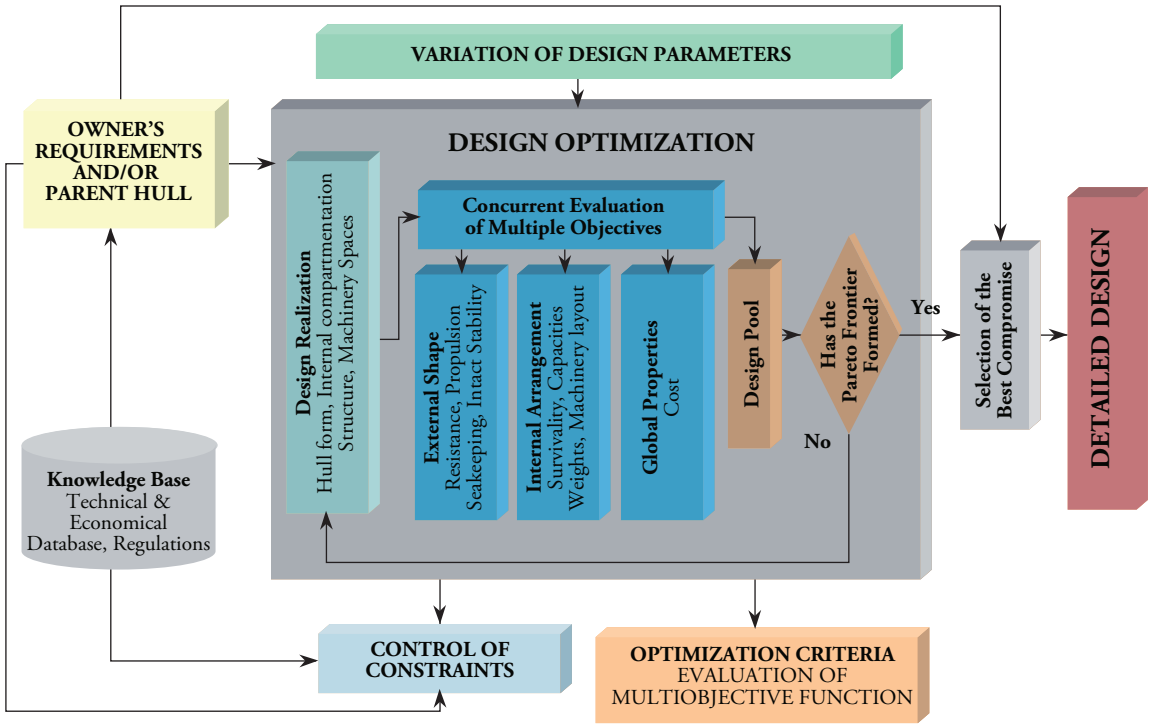

various constraints imposed by the latest MARPOL regulations (*Papanikolaou, 2009c*).

For the design concept development stage, a full parametric multi-objective design optimization platform by using Genetic Algorithms has been developed, taking into account probabilistic oil-outflow calculation methods for side and bottom damages. The resultant Pareto-optimal designs are evaluated from the point of view of oil outflow consequences, cargo capacity, design feasibility, ship maintainability and ballast water extent. Developed alternative designs dispose, compared to a standard double-hull design, increased cargo carrying capability and reduced structural weight, at a comparable or even slightly reduced risk for oil outflow; therefore, from the point of view of both economy and safety, they appear very promising compared to existing standard type double-hull designs. A preliminary economic analysis also showed that despite the anticipated slightly increased building cost, developed alternative designs are related to an appreciable decrease of unit transport cost, making them attractive to the shipping industry.

Reference Design

The, herein, optimized tanker vessel, code-named "Double Venture" is a double-hull construction tanker ship of AFRAMAX size also used in another EU-funded project POP&C (2004-2007). Table 1 presents the basic characteristics of the vessel. A double-skin construction is arranged along the cargo length area, consisting of six (6) pairs of side and bottom tanks for use of water ballast (Fig. 5). Two slop tanks are also provided, aft wards of main cargo area. Cargo handling is by means of centrifugal pumps installed in a pump room, which is located forward of the machinery space. It is noted that the above referenced double-hull design disposes of an increased double side and bottom clearance of 2.5 m, compared to the minimum 2.0 m required, according to MARPOL relevant requirements.

Fig 5. Sketch of Reference Vessel "Double Venture"

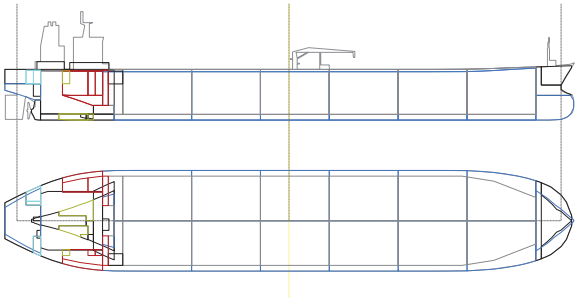

Alternative Configurations

Five different configurations were considered,

Table 1. Particulars of reference vessel "Double Venture"

Length, oa	250.10m
Length, bp	239.00m
Breadth, moulded	44.00m
Depth, moulded (main deck)	21.00m
Width of double skin sides	2.50m
Width of double skin bottom	2.50m
Draught scantling	14.60m
Deadweight, scantling draught (comparable with design proposed)	109,800dwt (cargo density 0.868 T/m3)
Cargo capacity Liquid volume, heavy oil, diesel oil, Water ballast	122,375m^3+2,830m^3 (Slop), 3,380m^3, 260m^3 41,065m^3 + 3,500 m^3 (peaks)
Classification	Lloyds Register
Number of Cargo tanks	12 (6x2) plus 2 slop tanks
Cargo Tanks block length	181.44 m

with six or seven tanks in the longitudinal direction, two or three tanks in the transverse direction and flat or corrugated bulkheads. The five different combinations of compartmentation are summarized in Table 2. A total of *21,500 designs* were examined in the present study. In Figs. 6 and 7, *only the feasible designs are shown*. The open circles correspond to dominated designs, while the full circles correspond to designs on the Pareto front. For comparison, the *reference design* is also included, marked by a *full triangle*. It should be noted that the steel weight of the reference vessel is not its actual weight as built, but the weight calculated by the POSEIDON software by Germanischer Lloyd, based on a corresponding structural design according to GL rules. This ensures full comparability with the generated optimal designs.

Discussion of Results

The five alternative configurations were selected to allow validating the characteristics of the reference design, as well as identifying possible improvements through analysis of the respective *Pareto frontiers*. Putting all Pareto frontiers into a single diagram provides a better insight of the relationships between design objectives, design parameters, and alternative configurations.

Fig. 6 clearly shows that the "6x3 flat" Pareto designs dominate all the other designs. Furthermore, there are several Pareto designs with significantly better

Fig 6. Outflow vs. cargo volume – Pareto designs from different configurations

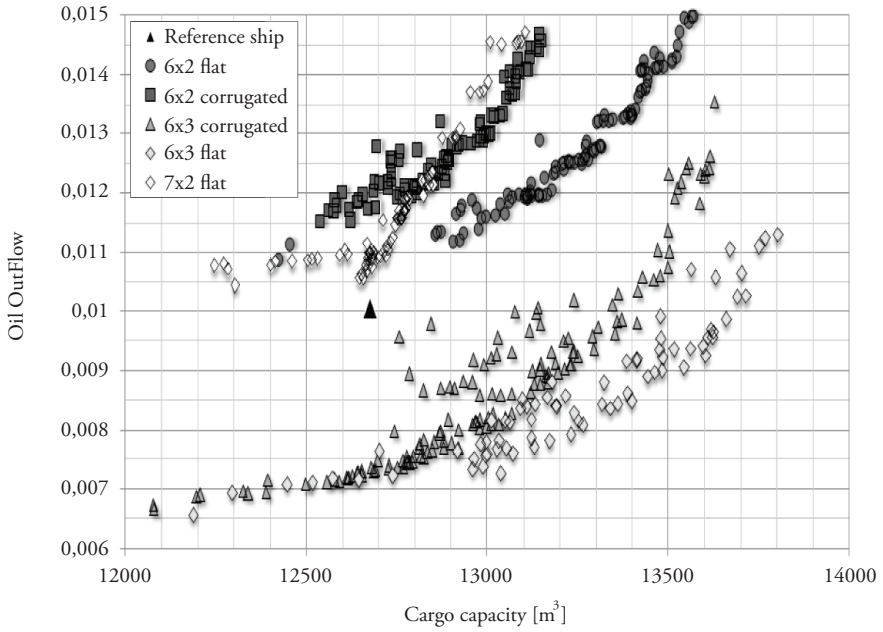

Table 2. Alternative compartmentation configurations

	Arrangement of cargo tanks	Bulkhead type	Number of designs
Configuration 1	6x2	flat	7287
Configuration 2	6x2	corrugated	1738
Configuration 3	6x3	flat	6147
Configuration 4	6x3	corrugated	3270
Configuration 5	7x2	flat	3043

oil outflow (in terms of the MARPOL mean oil outflow index, which must *be less than 0.015* for the reference AFRAMAX tanker) and cargo volume performance than the reference design.

As expected, Fig. 7 shows that for the same cargo volume, most generated "6x2 flat" Pareto designs have less steel weight than all the other configurations, noting that the structural weight of both the generated Pareto designs and of the reference ship were calculated by the same model, namely here based on POSEIDON structural designs. The reference design is here again dominated by several "6x2 flat" and "6x3 flat" designs.

In Fig. 8, the "6x3 flat" designs, as well as the "6x2 flat" designs dominate all other designs. The reference design is again clearly dominated by several "6x3 flat" designs. At the same time, practically all "6x2 flat" Pareto designs have *less steel weight than the reference design at acceptable oil outflow performance.*

Fig 7. Cargo volume vs. steel weight in cargo area – Pareto designs from different configurations

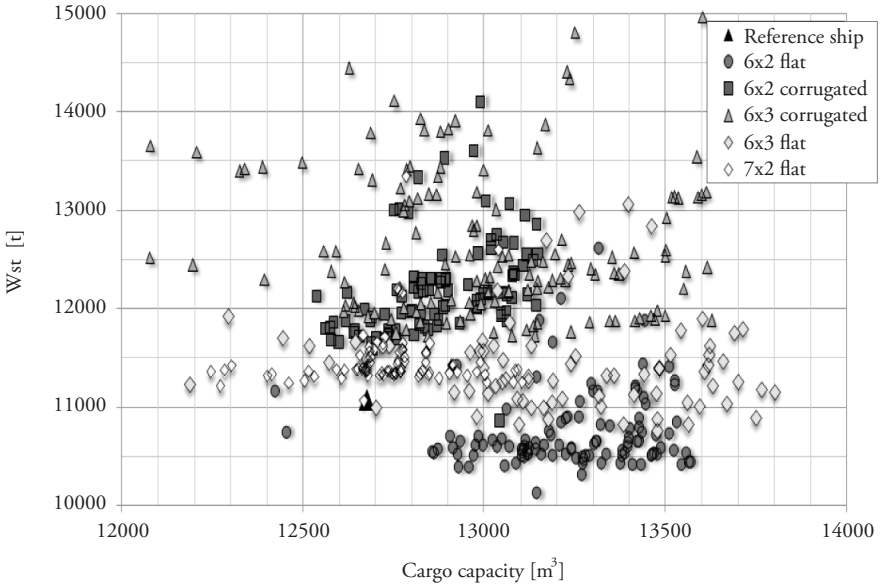

Fig 8. Outflow vs. steel weight in cargo area – Pareto designs from different configurations

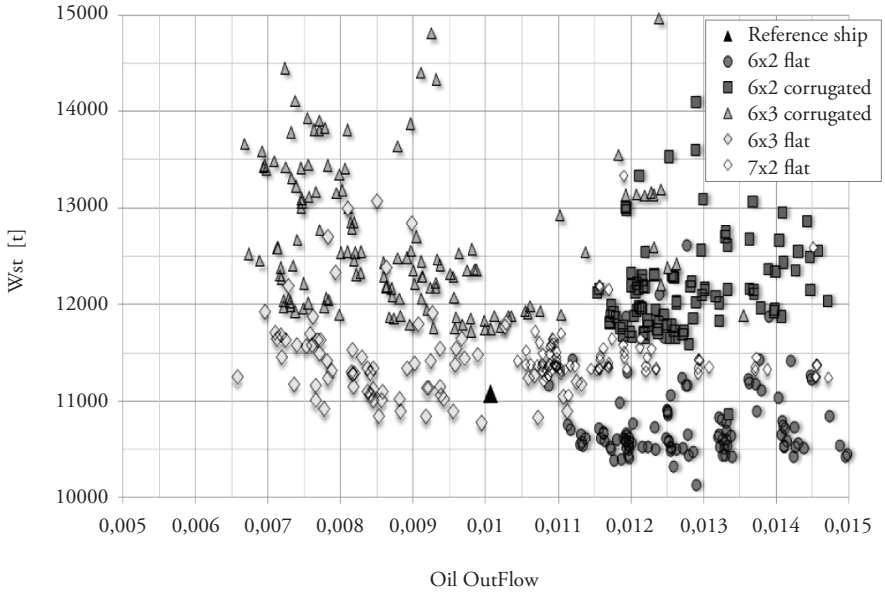

In addition to the above, the following observations can be made:

- None of the corrugated arrangements proves better than flat bulkhead designs. This does not mean that the corrugated geometries should be in general disregarded as alternative configurations. They have important advantages with respect to the ease of production and maintenance, which have not been considered in this study. Also, it should be noted that the flat bulkhead structural designs did not include some minor stiffeners, thus the comparison may be not entirely 'fair' in this respect.
- The "7x2 flat" arrangement performed poorly since the steel weight increases without any significant gains in the outflow or the capacity, respectively.

The reference design appears to be on the Pareto front of the "6x2 flat" designs. It was already noted earlier that the reference design is a well-proven design in practice, which was optimized with respect to steel weight (by the yard designer), most likely by use of Finite Element Method (FEM). .

Holistic Naval Ship Design

Introduction to Naval Ship Design

From the system's point of view, a naval ship may be regarded as an integrated, self-propelled combat system. It may be requested to provide accommodation space for personnel of the size of a small village and be hosted within a large mobile structure that continuously operates in a hostile environment (physical and operational); thus, many challenges come in addition to those of a merchant ship design.

In recent years, the task of formulating clearer goals and setting tangible design specifications for naval ships has been significantly improved with the use of the 2010 International Naval Ship Code (INSC, 2010). The INSC is based on a similar philosophy like the Goal Based Standards (GBS), currently discussed for merchant ships at the International Maritime Organization (IMO). It addresses, however, specific naval ship features and methods of operation. The goals are represented at the top tiers of the framework, below which the detailed requirements which the ship has to meet in design, construction, and operational phase are placed. The structure of the NSC 2010 (ANEP 77 v.2, 2010) version of the code is explained in Figs. 9 and 10. The code offers an *off-the-self* safety and performance management system for navies that need to establish a system of self regulation.

Compared to a merchant ship, the complexity of designing a naval ship is further increased by the multitude of disciplines that need to be considered

Fig 8. Outflow vs. steel weight in cargo area – Pareto designs from different configurations

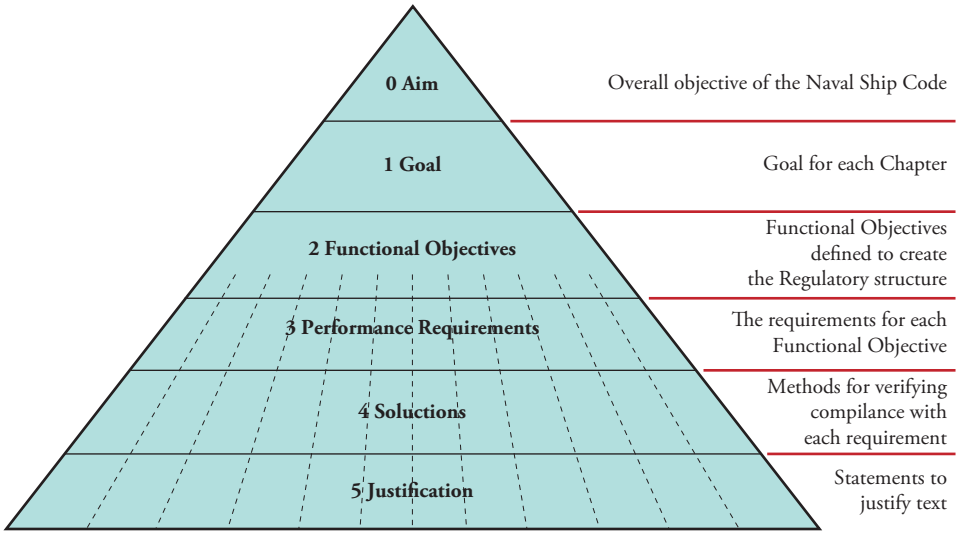

Fig 10. The GBS structure of the NSC (see RINA Warship Technology, 2011)

Tier 0	Aim Scope Introduction									
Tier 1 Goal	Ch I	Ch II	Ch III	Ch IV	Ch V	Ch VI	Ch VII	Ch VIII	Ch IX	Ch X
Tier 1 Functional Objective	General	Structures	Stability	Engineering Systems	Seamanship	Fire Safety	Escape Evacuation	Radio Comms	Navigation	Dangerous Goods
Tier 3 Performance Requirements	Reg 0-21	Reg 0-7	Reg 0-7	Reg 0-25	Blank	Reg 0-13	Reg 0-26	Reg 0-1	Reg 0-1	Reg 0-1
Tier 4 Solutions	Code	Class	National standard	Class	Ch V Blank	Code	Code	SOLAS	SOLAS	IMDG

and integrated in the ship design process, as shown in Fig. 11.

To enable major improvements in acquisition engineering design and analysis processes, many leading navies are working on developing and

Fig 11. Stakeholders disciplines of naval ship design (see Neu, 2000)

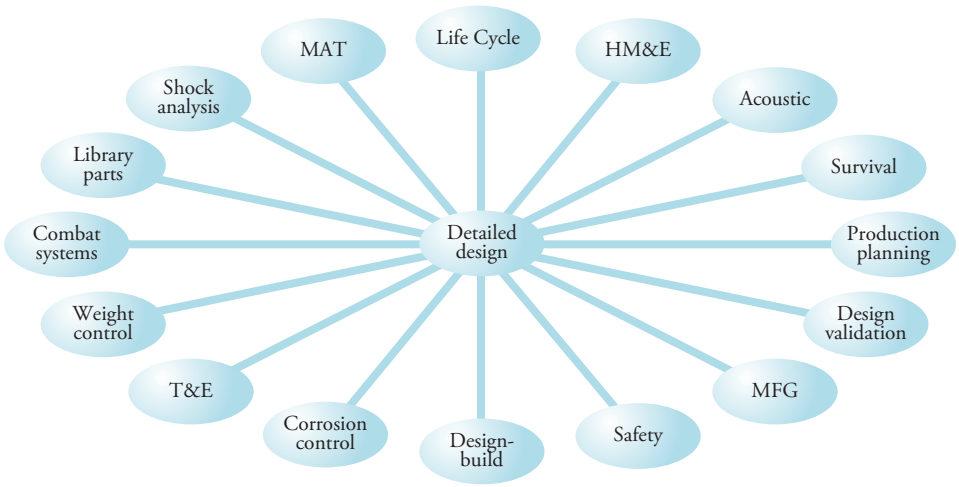

deploying scalable physics-based computational engineering software products aiming to replace empirical design based on historical data and experimental testing with physics-based computational design validated with experimental testing. This will allow the detection and resolution of any design flaws early in the design process before major schedule and budget commitments are made. Additionally, it will allow the innovation by the development of optimized designs for new concept and the integration of the various systems earlier in the acquisition process. The use of such a methodology will increase the acquisition program's flexibility and agility to respond to rapidly changing requirements (*Hurwitz, 2010*).

In that respect, *Holistic Ship Design Optimization* in naval ship design is achieved by the development of an integrated engineering software platform of tools that supports a reconfigurable ship design and acquisition process. This enables the designer to develop cost-effective ship designs on schedule

Fig 12. Sample Integrated Toolset (see ISSC Committee v.5, 2009)

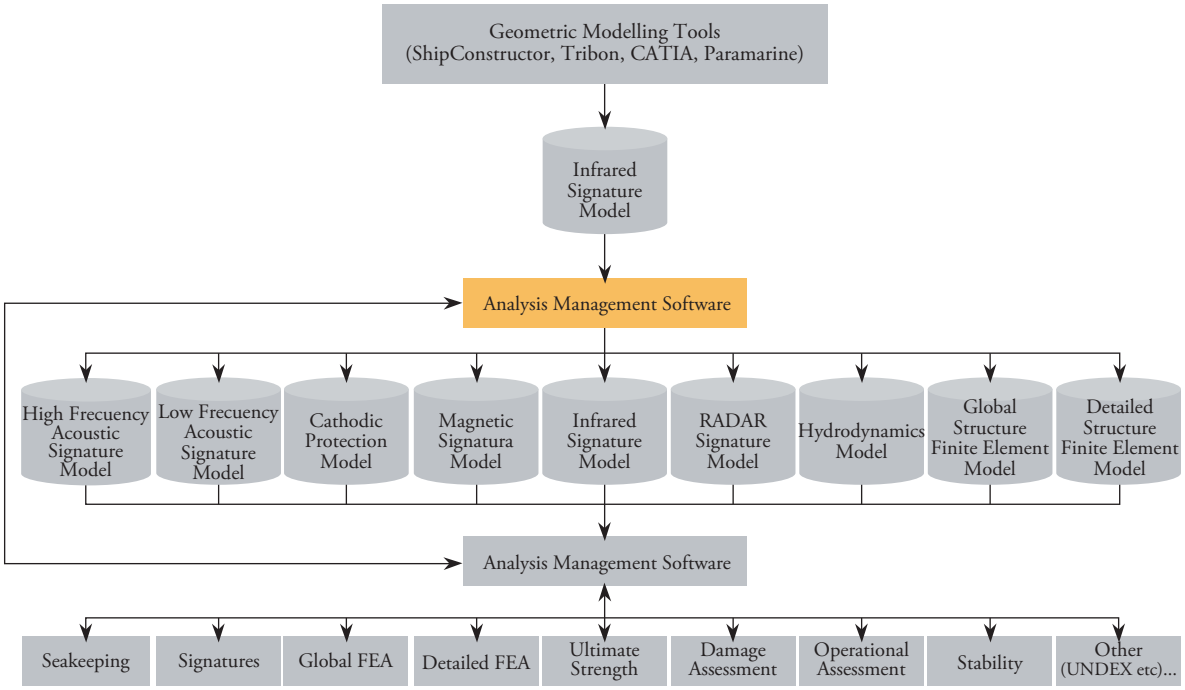

and within budget, able to perform as required and predicted. An example of such an integrated toolset is shown in Fig. 12.

At top level of Fig. 12, there are a number of geometric modeling tools (such as Tribon[6], ShipConstructor[7], CATIA[8], Paramarine[9], NAPA[10] etc.). These software tools generate ship's geometry and related data which are then passed over to the appropriate Analysis Model Synthesizer that uses specialized Analysis Management Software such as (e.g.):

- Davis' ShipIR/NTCS[11] for IR,
- IDS' Ship EDF for Radar Cross Section analysis (see Fig. 13),
- UCL and UoGs integrated PARAMARINE-SURFCON and maritimeEXODUS[12] for design, simulation of evacuation and enhanced operational effectiveness (see Fig. 14).

The development and validation of such integrated tool platforms is a very demanding task; two well known software platforms, which are used and continuously further developed by two major navies, are:

- NAVSEAS (US) Leading Edge Architecture for Prototyping Systems (LEAPS) (*Hurwitz, 2010*)
- QinetiQ-GRC's PARAMARINE software in UK (http://www.qinetiq.com).

The Ship Design laboratory at NTUA has also been developing integrated approaches to naval ship design, namely by utilizing its generic ship design optimization procedure (outlined in Fig. 4) together with a set of specific design tools for naval ship design. These are:

- A naval ship design version of the Parametric Design Tool (PDT) developed

[6] Now AVEVA Marine http://www.aveva.com/products_services_aveva_marine.php
[7] http://www.shipconstructor.com/
[8] http://www.3ds.com/solutions/shipbuilding/overview/
[9] http://www.qinetic.com
[10] http://www.napa.fi
[11] http://www.wrdavis.com/NTCS_intro.html
[12] http://fseg.gre.ac.uk/exodus
[13] http://www.idscompany.it/page.php?f=176&id_v=2

Fig 13. RCS warship analysis by Ship EDF (IDS Ingegneria dei Sistemi S.p.A.[13])

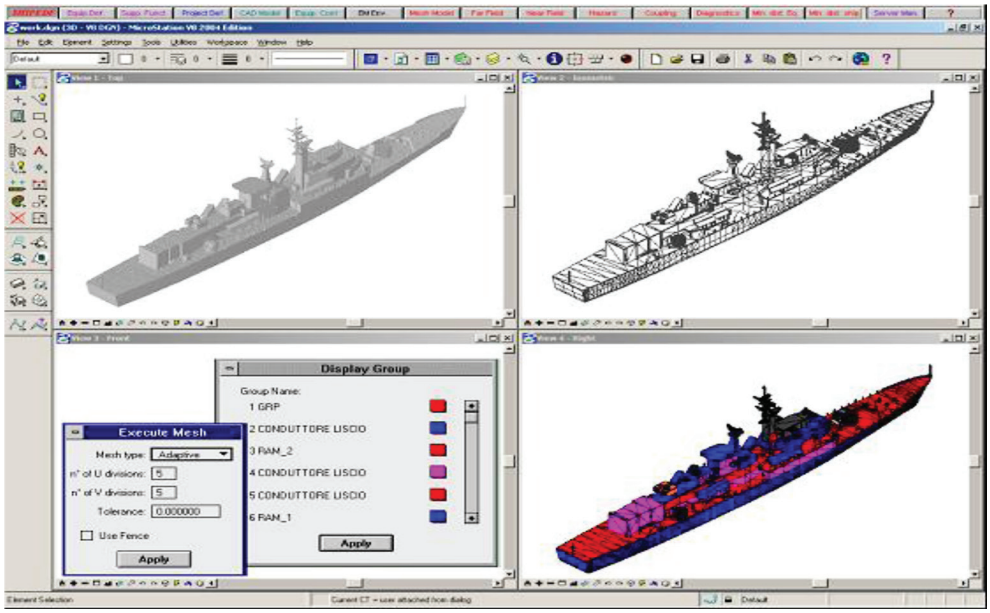

Fig 14. Personnel movement simulation results for RN Frigate (Andrews, 2009)

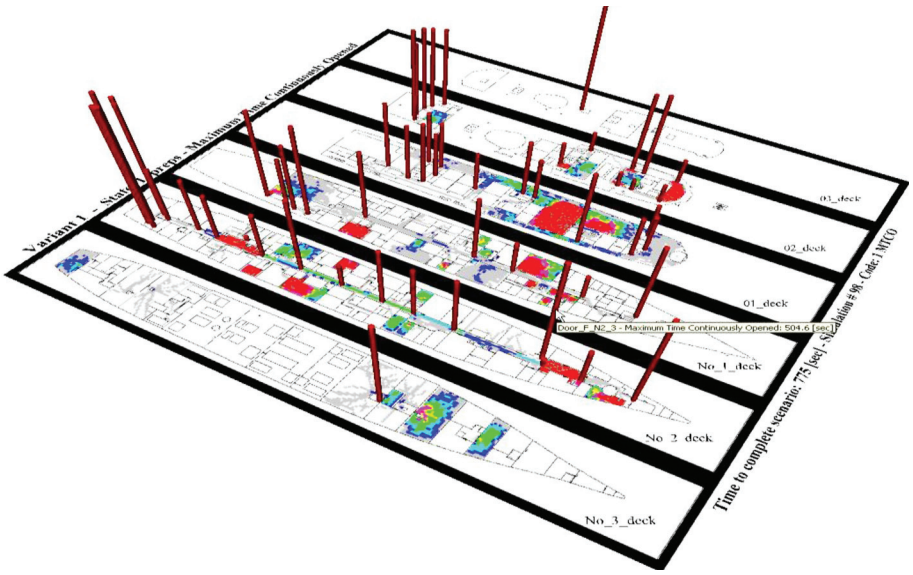

originally for the design of commercial ships (RoRo, tankers, bulkers, containerships) (*Boulougouris and Papanikolaou, 2009*) coupled with the general optimization software modeFRONTIER[14] (see ES.TE. CO, 2003). This is used for the fast population of the design space with conceptual solutions that can be further investigated (Fig. 15).

- An advanced toolset integrating the well-known ship design software package NAPA, modeFRONTIER and a number of external CAE tools such as NUMECA's[15] Fine/Marine CFD code, NTUA-SDL's NEWDRIFT[16] seakeeping (see *Papanikolaou, 2001*), Flowtech's

14 http://www.modefrontier.com

15 http://www.numeca.com

16 http://www.naval.ntua.gr/sdl

Fig 15. NTUA-SDL Parametric Design Tool Design Space Global Exploitation

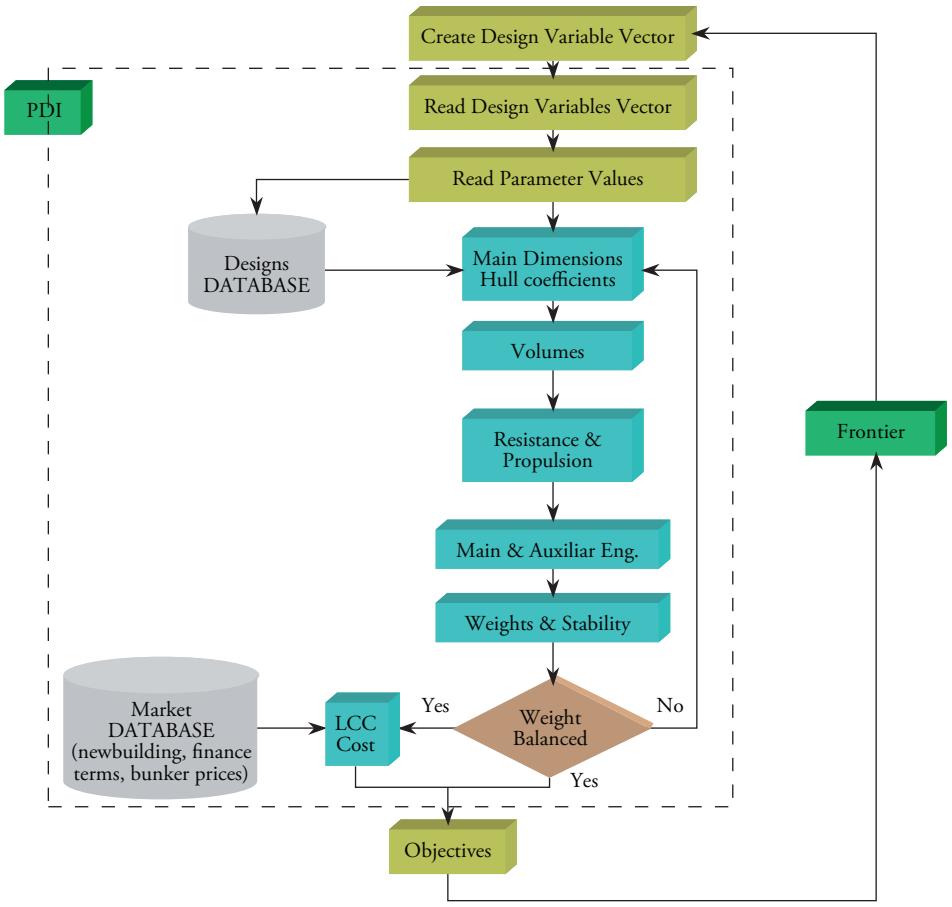

SHIPFLOW[17] (see *Larsson, 1990*) and GL's POSEIDON[18] structural design software. In addition a number of tools have been programmed in NAPA macro-language using NAPA BASIC.

- Using a Parametric Design Tool (PDT) the designer has a computationally efficient tool for the parametric exploration of the design space and the identification of the feasible solutions areas. This is basically a global optimization step. After this step, the more sophisticated tools are introduced to perform the local, more in-depth optimization of the design, taking into account the full set of objectives and ranking the designs according to decision maker's preference.

An example of application of this multi-objective optimization of a naval ship using genetic algorithms and including maximization of the survivability as one of the objectives may be found in the listed reference (*Boulougouris and Papanikolaou, 2004).*

Summary and Conclusions

The present paper provided a brief introduction to a *holistic* approach to ship design optimization, defined the generic ship design optimization problem, and demonstrated its solution by using advanced optimization techniques for the computer-aided generation, exploration, and selection of optimal designs. It discussed proposed methods on the basis of some typical ship design optimization problems of a tanker and naval ships

17 http://www.flowtech.se
18 http://www.gl-group.com/poseidon2/

related to multiple objectives, leading to improved and partly innovative design features with respect to ship economy, cargo carrying capacity, safety, survivability, comfort, required powering, environmental protection, or combat strength, as applicable.

It was shown that multi-objective mathematical optimization approaches are very valuable tools and greatly enhance the quality of ship design, even if applied to vessel concepts already optimized by traditional methods. The design developed and optimization methodology may be a useful tool for the designer in the preliminary design stage, facilitating the elaboration of a large number of design alternatives quickly and with little effort. The designer may explore this possibility to investigate the effect of crucial decisions on the vessel's operating performance before proceeding to the detailed design stage. The design methodology may also be effectively used in feasibility studies, providing assistance for the determination on a rational basis of the most suitable vessel size, transport capacity, speed, and other operating characteristics for a selected service. The integration of the parametric ship design application with a multi-objective optimization software facilitates the design space exploration in a rational and efficient way, enabling the identification of favorable and unfavorable areas of the design variables and ultimately for the determination of the optimal designs located on the Pareto Frontier (in case of multi-criteria optimization). Furthermore, once the optimum design has been selected, its detailed NAPA model including (but not limited to) the hull-form and the watertight subdivision is readily available for further elaboration and detailed design work, considerably reducing related effort.

A final comment on the way ahead: though the generic solution approach to the holistic ship design problem appears well established, it remains for researchers to develop and integrate a long list of application algorithms and related software, addressing the great variety of ship design for life cycle. This is a long-term task of decades, requiring profound skills and understanding of the physics and design of ships, a domain requiring properly trained naval architects and scientists from related disciplines.

Acknowledgements

The author likes to thank his associate, Dr. E. Boulougouris, Assoc. Prof. Dep. of Naval Architecture, TEI Athens, for his longstanding contributions to the herein presented work and particularly to the naval ship design section of the present paper.

References

ANDREWS D., PAWLING R., The Impact of Simulation on Preliminary Ship Design, 10th Int. Marine Design Conference (IMDC'09), Vol.1, Trondheim, May 2009.

ANDREWS, D. (COODINATOR), PAPANIKOLAOU, A., ERICHSEN, S. AND VASUDEVAN, S., State of the art report on design methodology, Proc. 10th Int. Marine Design Conference-IMDC09, Trondheim, May 2009.

BOULOUGOURIS E, PAPANIKOLAOU A., Hull Form Optimization of a High-Speed Wave Piercing Monohull, Proc. 9th Int. Marine Design Conference-IMDC06, Ann Arbor-Michigan, May 2006.

BOULOUGOURIS, E., PAPANIKOLAOU, A., Optimisation of the Survivability of Naval Ships by Genetic Algorithms, Proc. 3rd Int. Conference on Computer and IT Applications in the Maritime Industries (COMPIT'04), Siguënza, Spain, May 2004.

BOULOUGOURIS E. K., PAPANIKOLAOU A. AND ZARAPHONITIS G., Optimisation of Arrangements of Ro-Ro Passenger Ships with Genetic Algorithms. Ship Technology Research, Verlag Heinrich Söding, 51:3, pags. 99-105, 2004.

BOULOUGOURIS, E., PAPANIKOLAOU, A., Energy Efficiency Parametric Design Tool in the frame of Holistic Ship Design Optimization, 10th Int. Marine Design Conference (IMDC'09), Vol. 1, Trondheim, May 2009.

BRETT PO, BOULOUGOURIS E, HORGEN R, KONOVESSIS D, OESTVIK I, MERMIRIS G, PAPANIKOLAOU A, VASSALOS D. A Methodology for the Logistics-Based Ship Design", Proc. 9th Int. Marine Design Conference-IMDC06, Ann Arbor-Michigan, May 2006.

FLOWMART (2000-2003), Fast Low Wash Maritime Transportation. EU funded project, 5th Framework Programme, Contract number G3RD-CT 1999-00013.

GKOHARI, D., PAPANIKOLAOU, A., Optimization of Ship design within an Integrated Multimodal Transport System, Journal of Ship Production-SNAME, Vol. 26, 1, pp. 47-59, Feb. 2010, ISBN 8756-1417, ISSN: 1542-0469.

HURWITZ, M. , Plans and Status of the CREATE-SHIPS Project: Enabling Required Naval Warship Performance Throughout the Acquisition Lifecycle, 13th Annual Systems Engineering Conference, San Diego, CA, 27 October 2010.

INTERNATIONAL MARITIME ORGANIZATION (IMO), *Prevention of Air Pollution from Ships*. Report of the Working Group on Greenhouse Gas Emissions from Ships. MEPC 58/ WP. 8, October 2008.

INTERNATIONAL NAVAL SAFETY ASSOCIATION (INSA), *Naval Ship Code, NATO-ANEP-77 Edition 2*, July 2010, http://www.navalshipcode.org/.

ISSC 09-COMMITTEE V.5 (2009), *Naval Ship Design*, 17th Int. Ship And Offshore Structures Congress (ISSC 09), 16-21 August 2009, Seoul, Korea.

LEVANDER, K., Innovative Ship Design – Can innovative ships be designed in a methodological way, Proc. 8th Int. Marine Design Conference –IMDC03, Athens, May 2003.

LOGBASED (2004-2007), Logistics Based Design, EU funded project, 6th Framework Programme, Contract number TST3-CT-2003-001708.

NEU W.L. HUGHES O. MASON W.H. NI S. CHEN Y. GANESAN V. LIN Z. TUMMA S., A Prototype Tool for Multidisciplinary Design Optimization of Ships, Proc. 9th Congress of the Int. Maritime Association of the Mediterranean (IMAM'00), April 2000, Naples, Italy.

NOWACKI, H., Developments in Marine Design Methodology: Roots, Results and Future, Proc. 10th International Marine Design Conference, IMDC09, Trondheim, May 2009.

PAPANIKOLAOU A (ed). Risk-based Ship Design – Methods, Tools and Applications. SPRINGER Publishers, ISBN 987-3-540-89041-6, 2009c.

PAPANIKOLAOU A. (coordinator), Andersen P, Kristensen HO, Levander K, Riska K, Singer D, Vassalos D. State of the Art Design for X. Proc. 10th Int. Marine Design Conference-IMDC09, Trondheim, May 2009a.

PAPANIKOLAOU, A.; ZARAPHONITIS G., *Computer Program NEWDRIFT v.7*, Internal Report, NTUA, Greece, 2001.

PAPANIKOLAOU, A., Holistic ship design optimization. Journal Computer-Aided Design (2009), doi:10.1016/j.cad.2009.07.002, 2009b.

PAPANIKOLAOU, A., "Computer-Aided Preliminary Design of a High-Speed SWATH Passenger/Car Ferry," Proc. of the 4th IMSDC '91 Conference, Kobe, May 1991.

PAPANIKOLAOU, A., P. KAKLIS, C.

KOSKINAS AND D. SPANOS, "Hydrodynamic Optimisation of Fast Displacement Catamarans," Proc. 2l[st] Int. Symposium of Naval Hydrodynamics, ONR' 96, Trondheim, June 1996.

PAPANIKOLAOU, A., ZARAPHONITIS, G., BOULOUGOURIS, E., LANGBECKER, U., MATHO, S., SAMES, P., Multi-Objective Optimization of Oil Tanker Design, Journal Marine Science and Technology, Springer Verlag, Tokyo, 2010.

POP&C (2004-2007), Pollution Prevention and Control, EU funded project, 6[th] Framework Programme, Contract No. FP6-PLT-506193.

RINA WARSHIP TECHNOLOGY, (2011), *New safety standard will continue to evolv*e, The Royal Institute of Naval Architects, pp. 26-28, January 2011.

SAFEDOR (2005-2009) Integrated Project on Design, Operation and Regulation for Safety. EU-funded project, 6[th] Framework Programme, contract TIP4-CT-2005-516278, www.safedor.org

SKOUPAS, S., ZARAPHONITIS, G., PAPANIKOLAOU, A., Parametric Design and Optimization of High-Speed, twin-Hull Ro-Ro Passenger Vessels, Proc. 10[th] International Marine Design Conference, IMDC09, Trondheim, May 2009.

VRSHIP-ROPAX2000 (2001-2005), A Virtual Environment for Life-Cycle Design of Ship Systems, EU funded project, 5[th] Framework Programme, Contract Number G3RD-CT-2001-00506.

ZARAPHONITIS G, PAPANIKOLAOU A, MOURKOYIANNIS D. Hull Form Optimization of High Speed Vessels with Respect to Wash and Powering. Proc. 8[th] Int. Marine Design Conference-IMDC03, Athens, May 2003.

On the numerical prediction of the ship's manoeuvring behaviour

Acerca de la predicción numérica del comportamiento de maniobra de la embarcación

Andrés Cura-Hochbaum [1]

Abstract

A numerical procedure to predict the manoeuvrability of a ship based on Reynolds Averaged Navier Stokes simulations is described together with some recommended practices to obtain feasible results. The paper is dedicated to surface ships in unrestricted waters where usually only four degrees of freedom (DoF) are relevant. An example for a tanker shows the capability of the proposed method.

Key words: manoeuvring prediction, RANS, derivatives, virtual captive test.

Resumen

Se describe un procedimiento numérico para predecir la maniobrabilidad de un buque basado en simulaciones Reynolds promediadas de Navier Stokes, así como algunas prácticas recomendadas para obtener resultados factibles. Este documento está dedicado a embarcaciones de superficie en aguas sin restricciones donde usualmente sólo cuatro grados de libertad son relevantes. Un ejemplo para un buque cisterna muestra la capacidad del método propuesto.

Palabras claves: predicción de maniobrabilidad, RANS, derivados, prueba de cautivo virtual.

Date Received: January 23th, 2011 - *Fecha de recepción: 23 de Enero de 2011*
Date Accepted: February 17th, 2011 - *Fecha de aceptación: 17 de Febrero de 2011*

[1] Technical University Berlin, Department Dynamics of Maritime Systems. Berlín. Germany. e-mail: cura@tu-berlin.de

Introduction

RANS tools, *i.e.*, numerical methods for solving the Reynolds Averaged Navier Stokes equations for viscous turbulent flows, can be applied to predict the manoeuvring behaviour of a vessel. This is achieved either directly, by using the considered RANS code for calculating the hydrodynamic forces and moments acting on the hull in every new time step of the simulated rudder manoeuvre, or by using it to calculate the time histories of these forces and moments during selected forced motions. The latter results can be used to determine the manoeuvring derivatives of a mathematical model for manoeuvring prediction.

This second procedure is described in this paper from the practical point of view, together with recommended practices to obtain feasible manoeuvring prediction results. The numerical techniques used to discretise and solve the partial differential equations involved, e.g., finite difference method or finite volume method, to model the flow turbulence and to generate grids, have been described in many publications (Ferziger and Peric 2002, Wilcox 1993, Thompson *et al.*, 1985). This paper is dedicated to surface ships in unrestricted waters, where usually only four degrees of freedom (surge, sway, yaw, roll) are relevant for manoeuvring. In the example shown here for a very large crude carrier, however, the roll motion has no significant effect.

Manoeuvring Simulation

To predict a manoeuvre, the rigid motion equations of the ship in 3-DoF, 4-DoF, or even in 6-DoF are numerically integrated in time with a proper discretisation scheme, e.g., Euler implicit, Runge-Kutta, etc. In most applications, provided large accelerations are not expected, the first-order Euler explicit scheme can also be used. The motion parameters considered should be properly defined by means of an earth-fixed or "inertial" coordinate system, a ship-fixed coordinate system and/or with help of an intermediate or "hybrid" coordinate system to uniquely define angles and translations. The singularity typically (gimbal lock, for cos θ=0) occurring when using Euler angles is not relevant for a surface ship.

An example of motion equations in four degrees of freedom (4 DoF) for a free sailing (rigid) ship or model written in a hybrid coordinate system, which follows the ship motions excepting roll, reads:

$$m\left[\dot{u} - \dot{\psi}\ v - x_G^*\ \dot{\psi}^2 + z_G^*\left(2\,\dot{\psi}\,\dot{\varphi}\,\cos\varphi + \ddot{\psi}\,\sin\varphi\right)\right] = X \tag{1}$$

$$m\left[\dot{v} + \dot{\psi}\,u + x_G^*\,\ddot{\psi} + z_G^*\left(\left(\dot{\psi}^2 + \dot{\varphi}^2\right)\sin\varphi - \ddot{\varphi}\cos\varphi\right)\right] = Y \tag{2}$$

$$\left(I_{yy}\sin^2\varphi + I_{zz}\cos^2\varphi\right)\ddot{\psi} + 2\left(I_{yy} - I_{zz}\right)\dot{\psi}\,\dot{\varphi}\,\sin\varphi\,\cos\varphi + -I_{xz}\left(\ddot{\varphi}\,\cos\varphi - \dot{\varphi}^2\sin\varphi\right) + m\,x_G^*\left(\dot{v} + u\,\dot{\psi}\right) + m\,z_G^*\left(\dot{u} - v\,\dot{\psi}\right) = N \tag{3}$$

$$I_{xx}\ddot{\varphi} - I_{xz}\ddot{\psi}\cos\varphi + \left(I_{zz} - I_{yy}\right)\dot{\psi}^2\sin\varphi\cos\varphi - m\,z_G^*\cos\varphi\left(\dot{v} + u\,\dot{\psi}\right) = K \tag{4}$$

The surge and sway velocities u and v are the components of the velocity of the chosen ship origin O in the horizontal longitudinal and transversal directions x and y of the hybrid coordinate system, respectively. The Euler angles φ and ψ are the rotations around the x- and y-axes, respectively and describe the ship's roll and yaw motions. The dots in the equations above denote time derivatives. m is the mass of the ship or model and x_G* and z_G* are the coordinates of the centre of gravity, G, in the ship's fixed system. It is assumed that y_G* =0. I_{xx}, I_{yy} , I_{zz} are the moments of inertia about the ship's fixed axes through the origin O and I_{xz} is the product of inertia. It is assumed that I_{xy}* 0 and I_{yz}* 0 because of symmetry. X and Y (longitudinal and side forces) are the components in the hybrid system of the external force acting on the ship. K and N (roll and yaw moment) are the components in the hybrid system of the moment of the external forces. Given that heave and pitch motions are neglected, the state of movement of the ship is defined by the position of O (earth-

fixed coordinates), its velocity vector (u, v, 0), the Euler angles φ, ψ, and the angular velocity vector ($\dot{\varphi}$, 0, $\dot{\psi}$). The time history of these variables can be obtained by integrating equations (1) to (4) numerically over time. For this purpose, the forces and moments on their right hand sides are needed.

Rudder manoeuvres, like zigzag tests and turning circle tests, can be simulated directly by solving together equations (1) to (4) for the ship and the RANS equations for the fluid to calculate the forces and moments in every new time step. The rudder(s) is (are) turned according to the desired manoeuvre during the simulation. This kind of manoeuvring simulation is extremely time-consuming but, since there is no mathematical model for the hydrodynamic forces involved, in principle it is easier than by means of manoeuvring derivatives. It will represent the best approach once comprehensively validated. Some publications already show the potential of this procedure (Carrica *et al.*, 2008).

Rudder manoeuvres are traditionally simulated by using a mathematical model to calculate the hydrodynamic forces and X, Y, K, and N moments in every new time step of the time marching procedure used when solving the motion equations of the ship. An approach based on Abkowitz-type coefficients reads, e.g., for the non-dimensional side force:

$$Y' = Y'_0 + Y'_\delta \delta + Y'_{\delta\delta} \delta^2 + Y'_{\delta\delta\delta} \delta^3 + Y'_v v + Y'_{vv} v^2 + Y'_{vvv} v^3 + Y'_r r + Y'_{rr} r^2 + Y'_{rrr} r^3 + Y'_{vr} v\, r + Y'_{vrr} v\, r^2 + Y'_{vvr} v^2 r + Y'_{\dot{v}} \dot{v} + Y'_{\dot{r}} \dot{r} + \ldots Y'_{u\delta}\, \Delta u\, \delta + \ldots \quad (5)$$

The force has been written as a function of the rudder angle, δ, expressed in radians; the non-dimensional surge and sway velocities $\Delta u=(u-U_0)/U_0$ and v/U_0, where U_0 is the initial speed of the ship and the non-dimensional yaw rate $r = \dot{\psi}\, Lpp /U_0$, where L_{pp} is the ship length. The approach includes terms up to the third order and also mixed or coupled terms, accounting for interactions, but many other terms could be added. The sub-index u represents Δu. Dots denote time derivatives. Thus, $Y'_{\dot{v}}$ for instance, represents the hydrodynamic mass for transverse motion. Forces are made non-dimensional with $\frac{\rho}{2} U_0^2 L_{pp}^2$ and moments with $\frac{\rho}{2} U_0^2 L_{pp}^3$, ρ being the water density. All magnitudes in Equation (5) have been made non-dimensional with proper combinations and powers of $\frac{\rho}{2}$, U_0 and L_{pp}. Except for the coefficients, primes have been omitted for simplicity.

The coefficients are usually determined by means of captive model tests performed with a Planar Motion Mechanism (PMM) or a Computarized Planar Motion Carriage (CPMC). Once the coefficients have been determined for a specific ship it is very simple to predict all desired manoeuvres.

Manoeuvring Simulation

Due to the enormous computational effort required for the direct simulation of manoeuvres, another CFD (DEFINE FIRST) strategy has gained popularity instead. It consists in simulating usual PMM or CPMC tests numerically, solving the RANS equations around the ship or ship model when performing prescribed motions. Compared to direct manoeuvring simulations, this prediction procedure has the same advantages and disadvantages as between free and captive model tests. From the computational point of view, however, it is definitively more robust and less time consuming.

The strategy fully resembles the classical, well-accepted PMM tests followed by the determination of derivatives and seems already practicable for commercial applications. Nevertheless, a mathematical model (*i.e*, a set of coefficients of Abkowitz type or coefficients of formulae for diverse forces of a modular simulation method) is involved, introducing a further source of uncertainty into the prediction.

Motion equations are not solved in this instance. Selected motions, *i.e.*, harmonic pure sway, pure yaw, etc, are imposed; there are different ways to impose the motions. In order to resemble CPMC tests or to reproduce measured motions during free-model tests, it can be advantageous to read a file containing the time histories for the motion parameters.

Note that when disregarding that the ship motion is given, it would be best to let the ship or free model to sink and trim during the RANS simulation. However, contrary to direct manoeuvring simulations with RANS where the motions are predicted anyway and merely two more DoF should be considered to include sinkage and trim, this is less straightforward now and leads to a combination of given and predicted motions.

The analysis of the predicted time histories of the longitudinal and transverse forces X, Y, and the roll and yaw moments K, N is the same as when performing PMM or CPMC model tests. Moreover, since no artifcial time lag between predicted forces and prescribed motions arise and no inertial forces have to be subtracted (no filters, no swinging masses), the analysis is easier than performing model tests.

Similar to when performing model tests, there are different ways of determining the manoeuvring derivatives and the "virtual" test program has to be decided according to this and to the mathematical model used (e.g. the derivatives to be determined). The first step of any numerical investigation for manoeuvring consists in analysing the case considered and making decisions like limiting the calculations to double body flow or taking the free water surface into account, considering the free sinkage and trim or not, performing the simulations for the ship model or for the full-scale ship. This is followed by the proper choice of a turbulence model, discretisation schemes, grid and time resolution, and the choice of the boundary conditions at the borders of the grid.

In addition, several parameters of the code employed usually have to be chosen as well; for instance: the number of (outer) iterations within each time step, the number of (inner) iterations within an outer iteration, values for diverse under-relaxation factors, among others. Depending on the code, other settings could also be required and strongly influence the result of the computations. For these reasons, experience in viscous flow computations and insight on the RANS code to be used are prerequisites for successful CFD-based manoeuvring prediction.

General Considerations

In principle, RANS simulations can be performed for the full-scale ship, avoiding any scale effect. In practice, however, most simulations are performed for the model rather than for the full-scale ship because computations for Reynolds numbers in the order of 10^9 are yet to be fully validated and yield much more numerical difficulties than for Reynolds numbers at model scale, being two orders of magnitude smaller. In addition, prediction results for the model can be judged as a whole by comparing them with the results of a few selected free-model tests.

The Navier-Stokes (NS) equations and the continuity equation describe the conservation of momentum and mass in a viscous turbulent incompressible flow and are best suitable to describe the flow around a ship. To work with mean values of all flow variables (e.g. velocities, pressure) instead of instantaneous values, the RANS equations are obtained by averaging the NS equations. This averaging can be seen as time averaging in case of a steady mean flow, but has to be understood as ensemble averaging in case of an unsteady mean flow (Wilcox 1993, Cebeci *et al*., 2005). As a result of the averaging, the RANS equations contain some new unknown terms representing the effect of the turbulence on the flow. In order to solve the set of conservation equations, these terms are approximated by a turbulence model. The reason for doing so is that if not, the required space and time resolution for directly solving the NS equations would be impracticable (probably still in the next decades) for a turbulent ship flow.

Any turbulence model used by usual RANS applications can also be used for manoeuvring tasks. The most popular models are the k-ε and k-ω models (Launder and Spalding 1974, Wilcox 1993) and several variants with and without using wall functions, which allow a significantly coarser resolution of near-wall regions. When looking for accurate prediction of complex flow phenomena, however, e.g. detailed flow separation, more sophisticated turbulence models like Reynolds Stress Models (RSM) could be a better choice (Wilcox 1993). But, such models are less validated

and often less robust and more time-consuming than the classical two-equation models mentioned above.

The experience from published results and workshops shows that the dependence of side force and yaw moment on the turbulent model, i.e., of those forces which are most significant for manoeuvring, is less significant than expected. The reason is that these hydrodynamic forces are certainly viscosity dependent but firstly dominated by pressure. In fact, satisfactory results can be achieved even by using wall functions as they do not deteriorate the quality of the predictions to the same extent than when predicting resistance.

Disregarding cases where RANS tools are used for predicting forces on the bare hull only, e.g. to determine coefficients for hull forces in a modular mathematical model, the appendages have to be considered for manoeuvring tasks. Inclusion of rudders and even bilge keels has become usual in RANS applications. This complicates the grid generation and probably also some flow aspect, which can lead to increased convergence difficulties, but does not really represent a problem.

The main issue is how to treat the propeller(s), crucial for simulating the rudder inflow correctly when rudders are placed behind propellers. Taking the real geometry of the propeller into account and considering the rotating propeller during the RANS simulation is possible but extremely time consuming. Thus, body forces, which are added to the right hand sides of the RANS equations, are frequently used to approximate the effect of the propeller on the flow. These forces are distributed over the grid region corresponding to the spatial position of the propeller and are calculated so that they yield the propeller thrust and moment.

Body force models, mostly based on potential flow codes like vortex-lattice or panel methods, are often used to approximate the propeller effect including slip stream and swirl, which may also influence aspects of the flow like rudder stall angle, risk of cavitation, etc. The body force distribution inside the propeller region may be calculated in every new time step or in some larger time intervals, based on the current propeller inflow obtained during the RANS simulation and on the propeller rpm. This can be done either interactively, running the used potential code each time again, or determining the forces in grid cells within the propeller region from a data base calculated beforehand for the considered propeller. Fig. 1 shows the cylindrical body force region (rectangle) and the effect of the body forces on the axial velocity in the longitudinal central plane.

Fig. 1. Body force region and effect on the flow

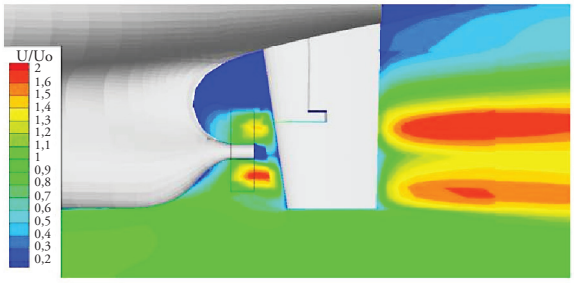

Fig. 2. Grid and boundaries of hexahedral computational domain

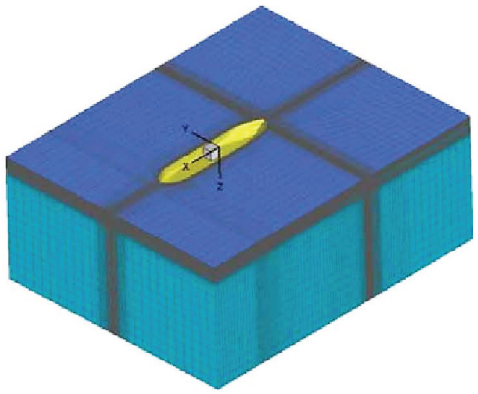

The choice of the propulsion point, corresponding to the full scale or to the model scale, should be decided by following similar criteria as for model tests. A way of determining the correct propeller rpm before starting the manoeuvre simulation is to calculate the flow for the steady straight ahead motion of the ship at the given approach speed for different rpm's and to determine the one which makes the total longitudinal force equal to the desired value (e.g. zero or estimated frictional deduction). A proper strategy for the propeller rpm dur-ing the manoeuvre, resembling the real

behaviour in full scale where the rpm often varies depending on torque, can also be implemented.

Commercial grid generators are widespread, but open source software is also gaining in popularity recently. Block-structured grids, often including non-matching interfaces, and unstructured grids with several million cells have become usual for manoeuvring tasks. Contrary to many CFD applications for ship resistance or propulsion, the nature of the problem now requires a grid covering the surroundings at both sides of the ship.

Not only for turning the propeller but also to deflect the rudder within direct manoeuvring simulations, a RANS code with sliding grid or overlapping grid capability is needed (Carrica *et al*.,). In the later case, a considerable amount of computational effort is required to transfer flow information from one grid part to the other. Otherwise and whenever possible, the grid is kept unchanged during the computation to avoid deteriorating its quality, which directly influences the convergence behaviour and the quality of the results. Nevertheless, this is obviously not possible in many cases of interest, for example when considering squat in shallow water or approaching a quay. In such cases, a suitable grid deformation technique can be an alternative to overlapping grids.

The grid can be generated in several ways and many different grid topologies can be chosen. The outer boundaries of the grid mostly consist of planes delimiting a box (hexahedron) surrounding the ship. Fig. 2 shows a typical configuration for a manoeuvring application for a double-body in deep water.

The grid has to cover the interesting flow domain so that non-physical boundaries (see below) are far from the region of interest, i.e., ship vicinity. Typical dimensions of a grid are 3-5 ship lengths in longitudinal direction, 2-3 in transverse direction and one length in vertical direction for deep water. The near-wall region has to be meshed so that the requirements of the used turbulence model are fulfilled (Wilcox 1993, Menter 1994). In any case, a certain number of grid points (say 20) within the boundary layer have to be placed. For the reasons mentioned above regarding the influence of viscosity on side force and yaw moment, wall functions are often used for manoeuvring cases.

If the flow computation is made in a ship-fixed coordinate frame, *i.e*., if the conservation of momentum is stated in terms of its components in a ship-fixed coordinate system, inertial body forces, e.g. centrifugal and Coriolis forces, have to be added to the RANS equations (Cura and Vogt 2002). These forces are usually treated explicitly during the computation and could affect the stability and convergence of the computation if they are considerably larger than the hydrodynamic forces themselves. On the other hand, if the flow computation is made in an earth-fixed or inertial coordinate frame, no inertial forces have to be added but cell boundary velocities will have to be considered to calculate the correct mass and momentum fluxes through the cell sides; see for instance Ferziger and Peric 2002. Both proce-dures are mathematically equivalent. The numerical advantages of one or the other procedure seem not significant for typical manoeuvring applications.

The boundary conditions (BC) are crucial for the accuracy of the numerical solution. Setting non-physical boundary conditions such as undisturbed flow (Dirichlet) or zero-gradient (Neumann) too close to the ship will affect the results. The way BC are imposed within the numerical technique may change from code to code, but does not differ for manoeuvring tasks from other tasks. However, during manoeuvring simulations there are often no longer unambiguous inlet or outlet borders of the computational domain but mixed forms. Further, in unsteady flow cases, the BC may have to be updated during the course of the simulation according to the instantaneous ship motion.

At an "inlet" border for instance, far in front of the ship (e.g. 1 Lpp) the absolute velocity is zero (in absence of current and waves). Within a ship-fixed frame, however, inlet velocities are relative velocities and, therefore, of equal magnitude but opposite sign than the velocity resulting in the considered point of the boundary from the translation (ship velocities u and v) and rotation (yaw rate r) of the

ship-fixed coordinate system, i.e., u inlet = – (u –y r) v inlet = – (v + x r)

Fig. 3. Velocities in horizontal plane around a ship in steady turning to starboard with drift angle 22°

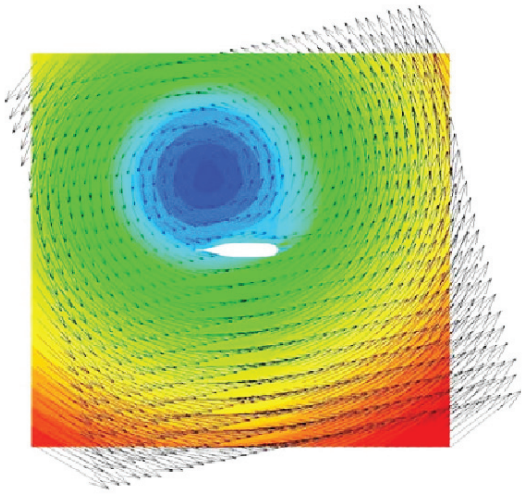

A pressure BC, either zero pressure for double-body flow or undisturbed hydrostatic pressure distribution for free surface flow, has proven be advantageous for the "outlet" border far behind the ship (e.g. 2-4 Lpp).

At the sides of the computational domain, e.g. placed 1-2 Lpp away from the ship, the velocities may also be given, but these borders could also be treated as inlet and outlet boundaries, for instance in case of a steady oblique towing motion at large drift angle.

At rigid walls like the hull, a "no slip" BC is mostly set, ensuring that the fluid particles have the same velocity as the wall. Sometimes, however, it is convenient to consider a wall without any friction, a "free slip" wall, for instance to delimit the computational domain. Note that, if planar, such walls behave similarly to symmetry planes.

The bottom of the computational domain can be seen as a free slip wall placed far below the ship for deep water (e.g. one Lpp). The same can be chosen for the top border of the considered hexahedral domain, placed at the waterline in case of double-body flow or at some distance (e.g. 0, 1 – 0, 3 Lpp) above the waterline in case of a free-surface flow.

Note that during manoeuvres often no real inlet and outlet boundaries exist and a border of the computational domain may change its character during the simulation. For these reasons, some adapted "mixed" BC taking this feature into account have proven advantageous. Hereby, the velocities are given if the flux is directed into the domain only and they are let free otherwise. This has been done at the left, upper and lower lateral borders in the example of Fig.3, while undisturbed pressure was assumed at the right border. The calculated velocity field differs from the undisturbed field in the close vicinity of the ship only.

Computations can be performed by taking the water free surface into account or not. The latter approach is reasonable for a slow ship in deep water and requires significantly less computational effort (e.g. factor 10 in a steady case). Nevertheless, even at low Froude numbers, the underwater shape and, thus, the forces could change significantly if the sinkage and trim of the vessel vary at large drift angle or yaw rate. A way to take such changes into account would be by including the free surface and using a 6 DoF motion model (see below) letting the ship free to sink and trim during the simulation.

Including the water free surface, however, even having become more standard in the last years, leads not only to more computational time but also to increased numerical difficulties. In particular, reflection of the waves generated by the ship on non-physical or open boundaries (outlet) should be avoided. Among other techniques to avoid such reflections, a strong coarsening of the grid towards the outlet has proven efficient in damping the outgoing waves, preventing reflections in a rather rude manner. This procedure would not be applicable if the boundary considered changes its type (e.g. from outlet to inlet) in the course of the simulated manoeuvre.

Example

The technique outlined above is applied here to predict the manoeuvrability of a Very Large Crude Carrier (VLCC), namely the tanker KVLCC1,

Table 1. Main particulars of KVLCC1

Lpp	320.0 m
B	58.0 m
T	20.8 m
CB	0.8101
LCB	3.48 %
GM	5.71 m
ixx/B	0.375
izz/Lpp	0.25
Rudder lateral area	136.7 m^2
Rudder helm rate	2.34 °/s
Ship speed U0	15.5 kn

used as a benchmark test in SIMMAN'08. Due to the low Froude number of the considered tanker and because negligible heel angles are expected during its manoeuvres, all RANS simulations were performed without taking the water free surface into account.

An in-house RANS code was used to calculate the flow around the tanker at several static conditions and during virtual pure surge, pure sway, pure yaw, and combined sway-yaw tests to obtain a rather simple set of hydrodynamic Abkowitz-type coefficients (Table 2).

All dynamic tests were simulated by using the same multi-block structured grid with about one million cells with (some) non-matching block interfaces. The semi-balanced horn rudder, embedded in an individual grid box, is not deflected during these simulations. For static cases with deflected rudder and constant drift angle and/or yaw rate only this grid box is replaced by another according to the rudder angle considered.

The grid dependency of the results has to be checked at least by means of selected calculations on different grids. In the present case, the values of all forces and moments acting on the ship obtained on coarse, medium, and fine grids behaved consistently and differed by less than 10% from each other. Although this check cannot replace a real Uncertainty Analysis (UA) it may be a good compromise in practise.

The computations are performed on a ship-fixed grid using a Cartesian non-inertial coordinate system. The standard two equation k-ω turbulence model with wall functions is used. During dynamic tests, the motions are imposed through the boundary conditions and corresponding inertial forces added to the RANS equations, see Cura and Vogt (2002).

Currently, the needed CPU time to simulate dynamic test amounts is still several days per period on a single processor of a normal PC, but it can be much less if a parallel code is run on a cluster with hundreds of processors. The static tests usually take some few hours depending on grid resolution.

Vortex lattice data for the propeller of a typical tanker was used in the present case. The rate of revolutions was set so that the resulting thrust balanced the resistance computed during a steady straight ahead motion of the model (model self propulsion point). This rate was kept constant throughout the computations. Fig. 5 shows the velocity distribution just behind the propeller plane during a simulated combined sway-yaw test at a certain time when the ship is turning to starboard. The white circle indicates the body force region.

In order to obtain all manoeuvring derivatives, except those depending on the rudder angle and surge velocity, five dynamic tests with large velocity amplitudes and a common non-dimensional period $T' = T\ U0 / Lpp$ of 3.369 (20 seconds in model scale) are simulated. Similar to real tests, the non-dimensional amplitudes of the harmonic motions should be chosen so that they cover the expected range of the motion parameters during the manoeuvres. In the present example, the amplitudes were: $\Delta u' = \Delta u / U0 = 0.10$ for pure surge, $v' = v / U0 = 0.35$ for pure sway, $r' = r\ Lpp / U_0 = 0.70$ for pure yaw and -0.35, 0.20 and -0.20, 0.40 for two sway-yaw tests, respectively.

Fig. 4a. Forces and yaw moment during one period of a virtual pure sway

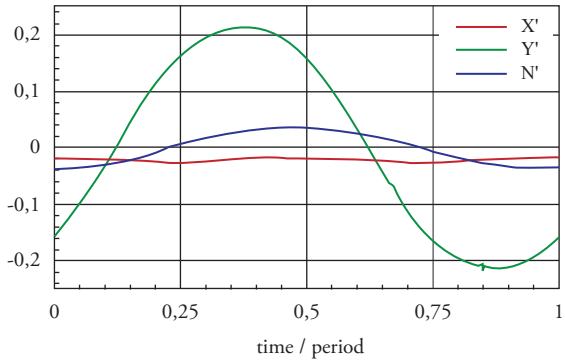

Fig. 4a. Forces and yaw moment during one period of a virtual pure yaw test

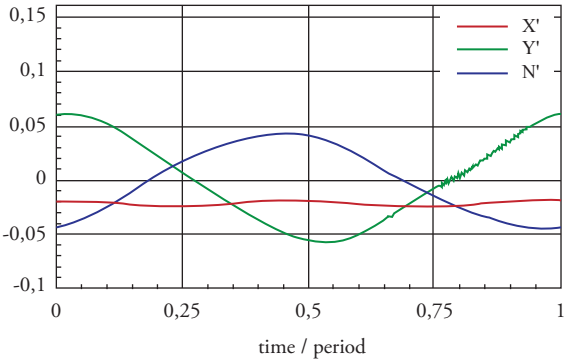

The simulations were carried out for the tanker model (scale 1:45.7) at a speed of 1.179 m/s, instead of for the full scale. The time step chosen for the RANS simulation corresponded to 1/2500 of the motion period in all cases.

The hydrodynamic forces and moments acting on the ship are obtained by integrating the pressure and shear stresses on the hull and appendages. The predicted time histories over one period of the simulated pure sway and pure yaw tests can be seen in Fig. 4. The longitudinal force *X'*, side force *Y'* and yaw moment *N'* have been made non-dimensional with water density, ship speed, length, and draught. Rudder angle, depending manoeuvring derivatives, can be determined by computing rudder angle tests at several drift angles and yaw rates resulting in a total of 42 cases.

Fig. 5. Snapshot of the velocity field behind the propeller

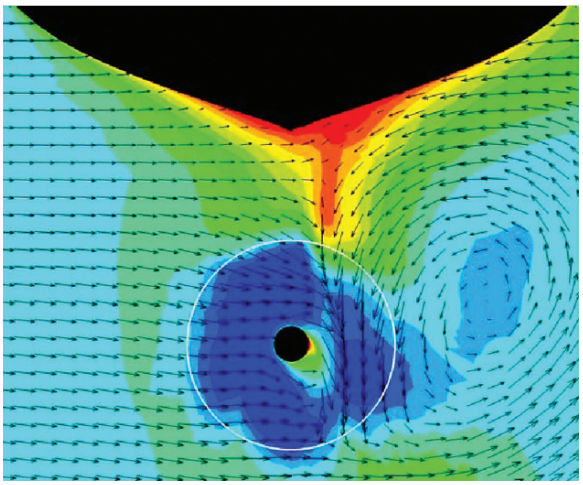

Fig. 6. Stern arrangement of the virtual ship model and during a simulated sway-yaw test computed pressure on the rudder deflected 35°

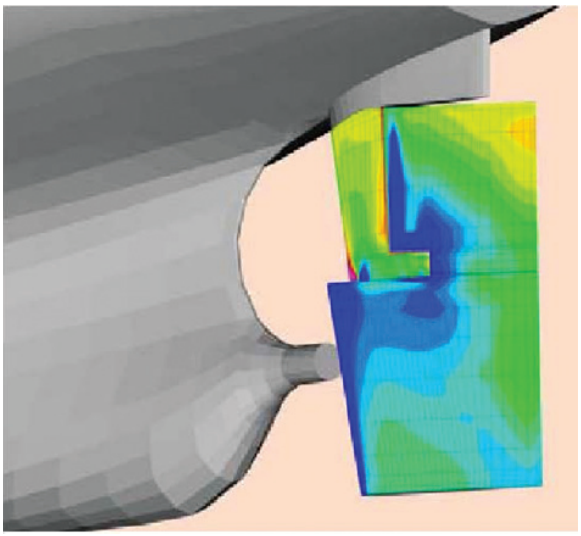

Fig. 6 shows the stern arrangement of the virtual model of KVLCC1 with the rudder deflected 35° to starboard. The pressure field on the rudder computed for steady straight ahead motion is influenced by the effect of the propeller, rotating to the right over the top. Negative pressure regions are depicted in blue, while positive pressure regions are in red.

Fig. 7a. Computed non-dimensional side force and yaw moment during rudder angle test at drift angle -10°, 0°, 10° and 20°

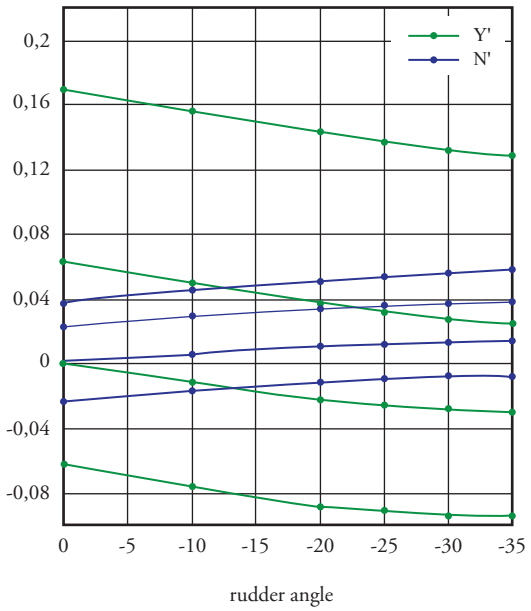

Fig. 7b. Computed non-dimensional side force and yaw rate -0,25, 0, 0,25 and 0,50

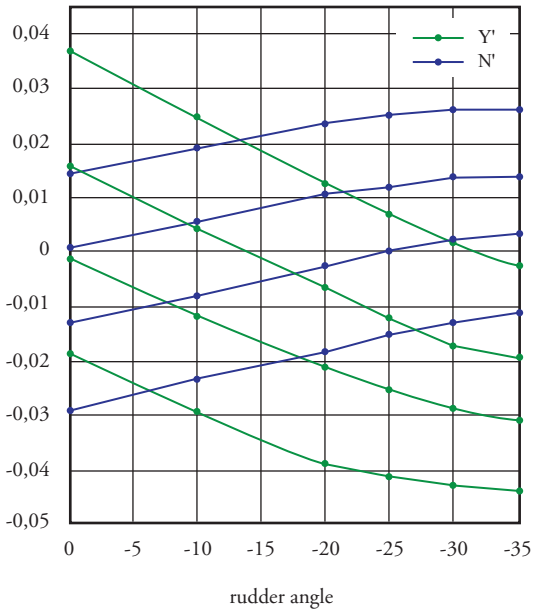

The computed non-dimensional side force and yaw moment acting on the hull for all static cases are summarised in Fig. 7 for oblique towing and steady turning conditions, respectively.

The time histories of the forces obtained from the RANS simulations for the five dynamic tests described above are used to determine the coefficients of the mathematical model in the same way as if PMM tests would have been done. This yields the coefficients in rows 4-18 of Table 2.

Regression analysis of the data obtained from static cases with deflected rudder yields the coefficients depending on the rudder angle written in rows 1-3 and 19-23 in Table 2.

The hydrodynamic coefficients shown in Table 2 have been made non-dimensional with water density, ship speed and length and multiplied by 1000, and are used to simulate standard rudder manoeuvres according to IMO (2002). For this purpose, the motion equations of the ship in four degrees of freedom (4 DOF) were used. However, the dependency of the non-dimensional magnitudes *X', Y', N'*, and roll moment *K'* (not shown) on heel angle and roll rate was neglected because no significant roll motion was expected for the considered tanker. The sub-indices *u, v, r* and δ denote the surge, sway, and yaw velocities and the rudder angle, respectively.

The main results of the simulated 10°/10° zigzag test starting at starboard are compared with experimental results in Fig. 8, which shows on the left side the heading angle, ψ, and the rudder angle, δ, versus time. The 2nd overshoot angle predicted for KVLCC1 is slightly larger than that measured and the overall agreement deteriorates with increasing time. Nonetheless, the characteristic parameters used to judge yaw checking and initial turning ability are predicted well, Table 3.

Any other rudder manoeuvre of interest can be predicted, as well. For instance, the result of a simulated turning circle to starboard with a rudder angle of 35° is compared with a free-model test in Fig. 8b. The main parameters of the turning circle tests are compared with experiments in Table 3 showing good agreement. Note that the tanker fulfils the IMO recommendations with margin.

Table 2. Manoeuvring Derivatives

0	X'_0	0	Y'_0	0	N'_0	0
1	X'_{δ}	0	Y'_{δ}	4,44	N'_{δ}	-2,06
2	$X'_{\delta\delta}$	-2,09	$Y'_{\delta\delta}$	-0,24	$N'_{\delta\delta}$	0,16
3	$X'_{\delta\delta\delta}$	0	$Y'_{\delta\delta\delta}$	-2,95	$N'_{\delta\delta\delta}$	1,38
4	X'_{u}	-2,20	Y'_{u}		N'_{u}	
5	X'_{uu}	1,50	Y'_{uu}		N'_{uu}	
6	$X'_{\mu uuu}$	0	$Y'_{\mu uuu}$		$N'_{\mu uu}$	
7	X'_{u}	-1,47	Y'_{u}		N'_{u}	
8	X'_{v}	0,11	Y'_{v}	-24,1	N'_{v}	-7,94
9	X'_{vv}	2,74	Y'_{vv}	2,23	N'_{vv}	-1,15
10	X'_{vvv}	0	Y'_{vvv}	-74,7	N'_{vvv}	2,79
11	X'_{v}		Y'_{v}	-16,4	N'_{v}	-0,47
12	X'_{r}	-0,07	Y'_{r}	4,24	N'_{r}	-3,32
13	X'_{rr}	0,58	Y'_{rr}	0,56	N'_{rr}	-0,27
14	X'_{rrr}	0	Y'_{rrr}	2,58	N'_{rrr}	-1,25
15	X'_{r}		Y'_{r}	-0,46	N'_{r}	-0,75
16	X'_{vr}	13,1	Y'_{vr}		N'_{vr}	
17	X'_{vrr}		Y'_{vrr}	-40,3	N'_{vrr}	8,08
18	X'_{vvr}		Y'_{vvr}	-9,90	N'_{vvr}	-3,37
19	$X'_{u\delta}$		$Y'_{u\delta}$	-4,56	$N'_{u\delta}$	2,32
20	$X'_{v\delta\delta}$		$Y'_{v\delta\delta}$	5,15	$N'_{v\delta\delta}$	-1,17
21	$X'_{vv\delta}$		$Y'_{vv\delta}$	7,40	$N'_{vv\delta}$	-3,41
22	$X'_{r\delta\delta}$		$Y'_{r\delta\delta}$	-0,51	$N'_{r\delta\delta}$	-0,58
23	$X'_{rr\delta}$		$Y'_{rr\delta}$	-0,98	$N'_{rr\delta}$	0,43

A detailed comparison of all results obtained with this method and with several other methods for manoeuvring prediction from other authors with experimental data is documented in the proceedings from the SIMMAN 2008 Workshop (Stern and Agdrup 2009). As can be seen, there the results of the present pure CFD-based method belong to the best results in the case considered.

Table 3. Characteristic parameters of 10°/10° test (left) and turning circle test (right)

10°/ 10°	SIM	EXP
time to attain	67 s	69 s
$x_{90°}$	1,66 L_{pp}	1,73 L_{pp}
α_{01}[°]	8,1°	8,2°
α_{02}[°]	21,4°	19,4°
r_{max}	0,42°/s	0,40°/s

10°/ 10°	SIM	EXP
$x_{90°} / L_{pp}$	3,10	3,03
$y_{180°} / L_{pp}$	3,13	3,25
$\varnothing_{st} / L_{pp}$	2,58	2,44
V_{st} / V_o	0,39	0,37
r_{st} [°/s]	0,43	0,42

Fig 8a. Characteristic parameters of 10°/10° test

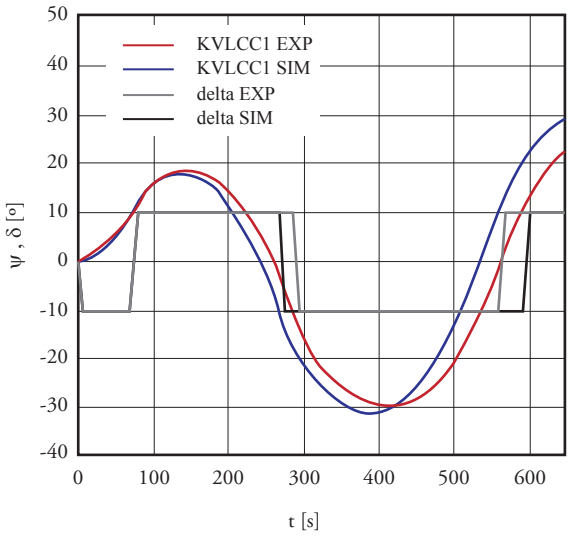

Fig 8b. Characteristic parameters of turning circle test

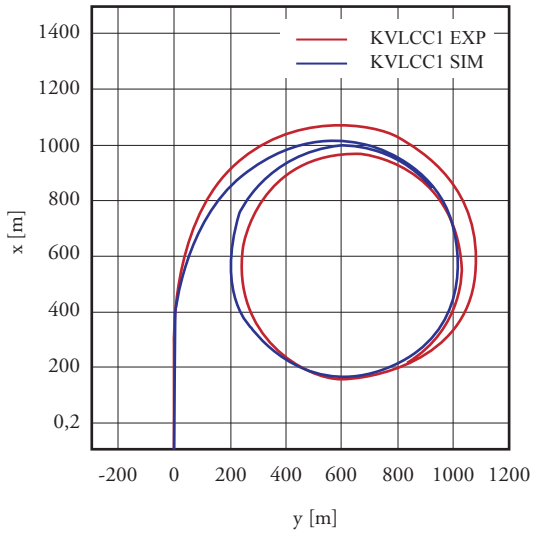

References

ABKOWITZ, M.A., (1964), *"Lectures on Ship Hydrodynamics - Steering and Manoeuvrability"*, HyA Report HY-5, Copenhagen.

CARRICA, P.M., ISMAIL, F., HYMAN, M., BHUSHAN, S., AND STERN, F. (2008), *"Turn and zigzag manoeuvres of a surface combatant using a URANS approach with dynamic overset grids"*, SIMMAN 2008, Copenhagen Cura Hochbaum, A. and Vogt, M. (2002), "Towards the Simulation of Seakeeping and Manoeuvring based on the Computation of the Free Surface Viscous Ship Flow", 24th ONR Symposium on Naval Hydrodynamics, Fukuoka.

CURA HOCHBAUM, A. (2006), *"Virtual PMM Tests for Manoeuvring Prediction"*, 26th ONR Symposium on Naval Hydrodynamics, Rome.

CURA HOCHBAUM, A., VOGT, M., GATCHELL, S. (2008), *"Manoeuvring prediction for two tankers based on RANS calculations"*, SIMMAN 2008, Copenhagen.

IMO, International Maritime Organization, (2002), Resolution MSC.137(76), *"Standards for Ship Manoeuvrability"*, London.

FERZIGER, J.H., PERIC, M. (2002), *"Computational Methods for Fluid Dynamics"*, Springer.

HIRT, C.W., AND NICHOLS, B.D. (1981), *"Volume of Fluid (VOF) Method for the Dynamics of free Boundaries"*, J. of Comp. Physics, Vol.39.

LAUNDER, B.E., AND SPALDING, D.B. (1974), *"The numerical computation of turbulent flows"*, Comput. Meth. in Appl. Mech. Eng. Vol.3.

MENTER, F.R. (1994), *"Two-Equation Eddy-Viscosity Turbulence Models for Engineering Applications"*, AIAA Journal, Vol.32, No.8.

OSHER, S., AND SETHIAN, J.A. (1988), *"Fronts Propagating with Curvature-Dependent Speed: Algorithms Based on Hamilton-Jacobi Formulations"*, J. of Comp. Physics, Vol.79.

STERN, F. AND AGDRUP, K. (editors) (2009), *"Proceedings of the Workshop on Verification and Validation of Ship Manoeuvring Simulation Methods SIMMAN 2008",* FORCE Technology, Lyngby, Denmark

THOMPSON, J.F., WARSI, Z.U.A., MASTIN, C.W. (1985), *"Numerical Grid Generation: Foundations and Applications"*, North Holland, New York Wilcox, D.C. (1993), "Turbulence Modeling for CFD", DCW Industries, La Cañada, California

Using anthropometrics in designing for enhanced crew performance

Utilización de antropometría en el diseño para mejorar el desempeño de la tripulación

J.M. Ross [1]

Abstract

Today's naval ship or craft designer routinely uses the principles of human factors (ergonomics) as a way to help enhance crew performance. But even though many aspects of human factors are well known, certain important categories often remain underutilized. One of these categories is anthropometrics, the study of human body dimensions and capabilities. Anthropometrics analyzes age, gender, and other data within populations of people, such as the general population of a nation or the special population of that nation's active duty naval personnel. For the naval designer, anthropometrics helps to ensure adequate ergonomic design for the population from which the crew is drawn. The naval designer can address in a quantifiable manner issues such as lines of sight, console height and valve handle accessibility. When anthropometric principles are thus applied, the ship better fits the capabilities and limitations of the crew, resulting in enhanced crew performance.

Key words: Human factors, ergonomy, anthropometrics, ship design, performance.

Resumen

El diseñador actual de buques navales o embarcaciones rutinariamente utiliza los principios de los factores humanos (ergonomía) como una manera para mejorar el desempeño de la tripulación. Pero, aunque muchos aspectos de los factores humanos son bien conocidos, ciertas categorías importantes a menudo permanecen subutilizadas. Una de estas categorías es la antropometría, el estudio de las dimensiones y capacidades del cuerpo humano. La antropometría analiza la edad, sexo y otros datos dentro de poblaciones de personas, como la población general de una nación o la población especial del personal naval en servicio activo de esa nación. Para el diseñador naval, la antropometría ayuda a asegurar el diseño ergonómico adecuado para la población de donde se obtiene la tripulación. El diseñador naval puede abordar confiablemente asuntos como linea de visión, altura de consola y accesibilidad de agarraderas de válvulas. Cuando los principios de la antropometría se aplican de esta manera, el buque encaja mejor con las capacidades y limitaciones de la tripulación, con el resultado del desempeño mejorado de la tripulación.

Palabras claves: Factores humanos, ergonomía, antropometría, diseño de buques, rendimiento.

Date Received: February 2nd, 2011 - *Fecha de recepción: 2 de Febrero de 2011*
Date Accepted: February 22th, 2011 - *Fecha de aceptación: 22 de Febrero de 2011*

[1] High Ground Initiatives LLC Telephone: 443-534-5671; E-mail: jonathan@highgroundinitiatives.com; www.highgroundinitiatives.com

Introduction

Often overlooked within the categories and subcategories of human factors (or ergonomics) is the topic of anthropometrics. Anthropometrics or anthropometry is derived from the Greek words anthropos (man) and metron (measure), and it is "the study and measurement of human body dimensions" (*Wickens, 2003*). Anthropometrics may also be defined as the science of dealing with measurement of the human body to determine differences in individuals, groups, etc. (*Panero, 1979*). Included are measurements of body weight and strength, as well as dimensions of various distances with regard to the body and the floor on which individuals are standing, or the seat on which they are sitting.

Anthropometrics is considered by many to be a vague subcategory of ergonomics, and receives only a fraction of the attention paid to topics such as motion sickness, fatigue, and airborne noise. However, the naval designer can benefit from knowing more about this specialized area; ship designing with anthropometrics in mind can substantially improve crew performance, not to mention safety and comfort.

This paper describes the importance of anthropometrics in designing for enhanced crew performance; discusses types, content, and examples of anthropometric data available to the designer; summarizes techniques for data selection and analysis; and presents a process and suggestions for using anthropometry in ship design.

The importance of Anthropometrics

Anthropometrics is a key ingredient in design, from furniture to underground mines to naval vessels (*Lossa, 2010; Hughes, 2006; Schute, 2003*). In particular, a working knowledge of anthropometry is essential to the successful design of a marine vehicle. This is especially true with regard to the placement of instrumentation and controls, accessibility for maintenance, visibility through bridge windows and clearance for safe and efficient movement about the vehicle. Poor anthropometric design can result in people bumping into overhead structures, not being able to easily reach controls, and not having visual contact with critical instrumentation. Examples of inappropriate anthropometric design include the following:

- Inability of Korean crew personnel to reach valve handles in the engine room of a Swedish-design container ship.
- Inability of US Navy personnel to access equipment for maintenance in a newly built auxiliary ship.
- Insufficient clearance between truck accelerator and brake pedals in utility trucks, resulting in unintended acceleration for drivers wearing large boot or shoe sizes (*Freier, 2010*).
- Computer keyboards that are too large and require too much key force for most users (*Hwang, 2010*).
- Undersized seat widths and personnel weight capacities of survival craft on oil rigs in the Gulf of Mexico (too small for present-day offshore workers) (BMT 2007, MMS 2001).
- Difficulty of Korean soldiers in operating US Army standard weapons, in particular the M-1 rifle (e.g., grasping the stock, reaching the trigger and sighting) (*Hart, 1967*).

There is an important distinction between anthropometrics and body mechanics. Anthropometrics makes distinctions among body variables of different populations, while body mechanics addresses practices common to any human. Examples of good body mechanics include the following (*Greenwich, ABS 2003*):

- Maintain a balanced, comfortable and aligned position.
- Sit in firm, straight chairs with arm rests; avoid low chairs.
- Arrange displays for easy reading.
- Place controls and actuators (e.g., valve handles) within easy reach (preferably above hip level and below shoulder level) and manipulation.
- Avoid twisting the back.
- Pushing is safer than pulling.
- Lift with the legs, not the back.
- Ensure proper eye height for comfortable viewing (Figure 1).

The same idea exists for ergonomics: common principles exist across the spectrum of humans, but dimensional details often vary from population to population, and indeed, from person to person within a given population. For example, the minimum comfortable distance and preferred angular lines of sight for viewing a console are constant for all humans (Fig. 1), but the height of the viewer's eye when standing or seated will vary among and within populations depending on body variables

The point to remember is that any mechanical design may result in excellent body mechanics or ergonomics for one population, but may fail for another population, sometimes with serious degradation to performance, safety, and comfort.

Fig. 1. Lines of Sight (Based on MoD Std 25-17)

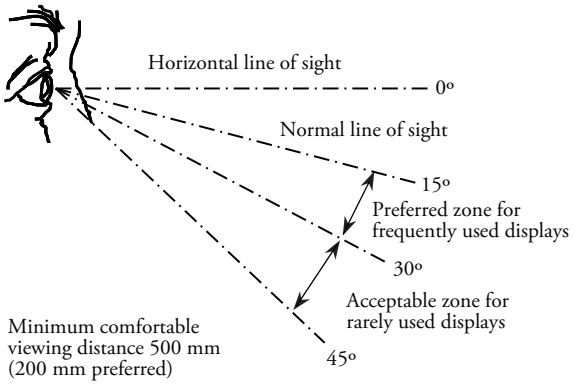

A number of modern design guides take the distinction between ergonomics and anthropometry into account. For example, the American Bureau of Shipping (ABS) notes that its numerical guidelines apply to the population composed of North American males. ABS provides comparative anthropometric data to adapt the guidelines to other populations. ABS recommends that (1) "the height of the lower edge of the front windows of the bridge should allow a forward view over the bow, from which a person seated at the workstations can monitor, navigate and maneuver," and (2) the height not be more than 1,000 mm (39 in) above the deck. The first recommendation applies to all human populations, but provides no specific design parameters. The second recommendation provides specific design guidance for the North American male population (ABS 2003a, 2003 b).

Anthropometric Data

General

Anthropometric data is a collection of measurements or "variables" of a sample set of individuals in a population. A sample set is collected because the population is almost always too large to measure all individuals. In a few cases, such as for Apollo astronauts, all individuals are measured. Variables and examples of data are described in the following paragraphs.

Variables

Anthropometric data has been standardized to a large extent, and variables have been developed that apply to numerous applications, from furniture to space craft. There are still differing definitions, conventions and levels of accuracy. The designer should compare data from different sources with care, as discussed in further detail in a following section. Typical traditional variables by which anthropometric data is characterized include the following (MoD Std 00-25-17):

1. Sitting height
2. Sitting eye height
3. Sitting shoulder ht.
4. Sitting elbow rest ht.
5. Thigh clearance ht.
6. Stool ht/popliteal ht.
7. Functional reach.
8. Vertical functnl reach.
9. Abdominal depth.
10. Knee height.
11. Buttock-popliteal lnth.
12. Buttock-knee lnth.
13. Inter-elbow span.
14. Standing shoulder ht.
15. Waist circumference.
16. Crotch height.
17. Hip breadth.
18. Elbow functional reach.
19. Stature.

20. Standing eye height.
21. Standing elbow height.
22. Bideltoid breadth.
23. Body breadth at elbow.
24. Foot breadth.
25. Foot length.
26. Hand breadth.
27. Hand length.
28. Wrist circumference.
29. Head breadth.
30. Head length.
31. Head ciucumference.
32. Bitragion arc.
33. Tragion to vertex.
34. Pupil to vertex.

The meaning of most of these variables is clear. Several that may not be immediately obvious are:

- Buttock popliteal length is the vertical height of the top of the left knee above the floor in sitting posture, with thigh parallel to the floor and the lower leg perpendicular to the floor.
- Bideltoid breadth is the width of the shoulders at the widest point (clearance at shoulder level).
- Bitragion arc is the distance from the tragion (think "ear" for the purposes of this paper) of one ear vertically overhead to the tragion of the other ear.
- Triagion to vertex is the vertical distance from the top of the head to the left tragion.
- Pupil to vertex is the vertical distance from the eyes to the top of the head.

Examples of Data

Significant amounts of anthropometric data exist, particularly for military personnel, both male and female. Example data is presented in Table 1 for males serving in US general military forces (MIL-HDBK-759C 1998). Table 2 presents data for the US general population.

Table 3 presents height data for ten international regions of the world.

Following convention, this data is summarized and presented in percentiles. The data is usually (not shown here) augmented with statistical measures that indicate the validity and spread of the data, as well as the size of the population of people from which the data was gathered. "5th percentile" indicates that for a given parameter (e.g., weight), 5% of the population has a lower value, and the remaining 95% have a greater value. "95th percentile" indicates that 95% of the population is below the value and only 5% are above the value.

Table 1. Example Percentile Values for US General Forces – Males (MIL-HDBK-759C 1998)

	5th	95th
Weight, kg	61.6	98.1
Overall Height, cm	164.5	187.1
Eye Height (Standing, cm)	152.8	174.3
Shoulder Height, cm	134.2	154.6
Vert. Arm Reach, Sitting, cm	128.6	153.2
Eye Height Sitting, Erect, cm	72.9	85.2
Hip Breadth, Sitting, cm	31.1	41.3

Table 2. Data for US General Population (Mean for Males 20 Years and Over)

	5th	95th
Weight, kg	62.2	122.6
Overall Height, cm	163.6	188.7

The following paragraphs describe representative sources of data.

CAESAR (Civilian American and European Surface Anthropometry Resource) is a survey of 40 traditional anthropometric measurements and 3-dimenisonal body scans of people in the US, Italy, and the Netherlands. A partnership of government and industry (e.g., apparel, aerospace, and automotive) developed the data base of 2,400 US and Canadian, as well as 2,000 European civilians. Data was gathered from 1998 to 2000. Subjects were male and female, aged 18-65 and representative of various weights, ethnicities, geographical regions, and socio-economic status. The data is presented in English and metric units

Table 3. 50th Percentile Height Data (cm) for Ten International Regions (Estrada 1995, ABS 2003 b)

Region	Male	Female
Sri Lanka	163.9	152.3
Colombian Workers	168.6	155.6
Japan	168.7	155.7
China	169.0	155.4
France	171.9	160.4
Germany	173.3	161.9
Sweden	174.0	164.0
UK	175.5	162.0
US	176.0	162.6
Netherlands	179.5	165.0

and includes the following (SAE 2010):

- 40 traditional 1D measurements carried out with tape measure or calliper.
- 3D scans of subjects' body surfaces in three poses (standing, relaxed seating, and coverage), with 100 landmarks placed on each subject.
- Extracted 1D measurements, using 3D scanning landmarks in the standing and relaxed seating positions.

NHANES (National Health Examination Survey) is a US Centers for Disease Control and Prevention program to assess the health and nutritional status of people in the US. The program began in the 1960s and examines a nationally representative sample of about 5,000 people annually. The latest data (2007-2008) includes 10 body measurements, nine of which are applied to adults. Of most interest to naval design are recumbent length, standing height, upper arm length, upper leg length, waist circumference and weight (NHANES 2007, 2009).

ANSUR is the name of an anthropometric survey of US Army personnel conducted in the 1980s (Gordon 1988) and documented in a 1988 database. The data may also be referred to as "NATICK" because the survey was conducted by the US Army Natick Soldier Research, Development & Engineering Center (NSRDEC). ANSUR data was used as the basis for anthropometric tables presented in MIL-HDBK 759.

ANSUR II involves the conduct of a new survey and development of new models, including digital models of humans. The purpose of the work is to assist in the design of working environments, clothing, and equipment. Included in the population will be Active Duty, National Guard, and Reserve personnel components. The Army goals are to (NSRDEC 2010):

- Produce valid anthropometric criteria for sizing and ordering equipment and materials.
- Reduce human factors risk in fast-track procurements.
- Improve operational readiness by integrating equipment and material requirements among Army components.
- Obtain 3D modeling capabilities for designing body armor.

American Bureau of Shipping "Guidance Notes for the Application of Ergonomics to Marine Systems" (ABS 2003) provides anthropometric data for the US and numerous other nations throughout the world. Much of the guidance on size and strength characteristics is based on a population of North American males.

International data is provided as well, and was derived from two sources:

- ILO 1990, which ABS notes is from data gathered in the mid-1960s. ABS states that certain Asian populations now have increased height, and recommends multiplying the length measurements by 1.02.
- ADULTDATA 1998, with data on people from selected Northern Europe nations.

The Universidad de Antioquia's "Investigación Nacional, Parámetros Antropometricos de la Población Laboral Colombiana," (National Investigation of Anthropometric Parameters of the Colombian Worker Population – 1995) provides data on weight, height, and of 70 other variables for male and female adults grouped by five age ranges and by percentiles, with a statistical analysis of the

data for each variable. "Worker" in this context included farm, factory, service, and office workers (Estrada 1995).

"Human Factors for Designers of Systems: Personnel Domain - Technical Guidance and Data," (MoD Std 0025-17) presents anthropometric data gathered between 1970 and 1995 on service personnel. The most recent data was gathered in 1990 and is considered by the Ministry of Defense (MoD) to be the most representative of present members of Royal Navy as well as Royal Army and Royal Air Force personnel. Thirty four variables are presented for male and female subjects. Range of movement and force data are included.

National Aeronautics and Space Administration (NASA) Human factors documents (NASA 1995, 2010b) provide example data for anthropometry, biomechanics (e.g., reach and grasp limits) and strength. Populations are 95th percentile US male and 5th percentile Asian Japanese female for the year 2000. This data is representative of the largest and smallest sizes of personnel who may crew or visit a space vehicle; NASA recognizes that actual crew and visitors may be outside this range.

Data selection and analysis

General

Anthropometric data is statistically analyzed to determine trends and to check that sufficient data has been gathered to validly represent the entire population. When the data is accepted as statistically appropriate, it may be used for design purposes. Using the data is straight forward for single variable design problems, such as ensuring that a valve handle can be reached by 95% of the population. However, when multiple variables are involved, such as in the design of a workstation, the design process is more complex, requiring special methods.

Mathematical Considerations

Anthropometric data is analyzed statistically to calculate distribution, standard deviation, mean, probability and similar metrics. The designer uses the results to determine whether the data is sufficient to model the entire population, or if there are gaps or outliers that show additional data is needed. The designer also uses the results to determine the maximum and minimum for the magnitudes of variables based on percentile. Fig. 2 shows a normal distribution of data, the 5th and 95th percentiles, and the quantity of the population contained within the entire data set (100%) and between the 5th and 95th percentiles (90%).

Fig. 2. Normal Distribution and Percentiles (ABS 2003 b)

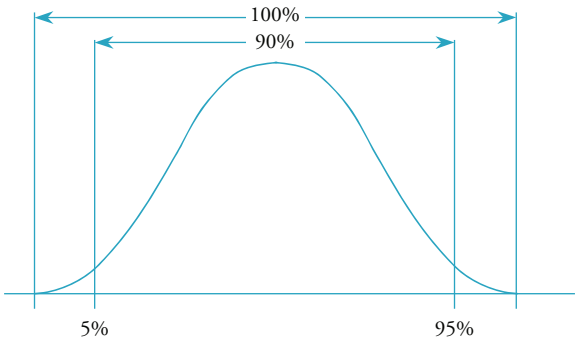

Variables (e.g., height) from two or more normal distributions can be combined to produce a single lumped distribution. However, the user must be aware of pitfalls, such as the need for iterative calculations to determine percentiles (*Nadadur, 2009; Pheasant, 2006*).

Selecting a data range

When using anthropometric data, the range of percentiles must be specified. For example the designer may choose to size a human-system interface to meet the dimensional needs of 90% (that is, the population between the 5th and 95th percentiles) of the military population.

In practice, larger people may be able to squeeze into tight spots, and smaller people may be able to reach a bit further than their comfort zone, but the idea is that data within specified percentiles provides the designer with a realistic dimensional framework. For US General Forces (males only, Table 1) within a range between the 5th and 95th

percentiles, the designer would use 61.6 kg as a minimum and 98.1kg as a maximum for weight. The minimum weight would be lowered at the 5th percentile end if females are included (MIL-HDBK-759C 1998).

Whether to use a 5th or 95th percentile or an inclusive range depends upon the design situation. For example, when designing for maintenance access behind installed equipment, the shoulder width of the 95th (larger size) percentile should be used. This ensures that only a small 5% of the population will have possible problems with access. On the other hand, when designing the location for a valve, reach can be important, and the designer will use a 5th (smaller size) dimension. As a result, all but 5 percent of the population can easily reach the valve (*Panero, 1979*).

Note that this approach results in an imperfect accommodation of the remaining 5%. For critical applications (e.g., emergency breathing apparatus) and for screened populations with specified anthropometric characteristics (e.g., helicopter pilot maximum height), the designer must accommodate 100% of the population.

Table 4 compares 5th percentile male data from US general forces, Army pilots (1966), US Air Force (1967) pilot officers (MIL-HDBK-759C 1998), and the UK Royal Navy (1990)(Mod Std 00-25-17). Note that the Royal Navy data is the most recent and are the only data applicable directly to marine vehicles. Sitting dimensions are measured from the top of flat, uncushioned benches on which subjects are seated.

Factors of Variability

Populations vary significantly. For example, the smallest male population is made up of the Pigmies of Central Africa, with a mean height of 143.8 cm (56.6 in), while the tallest, in the Sudan to the north of Africa, have a mean height of 182.9 cm (72 in) (*Panero, 1979*). Thus, the Sudanese are 27 percent taller than the Pigmies. A naval designer would certainly want to take this sort of difference into account when addressing critical dimensions in a ship or craft design. While such a large range is not found when comparing other populations, the variability can still be important and should be considered.

Variations may be categorized in the following way *(Panera, 1979; ABS, 2003b; NASA, 2010*):

- National origin.
- Age.
- Socioeconomic factors.
- Gender.
- Clothing.
- Posture.

In addition to the above variations, given populations such as "the general population of the US" will change over a period of time. An example is the increase in obesity (defined as the body mass index above 30) of the US general population from 13.4 % in 1960-1962 to 34.3% in 2007-2008 (*Flegal, 2010; Ogden, 2010*). Another example is the change in height, as shown graphically in Fig. 3.

Fig. 3. Change in Height over Time for US Males and Females (Ogden, 2004)

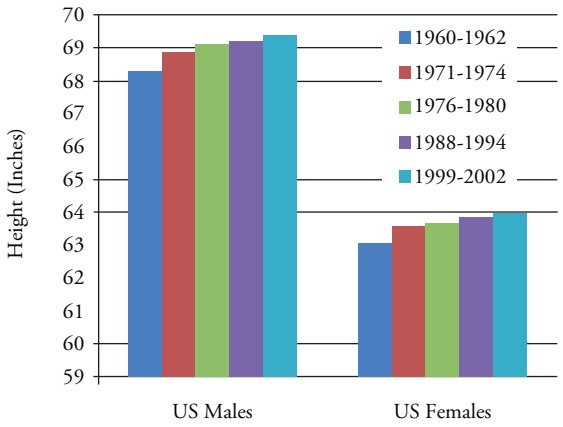

The Multivariant Challenge

Single and Multi-Variant Analyses

The traditional approach to analyzing and using anthropometric data is through 1D physical measurements. Indeed, a single variable is sufficient in certain contexts, such as a minimum clearance between deck and overhead, or a maximum allowable weight. However, the designer soon finds that more than one variable may be involved, such as height and width for a door opening. In these

cases, the designer needs to employ a "multivariant" analysis.

Table 4. Comparison of 5th Percentile Values Among Different Male Populations (MIL-HDBK-759C 1998 and MoD Std 00-25-17)

Variable	Population			
	US General Forces	US Army Pilots	US Air Force Pilots	UK Royal Navy
Weight, kg (lb)	61.6 (135.8)	64.5 (142.2)	63.6 (140.2)	(No Data)
Overall Height, cm (in)	164.5 (64.8)	165.9 (65.3)	167.2 (65.8)	166.0
Eye Height (Standing)	152.8 (60.2)	153.7 (60.5)	(No Data)	(No Data)
Shoulder Height	134.2 (52.8)	135.7 (53.4)	135.7 (53.4)	(No Data)
Vertical Arm Reach, Sitting	128.6 (50.6)	135.0 (53.1)	(No Data)	127.7
Sitting Height, Erect	85.2 (33.5)	87.1 (34.3)	88.1 (34.7)	87.1
Sitting Height, Relaxed	(No Data)	(No Data)	(No Data)	(No Data)
Eye Height Sitting, Erect	72.9 (28.7)	75.3 (29.6)	76.2 (30.0)	77.8
Shoulder Height, Sitting	54.9 (21.6)	56.4 (22.2)	56.5 (22.2)	62.0
Shoulder Breadth	41.8 (16.5)	46.0 (18.1)	44.1 (17.4)	43.8
Hip Breadth, Sitting	31.1 (12.2)	33.8 (13.3)	34.2 (13.5)	33.7
Foot Length	24.6 (9.7)	25.0 (9.8)	25.1 (9.9)	24.5
Foot Breadth	9.0 (3.5)	9.2 (3.6)	9.0 (3.5)	8.8

At first examination, carrying out a multivariant analysis may appear straight forward. Sometimes that is the case, because certain variables are statistically correlated. For example, stature, chest circumference and waist circumference are correlated and can be combined to develop specifications for clothing. In general, a high degree of correlation exists between height variables (waist height, crotch height, and sitting height) and arm and leg lengths. Thus, combining two or more variables can be valid (MIL-HDBK-759C). But the situation soon becomes more complex, because strong correlations do not exist between all variables. For example, there is only a weak correlation between height and strength.

The Average Person

The naval designer may be tempted to choose the 50th percentile anthropometric characteristics as the basis for an "average person model." This approach is not valid, and has been named the "average person fallacy," because different people vary in different ways; there is no average person. Also, percentiles are not additive. As shown by Robinette (1982) the sum of 5th percentile parts making up the height variable does not equal the 5th percentile height in a population.

Dr. H.T.E. Hertzberg states that men who are average in two variables are found in only seven percent of the population; those who are average in four variables are found in three percent of the population. There are no men who are average in ten variables (as reported in Penero 1979, MIL-HDBK-759C).

Consider the design challenge of a multi-dimensional work area, such as a cramped control station in a shipboard crane. All of the following variables may be important:

1. Sitting height.
2. Buttock-knee length.
3. Buttock-heel length.
4. Functional reach.
5. Sitting knee height.
6. Bideltoid breadth.

In this example, the designer may use anthropometric data from the UK Royal Navy and may want to design the work area to fit everyone from the 3rd to the 97th percentiles. For just one variable (e.g., "sitting height"), the goal is met: the work area can be designed to fit all individuals between the 3rd and the 97th percentiles. But if the work area must *simultaneously* fit the 3rd to 97th percentile individuals from both of the first two variables, then fewer individuals are included. The reason is that there is not a perfect overlap between the individuals within the 3rd to 97th percentiles for "sitting height" and those individuals within the 3rd to 97th percentiles for "buttock-knee length." As more variables are added, the work area fits fewer individuals. Only 78% of the population will fall within all six of the above "3rd to 97th percentile" variables (MoD Std 00-25-17).

One general anthropometric design approach considers three design solutions (NASA 2010):

- Single solution for all members of a population. This may be practical in cases where the population consists of screened individuals who meet specified dimensions, such as with helicopter pilot maximum height.
- Adjustment of equipment increases the range of accommodation. For example, height is a common adjustment for seats, where the lowest adjustment may be for the 5th percentile female popliteal height, and the highest adjustment for the 95th percentile male popliteal height.
- Several solutions are available and the user chooses the one that best fits their dimensions, such as with clothing sizes.

A similar approach uses the following four design principles (*ABS 2003b*):

- Design for the average - application is for nonadjustable situations such as work stations and desks
- Design for the range application is for adjustable situations, such as seating. Generally, the design will accommodate the middle 90% of the population.
- Design for the largest - applications are mostly for clearances (e.g., hatches and walkways). Generally, the design goal is to accommodate 95% of the population.
- Design for the smallest - applications are mainly for strength (e.g., pull, push) and reach distances. Usually the reach and strength of the 5th percentile person is used as the design criterion.

Fig. 4 relates the magnitudes of these four principles to percentiles in a normal distribution.

Fig. 4. Change in Height over Time for US Males and Females (Ogden, 2004)

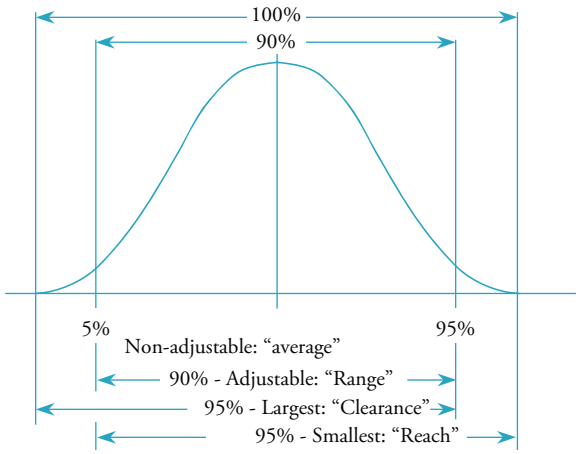

Digital Mannequins

Human Digital Modeling (HDM) tools simulate humans by means of 3D electronic models. These tools combine computer-aided modeling with anthropometric data, and for some years have been used effectively within industry and government. Mannequins, based on anthropometric data, are placed within CAD models and exercised to develop and refine the human-machine dimensional and strength interface. To effectively address the multivariant challenge, a family of mannequins is produced through a statistical method and exercised for a given design (e.g., 5th percentile female and 95th percentile male).

The Ford Motor Company developed a set of three male (5th, 50th, and 95th percentile) and three female

(5th, 50th, and 95th percentile) electronic models based on a Ford assembly worker population synthesized from NHANES and ANSUR data. The models were exercised in conjunction with automobile manufacturing processes, ensuring, for example, that the SDAR antenna could be mounted by a 5th percentile female worker (*Nadadur, 2009*).

NASA is active in the development of digital mannequins, using a set of "worst case" mannequins to form dimensional limits. Another solution that NASA uses to solve the multivariant challenge is to design space suits with standard size modular pieces (arms, legs, upper torso, etc.). These suits accommodate a wide range of operators and passengers and replace the expensive tailored space suits of the Apollo era. (*Thaxton, 2007*).

Since 1986, the German company Human Solutions has developed the RAMSIS mannequin, originally for automotive design, with emphasis on driver comfort and posture. The company has applications tailored to industrial vehicles and aircraft, and is presently entering the submarine design arena (Fig. 5). The mannequins are based on anthropometric data appropriate for each field of application (Heiner, Human Solutions 2010, van der Meulen 2007).

Fig. 5. Human Solutions' Mannekin RAMSIS for Use in Designing Submarine Interior (Human Solutions 2010)

Digital Mannequins

As made clear in the preceding sections, the field of anthropometrics is complex. Fortunately, a number of organizations (e.g., ABS, NASA, UK Royal Navy) have applied the principles of ergonomics, including anthropometrics, by using a known population and known variables, and have developed standards for sizes and clearances for numerous conditions directly related to ship design. These standards are already met by much existing commercial marine equipment, workstations, controls, and other instances of shipboard human-machine interfaces. In addition, most designers are familiar with these standards.

The challenge arises when the population that will operate and maintain a ship is significantly different anthropometrically from the population upon which numerical standards have been based. Often, this challenge does not arise at all. Most commonly, the challenge arises only for certain key factors, such as reach distance. Typically, mismatches are found when an existing design is exactly duplicated for a new population.

In general, the design process consists of nine steps, beginning at the start of a project and ending at the completion of Function Design. The steps are described as follows (diagrammed in Fig. 6):

1. Define the needs, that is, where anthropometrics can effectively improve crew performance. Needs may be driven by new design constraints for the particular ship (e.g., space constraints), or adapting the design to an existing design from another country, or adapting to design specifications based on another population.
2. Determine available resources, including budget, personnel, and schedule availabilities.
3. Gather anthropometric data, whether from a sample of an applicable population (e.g., measuring 1,000 individuals from a population of 10,000), or derived from a more general population (such as "all workers of a particular nation"). Analyze the data for validity and trends.
4. Determine the anthropometric approach, which may be single/multi-variant, coupled with a traditional application or with electronic mannequins. Determine how the anthropometric approach will be integrated with the ship design and with CAD modeling.

5. Develop design principles, which may be based on single solution/adjustment/several solutions, or average/range/largest/smallest, or some combination.
6. Produce the design criteria for use by the designer, through application of the design principles to the applicable ranges of data. Document this in a format that can be applied and monitored effectively. As appropriate, develop a family of electronic mannequins.
7. Conduct the design, from concept through functional.
8. Monitor the design to ensure that the criteria are being properly applied (this is quality assurance), and to detect unforeseen problems.
9. Adjust steps 1-8, adapting to project changes (such as budget and scope) and responding to unforeseen problems.

Fig. 6. Process for Applying Anthropometrics in Design

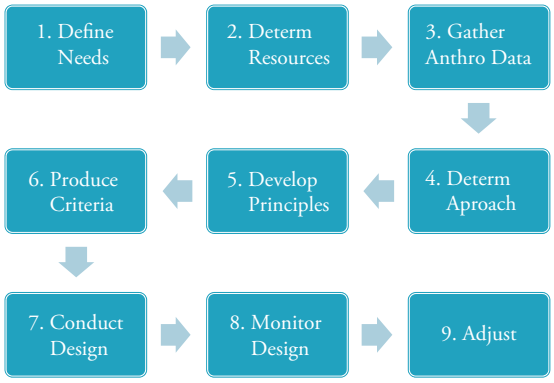

The following sections briefly describe particular suggestions to help maximize the fit of a marine vehicle to a particular user population. The designer applies certain anthropometric principles at increasing levels of detail as the ship design process proceeds. Only basic design phases (concept, preliminary, contract, and functional) are addressed. At their completion, virtually all human factor design, including elements of anthropometrics, will be complete. The stages that follow (transitional design and workstation/zone information preparation) are concerned not with dimensions, but rather with preparing the design for production.

Concept Design

Concept design may also be referred to as the cost and feasibility study phase; the goal is to clarify customer requirements and address the balance between ship capability and cost (Gale 2003). The product of this phase is a concept design that may include anthropometric considerations such as the following (Booher 2003, MIL-HDBK-759C 1998, Todd 2005):

- Define the scope of application of the anthropometric portion of the design to be responsive to owner's requirements, budget, and schedule. The scope may be limited to only a single system, such as bridge control and monitoring, or may be wider and address elements such as personnel clearances throughout the ship.
- Determine which body variables are relevant, such as reach, height, and weight. Table 5 shows typical variables required for the design of an office desk, a berth, and stairs.

Table 5. Using Different Anthropometric Data Depending on the Design Case (Panero, 1979)

Anthropometric Data	Office Desk (Seated)	Berth	Stairs
Stature		•	•
Sitting height erect		•	
Eye height			•
Eye height sitting	•		
Maximum body breadth	•	•	•
Hip breadth	•		
Thigh clearance	•		
Knee height	•		
Popliteal height	•	•	
Buttock-popliteal length	•		
Buttock-knee length	•		

- Determine the crew population and obtain required anthropometric data. If data is not available, define variable limits (e.g., maximum height) based on a more general population from which the crew will likely be drawn (e.g., general population of a country's workers).
- Use caution in applying anthropometric data. Most published data is for military personnel, much of that is up to 40 years old, and it is – at best – a general guide for today's military.
- Use caution in combining two or more variables in a design. For example, a 95th percentile male is not made up of the sum of 95th percentile variables. Rather, a real person may be within 95th percentile in height but 80th percentile in weight.
- Consider the variability of proportions of humans. For example knowing a height and weight is not necessarily sufficient to accurately predict shoulder width.
- Decide whether to design to accommodate all of a given population, such as with most naval marine ships or only a screened population, such as for certain environments where special, bulky clothing must be worn (e.g., very cold climates, special operations) (MIL-HDBK-759C 1998).
- Consider the characteristics of the user population of operators, passengers (e.g., scientists), and maintainers. Operators may be more fit than passengers; naval populations are different than civilian populations. A vehicle designed for a taller population may result in controls placed too high for members of another population to reach. Likewise, clearances sufficient for one population may be insufficient for another.
- As a baseline design guide, consider applicable published ergonomic standards and guidelines, such as minimum and the preferred work space dimensions in ASTM F116-07 (Table 6) and the ABS guides. Check the anthropometric source of the guideline and adjust to the crew population (e.g., ASTM F116 references US military, commercial, and regulatory sources).

Table 6. Mobile Work Space Dimensions (ASTM F116-07)

Work Space	Minimum		Preferred	
	mm	in	mm	in
Passageway				
Two persons passing	914	36	1370	55
Vertical entry hatch				
Square	459	18	560	22
Round	560	22	610	24
Horizontal entry hatch				
Shoulder width	535	21	610	24
Height	380	15	510	20
Crawling space				
Height	785	31	910	36

Preliminary Design

In preliminary design, top-level performance requirements are confirmed, second-tier requirements are developed, ship size and configuration are selected, systems are selected, performance is quantified, cost and technical risk are reduced, and an initial build strategy is developed (*Gale, 2003*). The designer may consider the following:

- Apply anthropometric principles according to the plan developed in the concept design. This may include ensuring maintenance clearance is generally sufficient among various major propulsion equipment components such as engines and generators.
- Employ computer-aided tools, such as *maritime*EXODUS, whose models are used to assess evacuation of personnel from a ship, and considers human behavior characteristics, the presence of fire, and vessel list. The model includes vehicle geometry (e.g., decks, stairs, and bulkheads) and characteristics of personnel (e.g., mobility, age, gender) (*Earl, 2006*).
- Exercise electronic mannequins within the ship CAD model and communicate with other designers when anthropometric limits are exceeded by aspects of the present design.

Contract Design

The contract design effort confirms ship capability and cost, develops information from which a shipyard can make a price bid and establishes criteria for ship owner acceptance of the ship upon completion (*Gale, 2003*). Anthropometric issues include the following:

- Using human subjects in a physical mock-up can help validate anthropometric assumptions (MILHDBK-759C 1998). Members of the actual commissioning crew can provide particularly valuable comments and advice.
- Electronic 3D "walk-through" modeling, especially with electronic mannequins, enables collaboration by designers, maintainers, users, and owners (MILHDBK-759C 1998).
- Specialized computer-aided tools such as the following can assist the naval designer at this stage of design:
  - *Crew Station Design Tool* provides a means to effectively select and arrange controls and instruments in a way that effectively considers human engineering and ergonomics principles (*MA&D, 2006; Walters, 2005*).
  - *Design Support and Evaluation System* is a tool used to help design bridges for new ships and to assess bridges for existing ships. The tool considers numerous factors, including physical layout, work environment, alarms, instrumentation, and controls (*Widdel, 2000*).
  - *Jack* is a modeling tool that simulates an ergonomically accurate human in a design environment (*Siemens, 2008*).

Functional Design

During function design, additional analyses are performed, such as structural and vibration analyses. Further detail is developed for structure and systems. The designer should consider the following:

- Continued use of physical mock-ups with prospective crew members and additional detailed computer analyses; particularly in critical areas of the ship, such as control stations.
- Continued use of an electronic 3D "walk-through" modeling with electronic mannequins for collaboration by designers, maintainers, users, and owners.

Conclusions

Major conclusions are as follows:

- One size does not fit all, whether for shoes or naval marine vehicles
- Applying anthropometric considerations to the design process is practical but can increase costs and time; usually, anthropometrics is needed in only certain instances
- Once determined, anthropometric data may be used for follow-on designs
- Even proven anthropometric data should be reviewed at the beginning of a design to include changes to the population
- The payoff of anthropometrics in design is an improved fit between the operator and the ship, and thus enhanced crew performance.

Acknowledgments

The author gratefully acknowledges the generous support and encouragement of Cotecmar and, particularly, Lt Cdr Angela Liliana Lossa Chamorro, Manager of the Accommodations Department, and Commander Oscar Darío Tascon Muñoz, Director of Research, Development and Innovation.

References

ABS (2003a). "Guidance Notes on Ergonomic Design of Navigation Bridges," American Bureau of Shipping," Houston, TX.

ABS (2003b). "Guidance Notes for the Application of Ergonomics to Marine Systems," American Bureau of Shipping," Houston, TX.

ADULTDATA (1998). "Adultdata, the Handbook of Adult Anthropometric and Strength Measurements – Data for Design Safety," UK

Department of Trade, Nottingham.

ASTM 1166-07, Standard Practice for Human Engineering Design for Marine Systems, Equipment, and Facilities, ASTM International, West Conshohocken, PA.

BMT (2007). "Human Factors Engineering Success Stories in the Oil and Gas Industry," BMT Designers and Planners, January.

Centers for Disease Control and Prevention (2006). National Center for Health Statistics. Data from the National Health and Nutrition, Examination Survey, Figure 13, http://win.niddk.nih.gov/ statistics/ #other (accessed Nov. 2, 2009).

ESTRADA, J., J. CANCHO, M. RESTROPO, C. PARRA (1995), "Investigación Nacional, Parámetros Antropometricos de la Población Laboral Colombiana," ACOPLA95, Universidad de Antioquia, Medellin, Colombia.

FLEGAL, K.M., M.D. CARROLL, C.L. OGDEN, L.R. CURTIN (2010). "Prevalence and Trends in Obesity Among US Adults, 1999-2008," The Journal of the American Medical Association, Vo. 303, No. 3, January.

FREIER, S., P. SEELEY, R. MARKLIN, K. SAGINUS (2010). "Application of Electric Utility Workers' Anthropometry to Clearance Between Vehicle Pedals and Adjacent Structures," 'Proceedings of the Unman Factors and Ergonomics Society 54th Annual Meeting – 2010,' October.

GALE, P.A. (2003). "The Ship Design Process," Chapter 5, Ship Design and Construction, T. Lamb, editor, The Society of Naval Architects and Marine Engineers, Jersey City, NJ.

GORDON, C., T. CHURCHILL, C. CLAUSER, B. BRADTMILLER, J. MCCONVILLE, I. TEBBETTS, R. WALKER (1988). "1988 Anthropometric Survey of U.S. Army Personnel: Methods and Summary Statistics," Technical Report NATICK/TR-89/044.

Greenwich (undated). "Body Mechanics – Patient/ Family Information Sheet," Greenwich Hospital, Greenwich CT, http://www.greenhosp.org/pe_pdf/ pt_bodymech.pdf (downloaded September 2010).

HART, G.L., G.E. ROLAND, R. MALINA (1967). "Anthropometric Survey of the Armed Forces of the Republic of Korea," Technical Report 68-8-PR, US Army Natick Laboratories, Natick, MA.

HEINER, B., F. ENGSTLER, F. FRITZSCHE, C. MERGL, O. SABBAH, P. SCHAEFER, I. ZACHER, (2006), "The Development of RAMSIS in Past and Future as an Example for the Cooperation Between Industry and University," 'International Journal of Human Factors Modelling and Simulation,' Volume 1, No. 1, December.

HUGHES, L.M., W.G. HORN (2006). "A Review and Comparison of Anthropometric Indices Applicable to the US Navy Submariner Population," Naval Submarine Medical Research Laboratory, NSMRL/TR—2006-1249, Groton CT, December.

Human Solutions (2010). http://www.human-solutions.com, downloaded December. Hwang, S., P. Johnson, (2010). "Computer Input Devices – Race and Gender: Is There a Mismatch Between Anthropometry and Input Device Design," 'Proceedings of the Unman Factors and Ergonomics Society 54th Annual Meeting – 2010,' October.

ILO (1990). "International Data on Anthropometry," Occupational Safety and Health Series: No. 65, International Labour Organization, Geneva.

LOSSA, A., G. ORTIZ, D. BAHAMON (2010). "Development of a Model for the Analysis and Evaluation of Ergonomic Risk on Board

Vessels," International Conference on Human Performance at Sea, HPAS 2010, Glasgow, Scotland, June.

MA&D (2006). Alion Science and Technology, Meetings, November.

McDOWELL, M.A., C.D. FRYAR, C.LL. OGDEN, K.M. FLEGAL (2008). "Anthropometric Reference Data for Children and Adults: United States, 2003-2006, 'National Health Statistics Reports,' Number 10, October.

MIL-HDBK-759C (1998). Human Engineering Design Guidelines, U.S. Department of Defense, March.

MMS (2001). "Water Survival Craft," 'MMS Safety Alert,' No. 192 Revised, US Department of the Interior Minerals Management Service Gulf of Mexico OCS Region, January.

MoD Std 00-25-17 (2004). "Human Factors for Designers of Systems: Personnel Domain -Technical Guidance and Data," Defence Standard 00-25 Part 17, Issue 1, UK Ministry of Defence, July.

NADADUR, G., J. CHIANG, M.B. PARKINSON, A. STEPHENS (2009). "Anthropometry for a North American Manufacturing Population," SAE International.

NASA (1995). "Man-Systems Integration Standards," NASA-STD-3000, Revision B, National Aeronautics and Space Administration, Washington, DC, July.

NASA (2010). "Human Integration Design Handbook (HIDH)," NASA/SP-2010-3407, National Aeronautics and Space Administration, Washington, DC.

NHANES (2007), "National Health and Nutrition Examination Survey, 2007-2008 – Overview," National Health and Nutrition Examination Survey, CS106114 (01/2007), T2650

NHANES (2009). "2007-2008 Data Documentation, Codebook, and Frequencies – Body Measurements," National Health and Nutrition Examination Survey, http://www.cdc.gov/nchs/ nhanes/nhanes2007-2008/ BMX_E.htm, September, downloaded October 2010.

NSRDEC (2010). "U.S. Army Anthropometric Models to Optimize the Human Systems Interface (ANSUR II)," US Army Natick Soldier Research, Development & Engineering Center (NSDREC), Natick, MA, http:// nsrdec.natick.army.mil/ media/print/Army_ ANSURII_Trifold2.pdf

OGDEN, C., C. FRYAR, M. CARROLL, K. FLEGAL (2004). "Mean Body Weight, Height, and Body Mass Index, United States – 1960-2002," 'Advance Data,' No. 347, US Department of Health and Human Services, Centers for Disease Control and Prevention, National Center for Health Services, October.

OGDEN, C., M. CARROLL (2010). "Prevalence of Overweight, Obesity, and Extreme Obesity Among Adults: United States, Trends 1976-1980 Through 2007-2008," Centers for Disease Control and Prevention, http://www.cdc.gov/nchs/data/hestat/ obesity_adult_07_08/ obesity_adult_07_08.htm, June.

PANERO, J., M. ZELNIK (1979). Human Dimension & Interior Space, Whitney Library of Design, Watson-Guptill Publications, New York.

PHEASANT, S., C. HASLEGRAVE (2006). Bodyspace: Anthropometry, Ergonomics and the Design of Work (Third ed.). CRC Press.

ROBINETTE, K.M. AND MCCONVILLE, J.T. (1982). "An Alternative to Percentile Models," SAE Technical Paper 810217,y 1981 SAE Transactions, pp. 938-946, Society of Automotive Engineers, Warrendale PA.

ROSS, J. (2009). Human Factors for Naval Marine Vehicle Design and Operation, Ashgate, Farnham, Surrey, England.

SAE (2010). "CAESAR – The Most Comprehensive Source for Body Measurement Data," SAE International, http://store.sae.org/caesar/.

SCHUTTE, P.C, M.N. SHABA (2003). "Ergonomics of Mining Machinery and Transport in the South African Mining Industry," Safety in Mines Research Advisory Committee Final Report, CSIR Mining Technology, Project Number SIM 02 05 04 (EC 2003-0252).

THAXTON, S., S. RAJULU (2007), "Anthropometric Accommodation in Space Suit Design," 10th Annual Applied Ergonomics Conference, Dallas, TX, March.

VAN DER MEULEN, P., A. SEIDL (2007). "Ramsis: The Leading CAD Tool for Ergonomics Analysis of Vehicles," Proceedings of the 1st International Conference of Digital Human Modeling.

WALTERS, B., J., BZOSTEK, J. LI (2005). "Integrating Human Performance and Anthropometric Modeling in the Crew Station Design Tool," SAE Digital Human Modeling for Design and Engineering Symposium, Iowa City, Iowa, USA, June.

WICKENS, C.D., J.D. LEE, Y. LIU (2003). An Introduction to Human Factors Engineering, Second Edition, Prentice Hall.

WIDDEL, H., F. MOTZ (2000). "Ergonomic Requirements for the Design of Ship Bridges," Human Factors in Ship Design and Operation, London, September.

Recent developments in the design of fast ships

Desarrollos recientes en el diseño de embarcaciones rápidas

J. L. Gelling [1]
J. A. Keuning [2]

Abstract

During the last twenty years, Damen Shipyards, a multinational shipbuilding group with 6000 employees worldwide, has done extensive research on the development of hull designs for fast monohull vessels. In the 1990s the Enlarged Ship Concept was developed, leading to highly improved sea keeping capabilities and vessel behaviour in waves at high speed. This hull design concept was applied in the Damen SPa 4207 patrol vessel and has proven extremely successful, reducing vertical accelerations by 50% and, thus, allowing vessels to keep operating at high speed in waves. Over 25 units of the Damen SPa 4207 have been delivered so far. After the successful introduction of the Enlarged Ship Concept, Damen and Delft University continued developing the next generation hull form: the axebow design. Compared to the already good sea keeping capacities of the Enlarged Ship Concept, model tests indicated a further reduction of vertical accelerations. This was proven by real-time measurements on the first built axebow vessels in 2006 and 2007. In the last 3 years, over 30 axe bow supply vessels have been delivered to very satisfied operators. As a next step, Damen has applied the axe bow design to the latest patrol vessel design, the Damen SPa 5009. The first vessel of this design is currently under construction and its trials are scheduled by the end of 2011. The paper describes the background of the research done by Damen and Delft University, focusing on the mathematical and scientific aspects of the axebow design and its application on various ship types. The development and design of the latest Damen patrol vessel, SPa 5009, will be introduced, describing its seakeeping performance, operatability and crew ergonomics. Finally, the paper will mention the current and future research topics that Damen and Delft University are working on together, identifying the developments of the future generation patrol vessels.

Key words: High-speed craft, Fast patrol vessels, Hull form design, Axe bow design, Seakeeping behaviour.

Resumen

Durante los últimos 20 años, los astilleros Damen, un grupo multinacional constructor de buques con 6000 empleados alrededor del mundo, han investigado ampliamente sobre el desarrollo de los diseños de cascos para embarcaciones rápidas monocasco. Durante los 90, el Concepto del Buque Ampliado fue desarrollado, conllevando a capacidades mejoradas de navegabilidad y comportamiento de la embarcación en oleaje a alta velocidad. Este concepto de diseño de casco se aplicó en la embarcación de patrullaje Damen SPa 4207, y se ha comprobado extremadamente exitoso, reduciendo aceleraciones verticales por 50% y, así, permitiendo que las embarcaciones sigan operando a alta velocidad en oleaje. Más de 25 unidades del Damen SPa 4207 se han entregado hasta la fecha. Luego de la presentación exitosa del Concepto del Buque Ampliado, Damen y la Universidad Delft continuaron desarrollando la forma de casco de la siguiente generación: el diseño de proa en arco (*axebow design*). Comparado con las ya buenas capacidades de navegabilidad del Concepto del Buque Ampliado, pruebas del modelo indican adicional reducción de la aceleración vertical. Esto se comprobó mediante mediciones en tiempo real en las primeras embarcaciones construidas con proa en arco (*axebow*) en 2006 y 2007. En los últimos tres años, más de 30 buques de suministro de proa en arco se han entregado a operadores muy satisfechos. Como paso siguiente, Damen ha aplicado el diseño de proa en arco a su más reciente diseño de embarcación de patrullaje, el Damen SPa 5009. La primera embarcación de este diseño está actualmente bajo construcción y sus pruebas están programadas para fines de 2011. El documento describe los antecedentes de la investigación realizada por Damen y la Universidad Delft, enfocándose en los aspectos matemáticos y científicos del diseño de proa en arco y su aplicación en varios tipos de embarcaciones. El desarrollo y diseño de la más reciente embarcación de patrullaje, SPa 5009, se presentará, describiendo su desempeño de navegabilidad, operabilidad y ergonomía de tripulación. Finalmente, el documento mencionará los temas de investigación actuales y a future sobre los cuales Damen y la Universidad Delft están trabajando conjuntamente, identificando los desarrollos de las embarcaciones de patrullaje de futura generación.

Palabras claves: embarcaciones de alta velocidad, Embarcaciones rápidas de patrulla, diseño de la forma del casco, diseño de proa en arco, Comportamiento de navegabilidad.

Date Received: Novembre 6th, 2010 - *Fecha de recepción: 6 de Noviembre de 2010*
Date Accepted: December 30th, 2010 - *Fecha de aceptación: 30 de Diciembre de 2010*

[1] Damen Shipyards - High Speed Craft Department. e-mail: jlg@damen.nl; eh@damen.nl
[2] TU Delft, Delft University of Technology - Shiphydromechanics Department. e-mail: J.A.Keuning@tudelft.nl

Introduction

The combination of high forward speeds and waves of any significance has since considerable time been a serious challenge for designers and operators of fast ships. The possibility of a fast ship to maintain its intended high forward speed under those conditions is a serious measure for its operability. For decennia, Damen Shipyards has put considerable effort into improving the operability of fast ships in a seaway. During the last two decades, this has resulted in close cooperation with the Ship hydromechanics Department at Delft University of Technology. As a result of this cooperation, some successful new concepts have been developed and brought to the market.

In the present paper an oversight of these developments will be presented and some results obtained with these new concepts when compared with existing contemporary designs will be highlighted.

Problem Definition

From full-scale experience, it is known for a long time that severe motions and, in particular, high vertical accelerations are the main reason for speed reduction of fast ships in a seaway. This speed reduction occurs primarily in head and bow quartering waves. Due to the large motions and the sometimes very high peaks in the vertical accelerations during impacts most crews apply voluntary speed reduction to maintain workable conditions on board of their ships to prevent possible structural damage to the ship and to guarantee the safety of the crew and the ship.

Principal reasons for these phenomena to occur in particular with fast ships originate from the fact that, both for practical and economical reasons, most fast ships are generally small, say smaller than 50 meters in overall length and, therefore, the waves they are sailing in are relatively large. Also, due to the high forward speeds in head waves the frequency of encounter is high, which has a very negative effect on the acceleration levels aboard these ships.

For a long time, the emphasis in the design of fast ships has been put on the minimal obtainable resistance at the required maximum speed. This had to be obtained under calm conditions. Operation of the ships in a seaway was for a long time not considered as an important design issue. In some design areas, such as the fast-ferry markets, the search for improved seakeeping behaviour was found in the design and application of ever larger vessels. By doing so, the mentioned deviancies in the behaviour in waves could be partly overcome, but this is not a solution applicable in most of the other areas of application of fast ships. The focus on calm water performance has lead to particular trends in the fast ship designs, such as low deadrise, low length to beam ratios, and relatively short and heavy hulls, i.e., low length – displacement ratios. These trends, however, showed unfavourable for the behaviour of these fast ships in a seaway. Thereby, when these ships moved their operational areas from the more sheltered inland waters to the more exposed sea areas a new design philosophy had to be developed.

The development of new design concepts

An important role in this new development, at least within the Damen and DUT cooperation, was played by the results obtained from a considerable amount of full-scale measurements carried on board various fast Patrol Boats and Search and Rescue (SAR) vessels of different sizes on the North Sea. As reported by Keuning in Ref [1] it became obvious that improving the operability in head waves meant reducing the peaks in the vertical accelerations on board as much as possible. The significant (or "average") value of the vertical accelerations did not prove to be the prime factor for the crews to voluntarily reduce the speed of the ship, but the occurrence of the more scarcely high vertical peaks or slams. Avoiding these high peaks, therefore, became a primary driving factor in the designs. To demonstrate this, Fig. 1 is introduced with the distribution of the peaks in the irregular time signal of the vertical accelerations of a fast ship.

The horizontal scale represents the change of occurrence and is "transformed" according to the Rayleigh distribution, the vertical scale presents the magnitude of the vertical accelerations in meters per second squared.

Fig. 1. Distribution of peaks and troughs of an acceleration signal

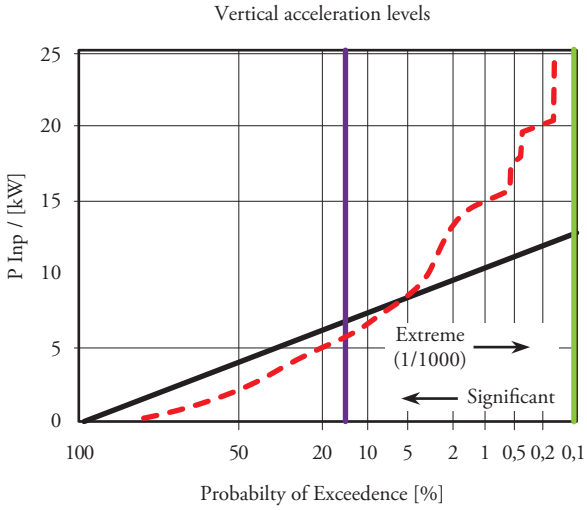

The wish to avoid the high peaks in the acceleration signal for improved operability in a seaway means that a distribution according to the black (straight) line is very much to be preferred above the distribution following the red line. This holds true even though the significant value corresponding with the black distribution line is higher than that of the red line.

These insights led to the development and introduction of the Enlarged Ship Concept (ESC) in 1995 [1], [2]. First by the so called "simple ESC 4100" in which only the length was increased without changing the section and bow shape of the design and which proved already a considerable improvement over the conventional designs. This concept was subsequently followed by the development of the more improved concept called "TUD 4100" in which improved bow geometry was introduced. These were followed by the more radical new design concept called the "AXE 4100" by applying the philosophy in full of the AXE Bow Concept (ABC) in 2001 [3], [4]. Based on an extensive research project FAST 1 carried out in 2003 by the Ship Hydromechanics Department at Delft University of Technology jointly sponsored by Damen, Royal Netherlands Navy, US Coast Guard and MARIN, all relevant aspects of the behaviour of the ABC in waves from any direction were analyzed and evaluated. This showed such promising results that Damen decided to introduce the ABC designs on the market in 2006 and these designs have been quite successful.

The philosophy behind these concepts is that, first of all, the length should be brought back into design. By increasing the length without changing the beam, the forward speed and the functionality of the design, the L/B ratio becomes larger, the L/DISP ratio also becomes larger and there is a more suitable place available to position the important areas on board such as the wheelhouse or passenger areas can be found, i.e., the ESC 4100.

By increasing the length without changing the functionality, more space (void space) also becomes available – enabling the design of the hull shape more from an optimal hydromechanics point of view.

To avoid severe impacts during sailing in waves, the hydrodynamic lift generated at the fore sections of the hull has to be reduced. Also, the dominant wave exciting forces for fast ships has been proven to be the so-called non-linear Froude Kriloff forces. These have to be reduced as far as possible, which is achieved by introducing changes in submerged volume below and above the waterline both in the horizontal and the vertical direction. This results, in particular at the bow, in taking care that only small changes in submerged geometry at the forward sections of the hull do occur when these sections are moving in and out of the water due to provoked motions in the incoming waves. This leads to very sharp bows with non-flared sections and very deep forefoots with possibly a negative contour. The sheer line is significantly raised to generate more freeboard forward and so increase the reserve buoyancy. To illustrate this, the lines of a Conventional, an ESC, and an ABC design are depicted in Figure 2. A more detailed description of these design concepts was presented by Gelling at the 2007 IPIN Conference [5].

Fig. 2. The line plans of the simple ESC, the improved ESC (TUD 4100), and the ABC designs

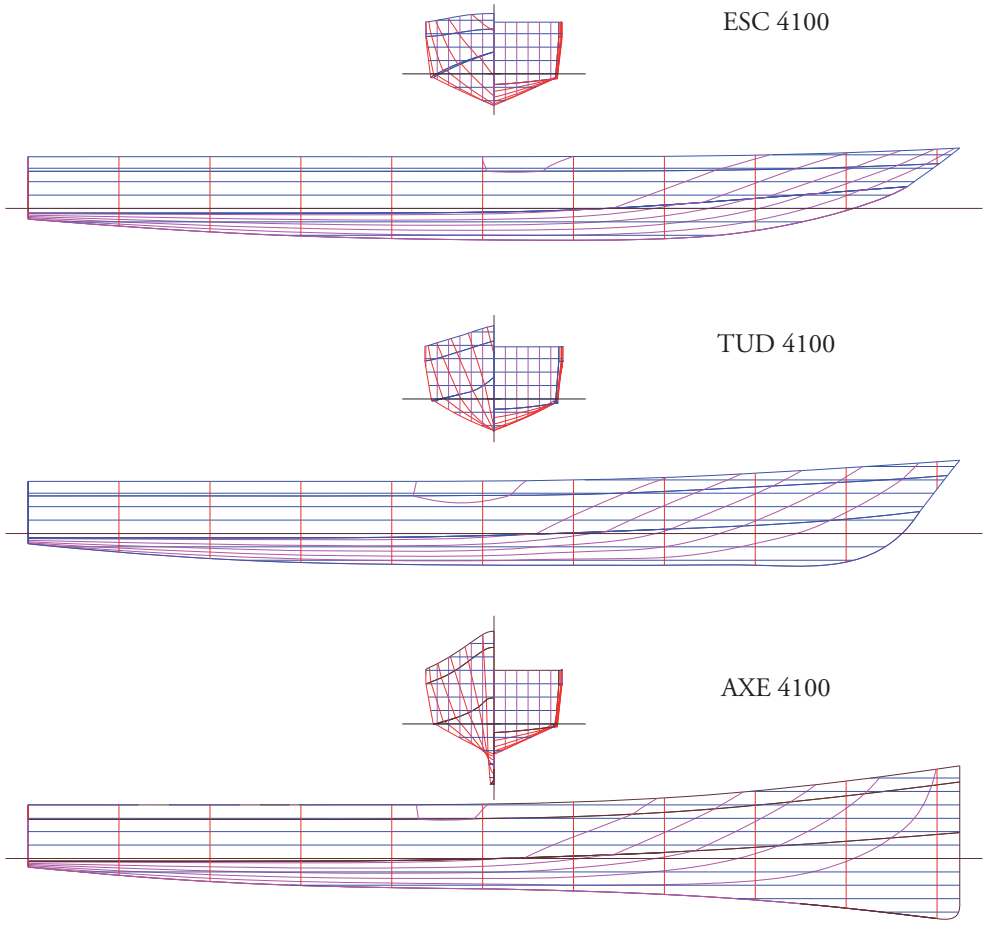

The improvements obtained with these designs in the vertical accelerations are clearly demonstrated by the results from a comparative study presented in Fig. 3. Here, the peak distributions in the vertical accelerations at the bow of the three concepts sailing at high speeds in head waves corresponding to a Seastate 5 on the North Sea are plotted on the basis of a Rayleigh distribution scale. From these plots, it is obvious that the application of the ESC and the ABC design philosophy leads to a significant reduction of the high peaks with limited occurrence, i.e., the right hand side of the figure is much lower. In particular, the AXE 4100 is superior in this respect. This leads to a large improvement in the operability of these craft. These theoretical results are in the meantime fully confirmed by full-scale experience with the actual ships.

On the market both concepts are very successful. This is amongst other things demonstrated by the fact that from the ESC design more than 75 vessels have been sold since 1997 and from the ABC design more than 30 since its introduction in 2007.

Fig. 3. The comparison of the distributions of the vertical accelerations at the bow for the new design concepts

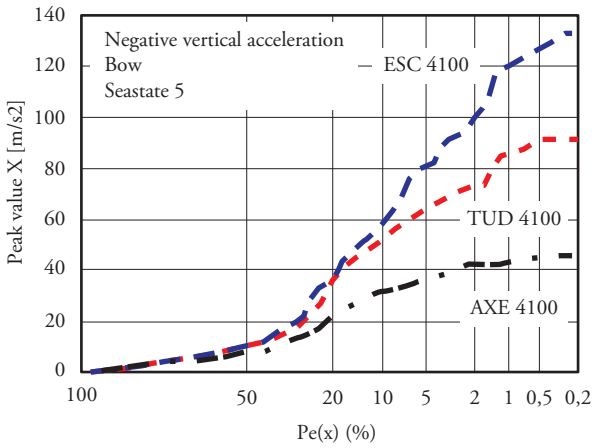

The ESC has been built primarily in the function of Patrol Boat in the range from 40 till 60 meters overall length with speeds ranging from 22 to 30 knots. The Axe bow designs range from 30 till 60 meters overall length and are primarily used as Fast Crew Suppliers, Fast Yacht Support Ships, and more recently Patrol Boats. Some typical examples are depicted in Fig. 4.

Fig. 4a. The AXE Bow Concept applied as Fast Yacht Support vessel of 50 m lengthconcepts

Fig. 4b. The ESC as 42 m Patrol Boat

One of the particular beneficial aspects of the application of the AXE Bow turned out to be the circa 20% lower fuel consumption in waves compared with conventional ships due to the considerable lower added resistance because of the waves. These good results obtained with the designs with the AXE Bow led to a new research project in 2009 into the possible application of this concept in catamarans. An important aspect was if and if so, which modifications had to be introduced for application of the concept with catamarans.

During the last decade, a considerable demand has come from the market for relatively small catamarans with improved seakeeping performance. These have to be operated from low to moderate sea states in particular for application as service vessels for the offshore wind mill farms at the North Sea. Typical length of these vessels is in the 20-meter range and typical speeds are up to 25 knots in calm water. In addition to the usual requirements for low levels of vertical accelerations

Fig. 5. The lines plan of the TwinAxe Catamaran concept

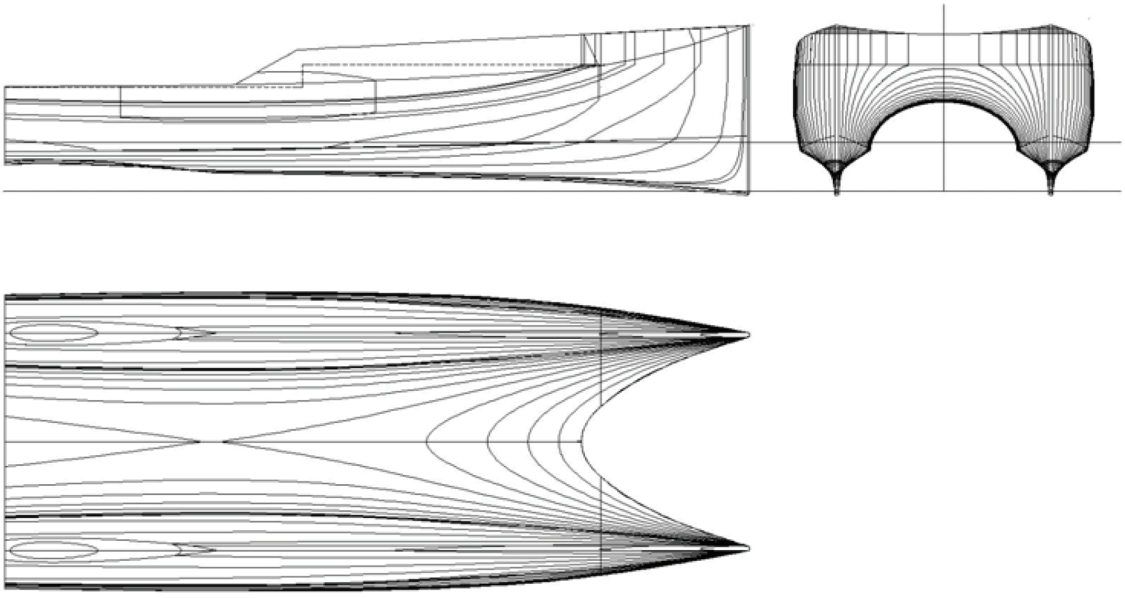

and small motions, the improvement in the seakeeping behaviour of the catamaran has also to be found in the avoidance of wet deck slamming. This put special focus on the design of the hull shape.

The solution for the optimized catamaran hull design was found in applying the Enlarged Ship Concept first and so to extend the overall length from 20 to 25 meters. Then the AXE Bow concept was applied on both hulls. To avoid wet deck slamming the vertical motion of the fore ship had to be introduced so that when sailing into the wave the deck was lifted but without violent accelerations. Thereby, a special geometry was designed between the hulls to gently introduce the wave forces, but not to eliminate them completely. Finally, the avoidance of the wet deck slamming was found in cutting away the foremost part of the wet deck about 20% of the overall length. This was also made possible by the application of the enlarged ship concept.

The research project aimed at comparing between the TwinAxe concept and a comparable conventional catamaran. It was decided that the comparison between the two designs would focus on the resistance in calm water and the heave and pitch motions and vertical accelerations in head waves. In addition, the possible tendency for bow diving in following seas was also investigated for both designs.

The calm water resistance of the two designs is compared in Fig. 6. From these results, it is obvious that the resistance of the TwinAxe is lower than that of the conventional catamaran. This is in particular due to the higher L/B ratio of the hulls and their bigger separation. A typical crossover is found at 25 knots.

From the results in waves only the vertical accelerations at a location 10% of the Loa aft from the bow are shown. The tests have been carried out in a typical North Sea Seastate and at a forward speed of 25 knots. These results are depicted in Figs. 7.

Fig. 6. Calm water resistance of the TwinAxe and the Conventional Catamaran

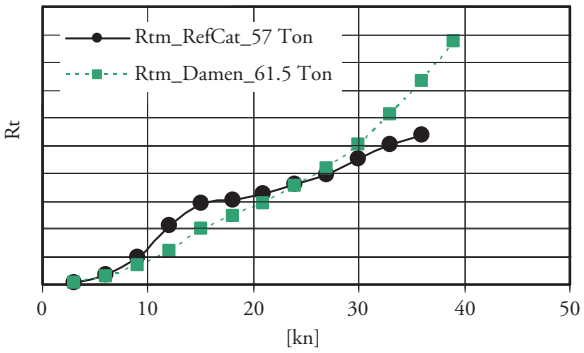

Fig. 7a. The distribution of the vertical accelerations at the bow for the TwinAxe Catamaran at 25 knots in irregular waves with significant wave height Hs of 1.5 m.

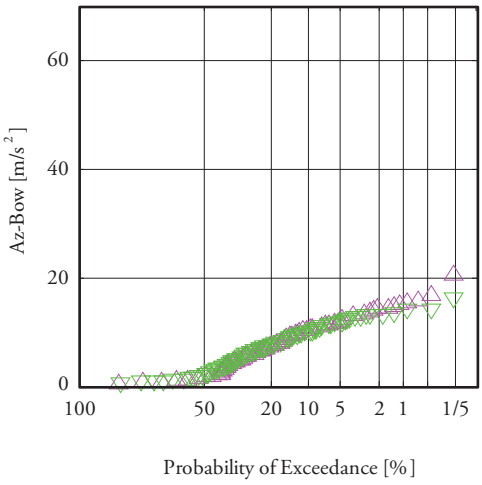

Fig. 7b. The distribution of the vertical accelerations at the bow for the Conventional Catamaran at 25 knots in irregular waves with significant wave height Hs of 1.5 m.

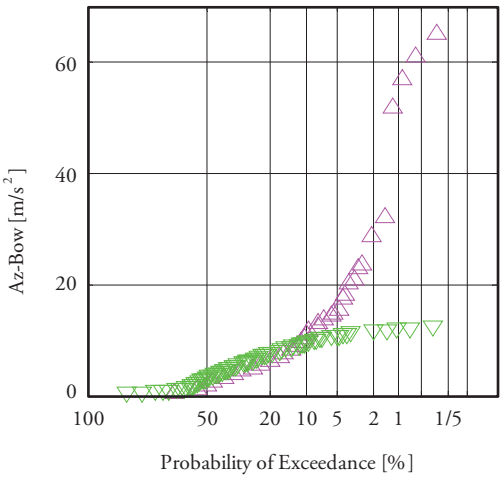

The enormous gains achieved in the vertical acceleration levels obtained with the application of the TwinAxe concept are rather obvious.

It is also well worth mentioning that under all the conditions tested, i.e., with significant wave heights ranging from 1.0 to 2.5 meters and forward speed of 25 knots no wet deck slamming occurred with the TwinAxe. In the following sea conditions no bow diving occurred also. Although the development time of this new catamaran concept was rather short, the results obtained were so promising that already a couple of these catamaran designs have been sold. A typical rendering of one of these designs is depicted in the next Fig. 8.

Fig. 8. Rendering of the TwinAxe Catamaran as windmill support ship

Another application of the new concepts was found in the design of a possible new Search and Rescue (SAR) vessel for the Royal Dutch Lifeboat Institute (KNRM). At present, they are looking for a possible replacement of their existing fleet of 18.5-meter long RIB vessels capable of a forward speed of maximum 35 knots and to be used on the North Sea under all weather conditions. Given the special functionality of these SAR boats and their possible use under very extreme environmental conditions, some modifications to the original AXE Bow design had to be made. The new SAR boats should have improved seakeeping performance when compared to the present ones when head and bow quartering seas are concerned. Under all other conditions, they should at least have similar performance and preferably better. Particular attention had to be paid to the possible occurrence of broaching in stern quartering seas. Also the tendency to bow diving in extreme following waves should be considered.

Finally, the manoeuvrability of these SAR ships in severe waves, both head and following, should be an issue. The boats should also be self righting. Based on these requirements, a new design has been developed. Particular points in the design were the enlargement of the hull, the application of the AXE bow but without the typical negative sloped contour (downwards) forwards because these SAR boats should be able to take the ground frequently and violently. For safety and manoeuvrability, reasons the boats are equipped with water jets of ample power. The tube along the entire length of the hull is there mainly for fendering reasons. The most striking difference with the existing boats is the very fine bow with increase sheer and freeboard. Compared with the existing boats, the deadrise and the hull L/B ratio are increased. A rendering of this design is depicted in Fig. 9.

Fig. 9. Proposal for a new SAR vessel for the KNRM with Loa = 21 m and Vs = 35 knots

From an extensive series of experiments carried out with a model of this new design and a model of the existing boat in the towing tank, it has been demonstrated that a considerable improvement in the head seas conditions has been achieved with the new concept, without any loss of performance under following and stern quartering conditions.

Development of new active controls

In addition to these new concept developments, research has also been carried out in the area of

active control for fast ships. This originates from the effect that both the size and the high forward speed of these craft make the use of actively controlled fins very attractive. Two typical examples with promising results will be mentioned here:

- an actively controlled trim flap or interceptor at the transom of the boat to control pitch, heave, and vertical accelerations and
- a retractable vertical bow rotor below the bow of a fast ship to improve directional control and reduce the roll and yaw motion in stern quartering and following waves.

The idea of controlling ship motions with an active control on the trim flaps at the transom is not new. In 1984 Wang [7], amongst others, published experimental and computational results of a hard chine planing hull equipped with actively controlled trim flaps. In his research, he already showed that considerable gains could be obtained with this control. Recently, Rijkens extended this research with model experiments to determine the forces and moments delivered by both active flaps and active interceptors at the transom. The results of these systematic series of experiments have been used to extend the calculation procedure used in the mathematical model for the motions of fast ships in waves. The type of flaps and interceptors investigated by Rijkens are depicted in Fig. 10.

Fig. 10. Type of flaps and interceptors investigated by Rijkens

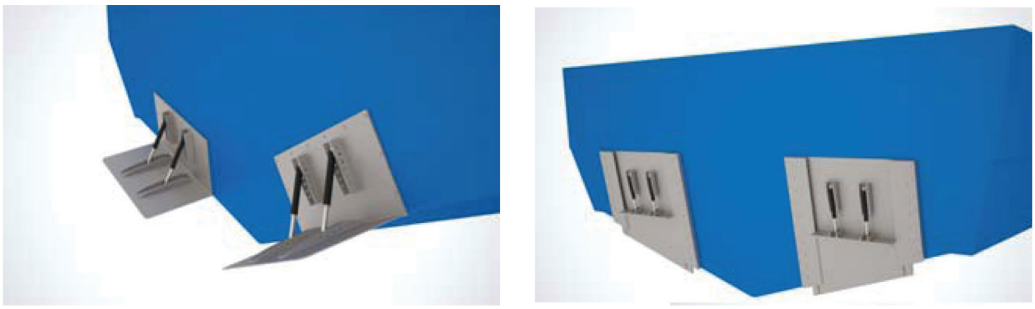

And the results he obtained with the flaps on the vertical accelerations at the bow are depicted in Figs. 11, for the tests with and without flaps.

Fig. 11a. Vertical acceleration at the bow without flaps

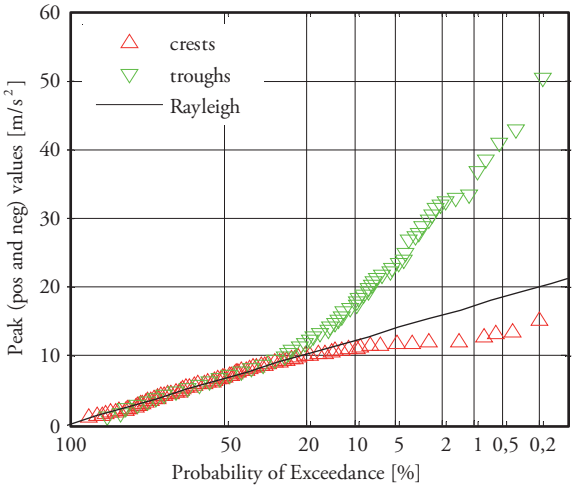

Fig. 11b. Vertical acceleration at the bow with active flaps

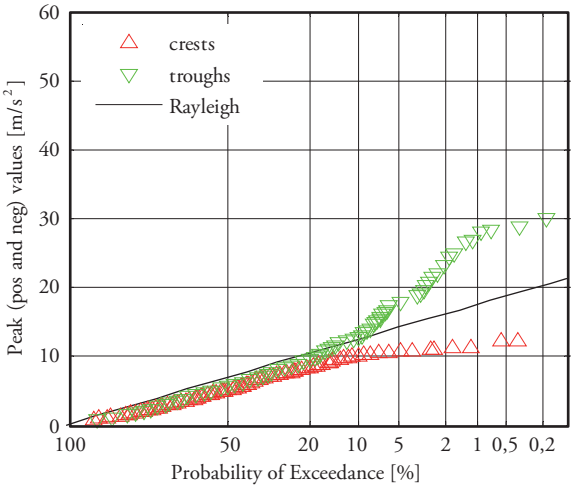

Finally, a new device has been developed for controlling the roll and yaw motions of fast ships in stern quartering waves.

It is known from full-scale experience and model experiments that quite a few fast ship concepts are sensitive for severe combined roll and yaw motions in stern quartering waves, sometimes leading to complete loss of control and a broach. This is aggravated once again by the fact that most fast ships are relatively small compared to the surrounding waves.

The phenomenon of the broach will not be fully explained here but an extended description can be found in Ref [8]. The Vertical Bow Rotor (VBR) device is a vertical and retractable Magnus Rotor underneath the bow of a ship, preferably an AXE Bow because the very geometry of such a bow easily enables the housing of such a device. An additional benefit of the AXE Bow and VBR combination is that the VBR cylinder is and will remain deeply submerged when the ship is heaving, rolling, and pitching in large waves. A Magnus Rotor has the property of efficiently generating a very high lift force when the cylinder is put into rotation. The combination of the forward velocity of the ship and the rotation of the cylinder produces a lift force perpendicular to the forward velocity of the ship. By changing the rotations per minute (RPM) of the rotor and/or the direction of rotation, the lift force can be fully controlled both in magnitude and direction; almost like a rudder, but more efficiently. The VBR in this application is made retractable because under those situations or conditions in which its application is not necessary it can be easily retracted and so the effect of the rotor on the ship resistance remains. A typical configuration of such a rotor is depicted in Fig. 12.

Fig. 12.

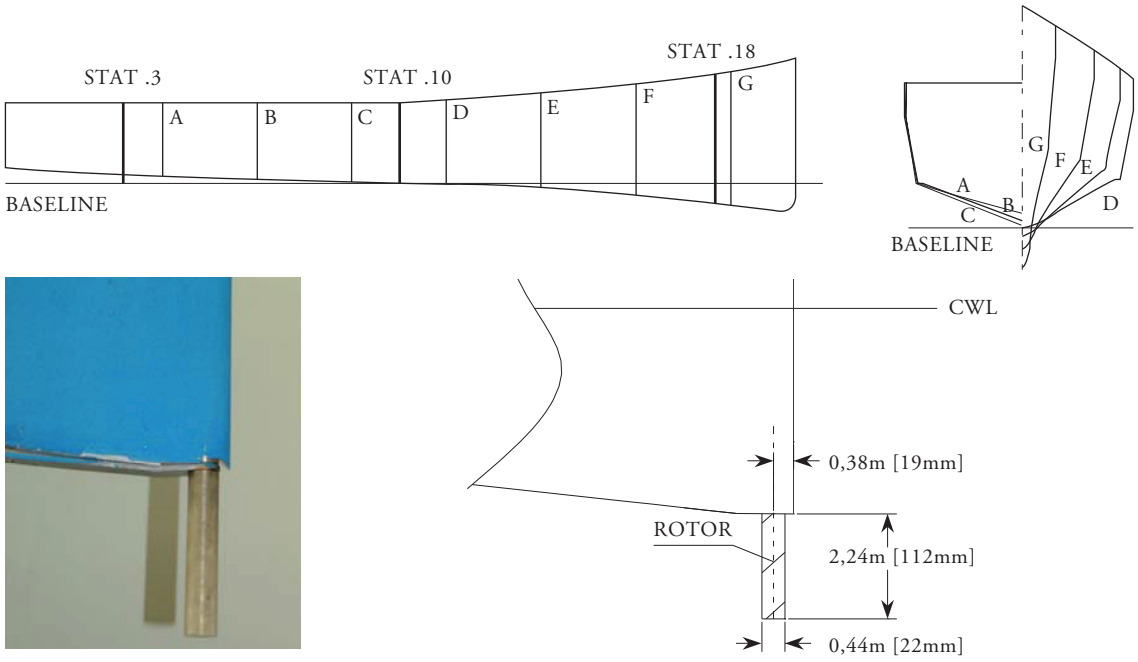

To investigate the effect of the VBR on the dynamic behaviour of a fast patrol boat in stern quartering waves, extensive experiments have been carried out in the MARIN Ship Motion Basin in Wageningen. The ship tested was a 35-meter Length over all (Loa) Fast Patrol Boat from DAMEN and the VBR was dimensioned based on an extensive systematic test with various rotors in the towing tank of the Delft University of Technology. A few of the results are presented here. They show the effect of the VBR on the roll and the yaw motion in an irregular sea with a significant wave height of

2.5 meters and a peak period, Tp, of 7.6 seconds, a typical North Sea spectrum energy distribution over the frequency range. The waves approached from 315 degrees (stern quartering) and the ship travelled at a forward speed of 22 knots. From earlier tests, it was found that this was the worst combination of waves, heading, and forward speed. The distribution plots show the crests and troughs of the roll and yaw motions with and without the VBR.

Fig. 13. Distribution of roll and yaw motions in stern quartering seas with Hs = 2.5 meter at 22 knots with and without VBR

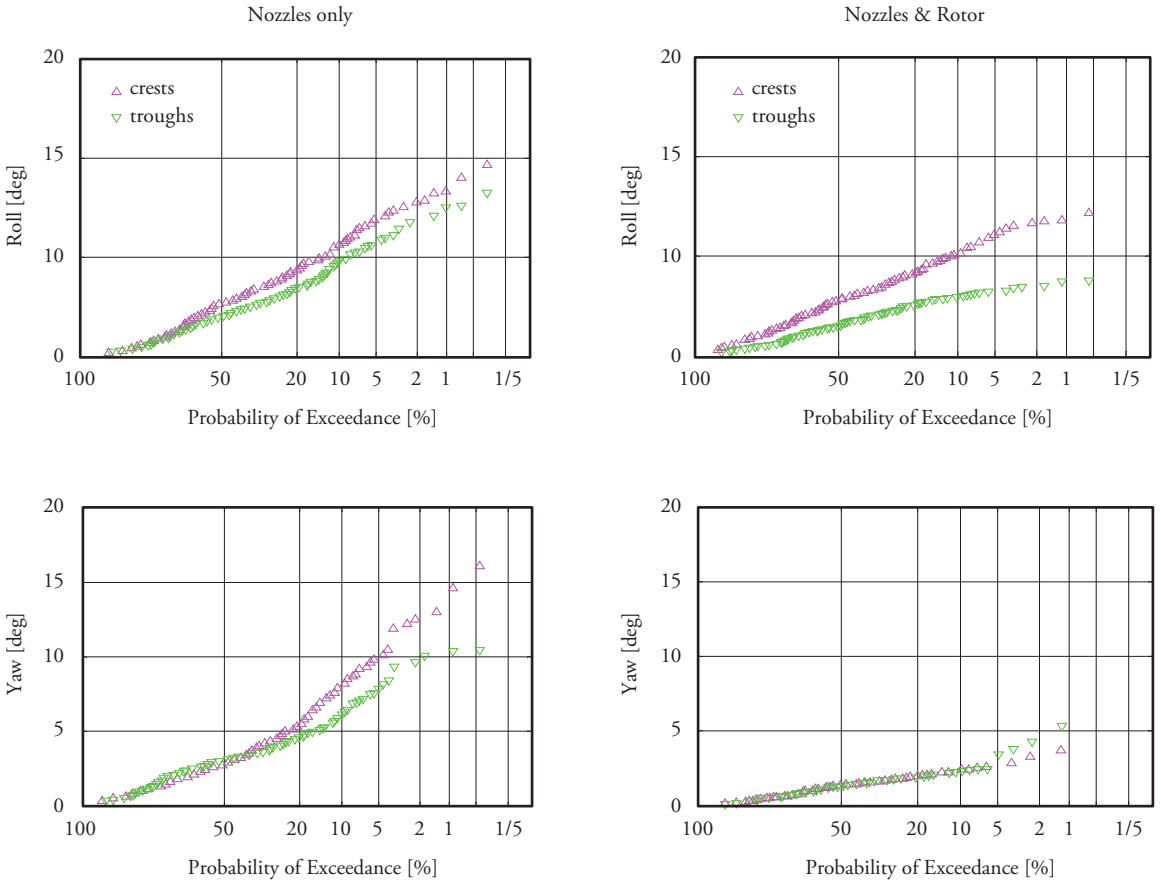

These results show that a reduction of almost 40% on average in the roll motion and of almost 60% in the yaw motion can be achieved under those conditions. To investigate the extended application of the VBR, measurements have also been carried out in Seastate with 3.5-meter significant wave height, conditions under which the ship without the active VBR now and then broached. These results are presented in different manner in the following figures, i.e., in Fig. 14 as Significant Double Amplitudes (SDA) of the motions and as Maximum Plus and Minus amplitudes in Fig. 15.
From these results, it can be concluded that the introduction of the VBR has very positive effects on the controllability and the reduction of the roll and yaw motions in stern quartering seas. The operability of fast vessels under those conditions can be very much improved by applying VBR. Under the conditions tested, the vessel used for the experiments did not experience any broaching behaviour with the VBR activated whilst without the VBR some broaches did occur. Although not specifically investigated yet, it appears that using the VBR is especially suited in combination with the AXE Bow.

Fig. 14. Significant Double Amplitude for Roll and Yaw with and without the Bow Rotor at 22 knots in a seaway from a angle of incidence of 315 degrees and with a significant wave height of 3.5 meters

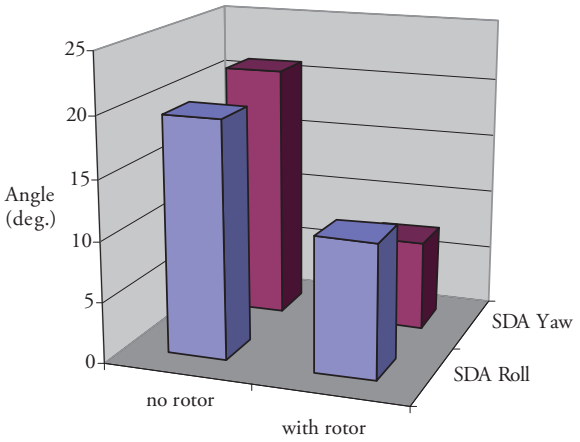

Fig. 15. Maximum Roll and Yaw angles with and without the Bow Rotor at 22 knots in a seaway from an angle of incidence of 315 degrees with a significant wave height of 3.5 meters

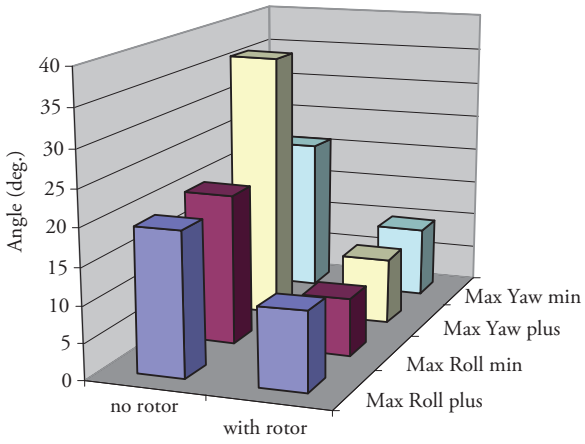

Conclusions

The High-Speed Craft area lends itself very much for improvements in design. In particular, in improving the operability – in general – of fast ships in a seaway is a very interesting field of research and development. Some noticeable results have been achieved in this area over the last decades through intensive cooperation among universities and research institutes with the industry. It is to be expected that if this cooperation is continued and intensified, in the years to come new and very fruitful results will again be achieved.

References

[1] BOSCH, J.J. VAN DEN "Tests with two planing boats in waves" TU Delft Laboratorium voor Scheepsbouwkunde, Report 238, June 1969.

[2] BLOK, J.J. AND ROELOFFS, H.W. 'The influence of the Forebody Deadrise on the performance in a Seaway" MARIN Report No 49207-1-HT April 1989.

[3] KEUNING, J.A. "Nonlinear Heave and Pitch Motions of Fast Ships in Irregular Head Waves" ASNE High Speed Marine Vehicles Conference, Washington, June 1992.

[4] KEUNING, J.A. "The Non Linear Behavior of Fast Monohulls in Head Waves" PhD Thesis, Delft University of Technology, September 1994.

[5] GELLING, J.L. AND KEUNING, J.A. "Developments in hullshapes for high speed craft" IPIN Conference 2007, Cartagena, Colombia.

[6] KEUNING, J.A. AND PINKSTER, J. "Further Design and Seakeeping Investigations into the Enlarged Ship Concept" FAST Conference Proceedings 1997, Sydney Australia.

[7] KEUNING, J.A., PINKSTER, J. AND WALREE, F. VAN "Further Investigation into the Hydrodynamic Performance of the AXE Bow Concept" Proceedings of the WEGEMT Conference on High Performance Marine Vehicles September 2002 Ischia, Italy.

[8] KEUNING, J.A., TOXOPEUS, S. AND PINKSTER, J. "The Effect of Bow Shape on the Seakeeping Performance of a Fast

Monohull" FAST Conference Proceedings Southampton, September 2001.

[9] OOMS, J AND KEUNING, J.A. "Comparitive Full Scale Trials of Two Fast Rescue Vessels" International Conference SURV 4, 13&14 may 1997 Gothenburg.

[10] KEUNING, J A AND VISCH, G. The Application of a Vertical Bow Rotor on an AXE Bow FAST Conference Athens, Greece 2009.

Ship maneuverability: full-scale trials of colombian Navy Riverine Support Patrol Vessel

Maniobrabilidad de buques: pruebas a escala real del Buque Patrullero de Apoyo Fluvial de la Armada de Colombia

Jorge E. Carreño Moreno [1]
Etty Y. Sierra Vanegas [2]
Victor H. Jiménez González [3]

Abstract

Methodology and results of full scale maneuvering trials for Riverine Support Patrol Vessel "RSPV", built by COTECMAR for the Colombian Navy are presented. This ship is equipped with a "Pump – Jet" propulsion system and the hull corresponds to a wide-hull with a high Beam – Draft ratio (B/T=9.5). Tests were based on the results of simulation of turning diameters obtained from TRIBON M3© design software, applying techniques of Design of Experiments "DOE", to rationalize the number of runs in different conditions of water depth, ship speed, and rudder angle. Results validate the excellent performance of this class of ship and show that turning diameter and other maneuvering characteristics improve with decreasing water depth.

Key words: maneuverability, shallow waters, sea trials, ship dynamics.

Resumen

En el presente trabajo se presenta la metodología y los resultados de las pruebas de maniobrabilidad a escala real del Buque Patrullero de Apoyo Fluvial Pesado "PAF-P", construido por COTECMAR para la Armada Nacional de Colombia. El buque está equipado con un sistema de propulsión de bomba de agua tipo "*Pump – Jet*" y su casco corresponde a un casco con una relación Manga – Calado muy alta (B/T = 9.5). Las pruebas se basaron en los resultados de simulación de círculos evolutivos obtenidos en el software de Diseño TRIBON M3©, aplicando técnicas de Diseño de Experimentos "DOE", para racionalizar el número de corridas en diferentes condiciones de profundidad, velocidad y ángulo de timón. Los resultados validan el excelente desempeño de esta clase de buques y muestran que el diámetro de giro y otras características de maniobrabilidad mejoran con la disminución de la profundidad.

Palabras claves: maniobrabilidad, aguas poco profundas, pruebas en mar, dinámica del buque.

Date Received: November 26th, 2010 - *Fecha de recepción: 26 de Noviembre de 2010*
Date Accepted: January 20th, 2011 - *Fecha de aceptación: 20 de Enero de 2011*

[1] COTECMAR. Oldenburg, Lower Saxony. Germany. e-mail: jorgec@cotecmar.com
[2] COTECMAR. Cartagena, Bolívar. Colombia. e-mail: esierra@cotecmar.com
[3] COTECMAR. Cartagena, Bolívar. Colombia. e-mail: vjimenez@cotecmar.com

Introduction

The Colombian Science and Technology Corporation for the Development of the Naval, Maritime, and Riverine Industry (COTECMAR, for its name in Spanish) designed and constructed a series of Riverine Support Patrol Vessels "RSPV" for the Colombian National Navy to comply with missions in over 13,000 Km of the nation's navigable rivers. The first and second generations of these vessels, are comprised of four units equipped with propulsion systems consisting of two propellers driven by diesel engines and a steering system composed of two compensated rudders. These vessels fulfill missions in Tropical rivers, characterized by a wide course, without canalization or marked, with very shallow waters, especially during dry season months, so much that the depth – draft (h/T) ratio may be reduced to 1.5.
The first vessel of the series, "ARC GUILLERMO LONDOÑO" was commissioned in January 2000 and the fourth vessel started operations in 2004.

The operational experience gathered with these vessels evidenced the need to introduce different technologies for the propulsion and steering of these vessels. Propellers with a minimum immersion generate pressure pulses transmitted through the sternpost to the vessel structure, not only causing harmful effects to equipment and less rigid structures, but deteriorating crew comfort conditions; likewise, objects floating on river waters like tree trunks frequently become strong causes of damage, by deforming the propeller blades and the rudders. Also, conditions of maneuverability of vessels with very high beam - draft ratios (B/T=9.5) are critical because there is route instability, a situation exacerbated by navigation in very shallow waters with presence of currents.

This prior problem, as well as the review of the roles and operational capacities of the RSPV vessels called for re-engineering, which began during September 2003 with trials in the hydrodynamic experience towing tank at the "Centrum Techniki Okretowej" (CTO) in Gdansk, Poland, where resistance trials were developed on the vessel's advance under different depth conditions, along with self-propulsion tests with a new type propulsion configuration -Pump Jet-.

The third generation RSPV (Fig. 1) comprises four vessels, the first of which was commissioned in 2005 and the last two in March 2009. Improvements in terms of maneuverability and reliability of the propulsion and steering system are evident, on one part the appendages are totally eliminated such as buttresses, propellers, axes, and rudders, which implies that there are no possibilities of damage due to impact with floating objects; while the possibility of independently controlling water jets from each pump in any direction confers exceptional maneuverability conditions to the vessel in terms of ease of turning and change of course, tactical ability – important during combat to aim its weapons through the appropriate flank; despite the aforementioned, routing instability persists, that is, the coursekeeping ability because of the low drift area (L x T) and the lack of control surfaces.

Bearing in mind the existing problem, the "Sea trials" Project was undertaken in which one of the objectives was to run full-scale trials on the RSPV to identify its maneuverability characteristics, following the vessel maneuverability standards, adopted by the International Maritime Organization (OMI) and issued by resolution A. 751 (18) in 1993 [5], in addition to circular MSC/Circ.644 published in June 1994 [6]; the maneuverability characteristics, issued by the OMI, are typical measurements with nautical interest in vessel performance.

To assess these qualities, the OMI recommends performing turning circle trials, zig-zag trials, and stop collision tests; however, the referred standards do not cover all types of vessels or the operational circumstances in which some of them navigate. Particularly, in 2006 the European Union adopted directive Nº 2006 C/166-E/01 [3], which establishes the requirements of maneuverability that must be complied with by vessels navigating the European riverine network and these are summarized in the stopping ability, back-up ability, ability to execute evasive maneuvers, and ability to turn against the current.

The full-scale sea trials were conducted by COTECMAR, on board the "ARC STCIM EDIC CRISTIAN REYES HOLGUÍN", the last vessel of the third generation RSPV, in the Cartagena Bay on the Colombian Caribbean Coast, during March and April 2009 in shallow waters (h/T = 2.2) and deep waters (h/T = 24). The vessel was subjected to turning circle trials at different approach velocities and rudder angles, zig-zag, and emergency stop; the instrumentation used during the trials included a Differential Global Positioning System (DGPS), an inertial gyro, sensor transmitters of thrust direction of propellers, vane and anemometer, a pair of optical sensors to measure angular velocity of the axes, and a torque measurement system. The data sensed were acquired through virtual instruments developed via LabVIEW for this purpose, centralizing the information in a computer located on the ship's bridge.

Description of the Vessel

The main characteristics of the RSPV are described in Table 1. The hull corresponds to a river vessel with very little dead-rise and high beam - draft ratio, designed to navigate in very shallow waters, the frame box is shown in Fig. 2.

Fig. 3 shows in detail the disposition of the propellers on the model ready for the self-propulsion test; as noted, the pumps are placed on the vessel sternpost and there are no exposed surfaces. The hull has no appendices except for a central skeg that permits separating the flow of water in each pump, as well as two deflector plates that guide the pumps output flow and contribute to diminishing the thrust deduction.

The propulsion system is composed of two "Pump – Jet" type centrifuge pumps model SPJ 82RD, manufactured by Schottel, driven by MTU diesel engines Series 60 450BHP@1800RPM with a connection composed of an investor reduction gear and a cardan shaft. The jet from the pumps may be aimed 360 degrees individually or in tandem through a joy stick control from the bridge or locally from the engine control room.

Table 1. Main Particulars of RSPV

Length overall	L_{OA}	40.3 m
Length between perpendiculars	L_{BP}	37.9 m
Beam	B	9.5 m
Design Draft	T	1.0 m
Displacement	Δ	303 tons
Block Coefficient	C_B	0.78
Prismatic Coefficient	C_P	0.87
Longitudinal Center of Gravity	L_{CG}	17.31 m
Design speed @ deep water	VM_{AX}	9.5 knots
Main Diesel Engines	2 x MTU Series 60, 450BHP@1800RPM	
Propulsion device	2 x SCHOTTEL Pump Jet, model SPJ 82RD	
Shipyard	COTECMAR	
Owner	COLOMBIAN NAVY	

Source: COTECMAR

Fig. 1. Picture of RSPV during sea trials

Experimental Design

The number of runs and the cost represented by experimenting with a vessel at full scale exceeds the resources available and make it non-viable. Making use of experimental design methodology and two-level fractional factorial design, Montgomery [13], the experimenter may reasonably suppose that certain higher order interactions are insignificant,

Fig. 2. Body plan of RSPV

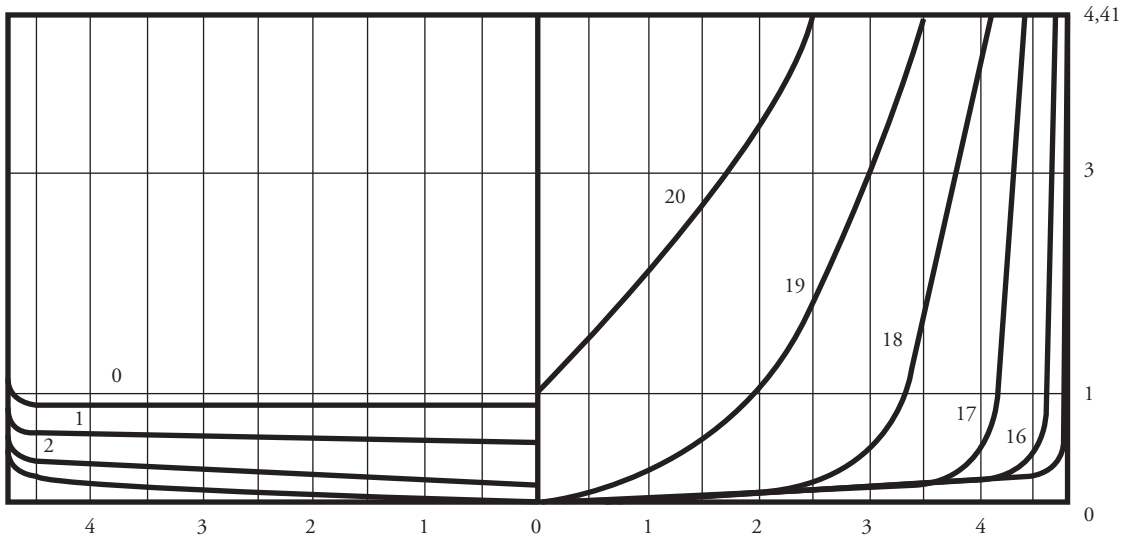

Source: COTECMAR

Fig. 3. Detail of ship model ready for self-propulsion test

Source: CTO Report

permitting them to obtain information from the main effects and from the lower order interactions running only one fraction of the complete factorial experiment.

Following the same methodology introduced by Islam *et al.*, [8], herein present the screening experimental design to conduct the sea trials for the turning circle maneuver. First of all, a dimensional analysis has been made of the main factors intervening in the maneuver mentioned, bearing in mind the interest of studying the influence of the navigation in shallow waters, the objective is to identify the most significant factors, so they can be eliminated to – in a later stage – rationally design the experiment with the remaining factors. Table 2 shows the screening design characteristics conducted via STATGRAPHICS Centurion XV© Version 15.2.14 software.

For the purpose of evaluating the linearity of the effect of the factors, four central points per block has been aggregated, yielding a 2^{k-1} design, *i.e.*, 2^{4-1}, 8 runs plus four central points for a total of

12 random runs. It has been intentionally omitted the maneuver execution flank factor, which was introduced during the final design phase of the experiment. The reason is that it is not possible to obtain a variation in the response from simulation with the TRIBON-M3© software, which has been used to obtain the turning diameter values.

The contour of the response surface estimated for the turning diameter is shown in Fig. 5; this result has been obtained from simulation in TRIBON M3© using the mathematical models of filled form vessels and equipped with conventional rudders and propellers, given that there was no calculation tool to predict maneuverability characteristics of vessels with non-conventional, Pump-Jet type propulsion and steering systems. The models used in this software correspond to the work developed by Khattab [11], who developed multiple regressions to find the linear and non-linear hydrodynamic derivatives in deep and shallow waters, for filled form vessels. It was noted that for a velocity of 9 knots, the turning diameter diminishes as depth is diminished, that is, the maneuverability characteristics improve contrary to what occurs with most vessels.

This disagrees with the widely known literature for vessels of conventional proportions and equipped with propellers and rudders. Kijima (2003) [12] presents results of turn simulations in shallow waters for four different vessels and in all instances, the turning diameters and tactical diameters increase as depth diminishes. Delefortrie (2007) [2] has studied the effect of the under keel clearance in container ships and validates the increase in the dimensions of the vessel's turning diameter as the under keel clearance diminishes. The Maneuverability Committee (2002) of the 23rd International Towing Tank Conference (ITTC) [9], presented the effects of depth on standard maneuvers, describing an increase of up to 75% of the tactical diameter in vessels navigating with an under keel clearance of 20%. There are few results of full-scale maneuvers in shallow waters; this added to the specifics of the propulsion system and to the hull geometry makes the present experiment particularly important for the scientific community.

The statistical analysis of the two-level fractional model with four central points focuses on gathering the most significant factors in the response, according to that presented in Table 2. Fig. 4 shows the Pareto diagram, which can be used to identify the most significant factors. In the case study, were eliminated the second, third, and fourth-level interactions, as well as the load factor. The velocity factor was maintained to give the experiment greater robustness.

The three significant factors studied are: Rudder angle, vessel velocity, and depth. Likewise, and as required by IMO norms, a factor generator of random errors will be included to design the final experiment. This factor will be the flank on which the maneuver is executed, that is, starboard or port.

The design of the 2^k factorial experiment is shown in Table 3, with two central points and four factors, i.e., 18 runs in total. This process permitted eliminating a factor and insignificant interactions, as well as optimizing the number of runs against what was initially sought through a design with three factors of three levels each (Velocity, depth, and rudder), along with two discrete factors with two levels each, that is, load condition and flank of the maneuver. In total, the number of runs was reduced from a value of 108 (3^3 x 2 x 2) to merely 18.

The number of runs defined in Table 3 is justified from the scientific interest point of view of the present research to validate the mathematical models of vessel maneuverability with non-conventional propulsion systems navigating in shallow waters. The low and high values of the factors described differ from those shown in Table 2 for practical reasons. In the case of depth, it is conditioned by the area where the maneuvers take place within the Cartagena Bay, finding only constant depths between 2 and 3 meters, for ratios of h/T = 2.2 and depths greater than 13 meters for the case of ratios of h/T > 10 in which it is considered that there is no canal effect. Similarly, before the formal start of the tests, It was decided to increase the angle of incidence of the water jet from the pumps, increasing it from 10 to 20 degrees, given that there is no significant response effect upon the vessel with lower angles.

Table 2. Screening experiment design for Turning Diameter

Base Design
Number of experimental factors: 4
Number of blocks: 1
Number of responses: 1
Number of runs: 12, including 4 center-points per block
Error degrees of freedom: 4
Randomized: Yes

Factors	Low	High	Units	Continuous
Ship Speed	3.0	9.0	knots	Yes
Load Condition	LIGHT	FULL		No
Water Depth	1.5	10.0	meters	Yes
20,3	5.0	15.0	degrees	Yes

Responses	Units
Turning Diameter	m/L

Table 3. Factorial experiment design for Turning Diameter

Design name: Factorial 2^4
Comment: Turning Circle
Base Design
Number of experimental factors: 4
Number of blocks: 1
Number of responses: 1
Number of runs: 18, including 2 center-points per block
Error degrees of freedom: 7
Randomized: Yes

Factors	Low	High	Units	Continuous
Ship Speed	STRB	PORT		No
Load Condition	3	12	meters	Yes
Water Depth	3	9	knots	Yes
20,3	10	20	degrees	Yes

Responses	Units
Turning Diameter	m/L

Fig. 4. Pareto Chart for Turning Diameter

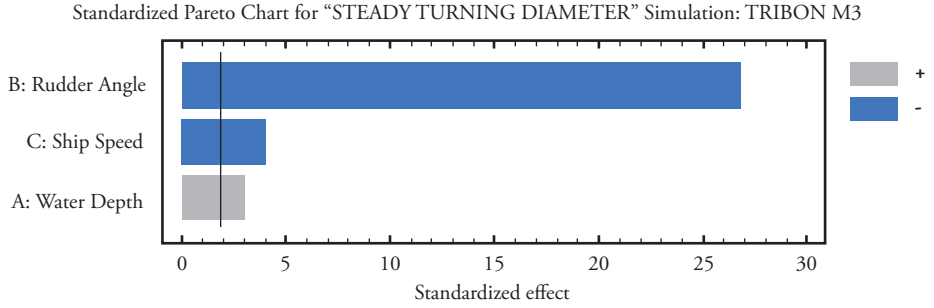

Fig. 5. Contour of the estimated response surface for Turning Diameter

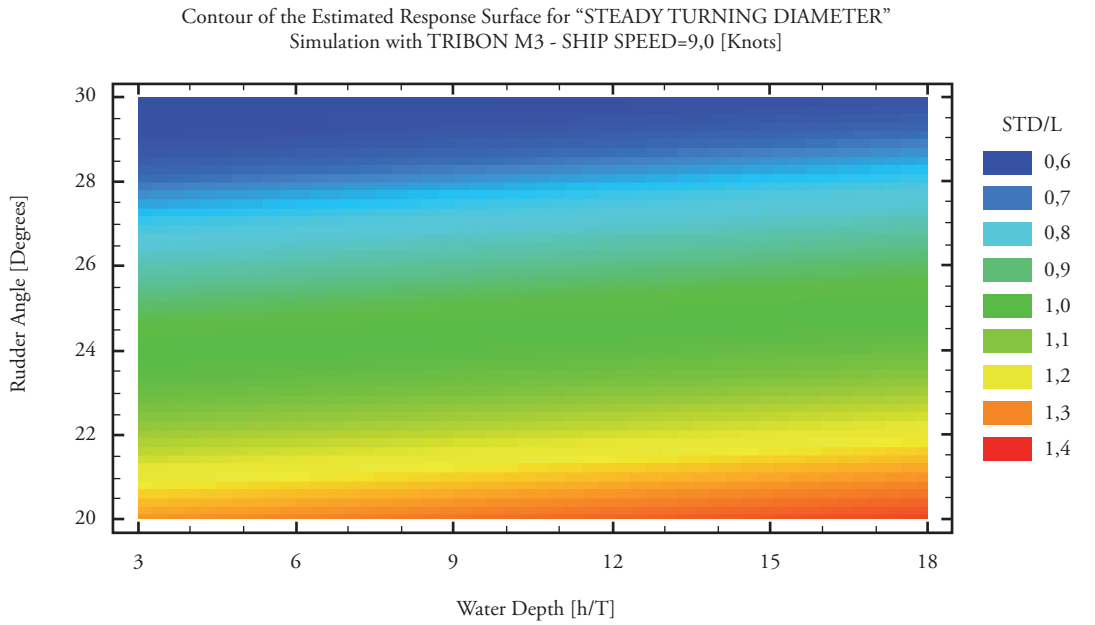

Recommended Maneuverability Trials

The maneuverability trials seek to determine vessel behavior in the change or coursekeeping ability, route stability, and ease of turn; said features can be evaluated quantitatively given that they are directly related to the magnitudes measured during the execution of the trials.

SNAME [15] has conducted sea trials to evaluate maneuverability; in 2002, IMO adopted Resolution MSC 173(76) which exposes the standards and maneuverability characteristics that must be complied with by each vessel. That same year, ITTC exposed three documents containing the procedures to conduct full-scale sea trials of vessels and in 2006 the European Union adopted directive Nº 2006 C/166-E/01 which established the maneuverability requirements to be complied by vessels navigating the European riverine network.

According to the final report and recommendations to the 22nd ITTC (2005), among the maneuverability trials recommended by several organizations, COTECMAR selected zig-zag, turning circle, reverse spiral, and emergency stop to evaluate maneuverability in the RSPV "ARC STCIM Edic Cristian Reyes Holguin".

Data Acquisition System

Data acquisition during the sea trials was conducted in distributive way by using different types of sensors, integrated in centralized and synchronized way through a portable computer and data acquisition and digitization cards. The data obtained from the acquisition system were sampled according to ITTC recommendations

Table 4. Instrumentation recommended by ITTC

Heading	Position	Speed	Rudder angle	Shaft RPM	Rate of turn	Torque
Gyrocompass	GPS	GPS	Angular Potentiometer	Tachometer	Heading change per second	Strain Gauges

(0.5 - 2 samples per second); these are stored in the computer for post-processing and to obtain information on the maneuverability characteristics of the vessel by quantifying the evaluation parameters. Table 4 specifies the instrumentation recommended by ITTC [9] and [16].

The instrumentation used to carry out sea trials in COTECMAR (Table 5), selected according to ITTC recommendations, can provide a time history of the measurements during the execution of the maneuvers.

Table 5. Data acquisition equipment

Parameter	Units	Measurement equipment	Range	Accuracy
Heading	Degrees	Gyroscope 3d	0-360°,-180-+180°	<1.0°
Position & Course	degrees/min/s	GPS	-	<10m
Speed	Knots	GPS	0-9kn	0.05m/s
Rudder angle	Degrees	Linear Potentiometer	0-360°	0.05Ω
Angular velocity	RPM	Optical sensor	1-250000RPM	-
Rate of turn	degrees/s	Inertial gyroscope 3d	±300°/s	-
Wind speed	Knots	Anemometer	0-86.9kn	±0.87kn
Wind direction	Degrees	Vane	0-360°	-

Data corresponding to time, heading, course, position, speed, and rate of turn are gathered from the bridge; while torque and angular velocity of propeller shafts, direction and wind speed are collected from the engine room. The sensors, interfaces, and input sources installed in the engine room are integrated on portable equipment that permits the connections of the equipment required for each trial and which also has wireless or cable communication with the PC located on the bridge. The data acquired are collected by using an application developed via LabVIEW. Fig. 6 shows the location of the instrumentation used in the RSPV sea trials.

Performance of the Experiment

COTECMAR conducted full-scale sea trials on the "ARC STCIM EDIC CRISTIAN REYES HOLGUÍN", last vessel of the third generation of RSPV, in the Cartagena Bay on the Colombian Caribbean Coast (Fig. 7) during March and April of 2009 in shallow waters (h/T = 2.2) and deep waters (h/T = 24). The tests on 6-m depths, corresponding to the two central points defined in the experimental design, were not possible because of difficulties in finding a safe navigation zone within the Cartagena Bay.

The selection of the area for sea trials was carried out by the Hydrographic Area of the Colombian National Navy's Center of Oceanographic and Hydrographic Research (CIOH, for its name in Spanish), who also participated in conducting the tests with the acquisition of position data by using a Differential Global Positioning System (DGPS) and then providing trajectory images and data of the tests processed by using the HYPACK software, high-precision information used in data validation.

HYPACK is a hydrographic software that integrates the necessary tools for each of the hydrographic

Fig. 6. Data Acquisition System

Fig. 7. Area of sea trials

Source: CIOH

survey stages[1]; CIOH carries out marine depth surveys under the single-beam system, with an echo-probe and a DGPS complemented with the HYPACK MAX package, generating a relief map of the seafloor with useful information for surface navigation. HYPACK MAX permits configuration of geodesic parameters (zone, ellipsoid, geoid model) so that it provides the position data in geographic and plane coordinates; for the calculations necessary to analyze maneuverability, it is more convenient to use the data in plane coordinates.

Data Processing

The following was the procedure for data processing:

1. Data filtering: it is the first item performed in the information analysis procedure, considering that there is always noise included in the signals acquired. Tool used: Microsoft Excel (Mathematical Software).

[1] HYPACK MAX (single-frequency echo-probes), HYSWEEP (multi-beam echo-probes). DREDGEPACK (dredging), planning and design of the work, acquisition, and editing of data, final product (volumes and plotting)

2. Synchronization over time of data acquired: carried out to synchronize over time the data acquired by the COTECMAR data acquisition system with data acquired by CIOH (DGPS). Tool used: Microsoft Excel.

3. Interpolation: carried out on files of incomplete data in fractions of time. Tool used: Microsoft Excel.

4. Smoothing of data acquired to analyze some signals that were more affected by noise, signals like drift and yaw rate. Tool used: STATGRAPHICS Centurion XV© Version 15.2.14.

5. Synchronization of data with the initial test heading is necessary to start the information analysis.

6. Identification of critical points, bearing in mind information of speed, heading, and balance.
   - Start of maneuver
   - Rudder order
   - 90° heading variation
   - 180° heading variation
   - Complete maneuver or start of spiral

7. Correction for wind and current according to recommendations by the OMI "Resolution A. 751(18), 1993" [5] for maneuvers whose trajectories were deformed by the effects of wind and current during tests.

8. Graphing the time series that describe vessel behavior during tests, under transitory and steady state, for speed, heading, course, drift, yaw rate, and roll. Tool used: Microsoft Excel.

9. Calculation of variables: turning diameter, tactical diameter, advance and transference; necessary to conduct the analysis of vessel ease of turn and change of course.

10. Graphing the path followed by the vessel in each test, taking into account that the information of position per second corresponds to plane coordinates, it was only necessary to translate and rotate the trajectory. Tool used: Microsoft Excel.

11. Processing and analysis of images from videos taken during tests to extract heading information in instances where it was not possible to obtain such by means of the gyroscope and validate it in cases in which it was possible to acquire said information. Tool used: Boat_Tracking[2] [17].

    Processing of video image analysis consists in tracing a straight line between two points located on the image of the vessel, one on the bow and another on the stern, the angle of this line with respect to the cardinal points would be the heading of the vessel if the videos had been made on the horizontal plane; however, given that the videos were filmed from a building, the straight line (with determined position) determining the heading of the vessel, is found on another reference heading and, thus, the straight line is defined by the heading, as well as a slope. To measure the heading, it was necessary to find the projection of the horizontal plane in real magnitude and in consequence of the "θ" slope (Fig.8). Once the slope is found, the horizontal projection can be made and the heading value can be found via Equation 2.

$$\theta = \tan^{-1}\frac{H}{D} \quad (1)$$

$$\psi = \operatorname{atan}\left(\frac{\vec{y} * \operatorname{sen}(\theta)}{\vec{x}}\right) \quad (2)$$

    Where $\vec{x}$ and $\vec{y}$ are measured in the video as the components of the straight line traced between the vessel's bow and stern.

12. Graphing response surfaces and Pareto diagrams for variables of turning diameter, tactical diameter, advance, and transference. Tools used: STATGRAPHICS Centurion XV©.

[2] Constructed under an environment based on Java "Processing", the software analyzes the heading of the vessel during sea trials.

Fig. 8. Calculation of slope

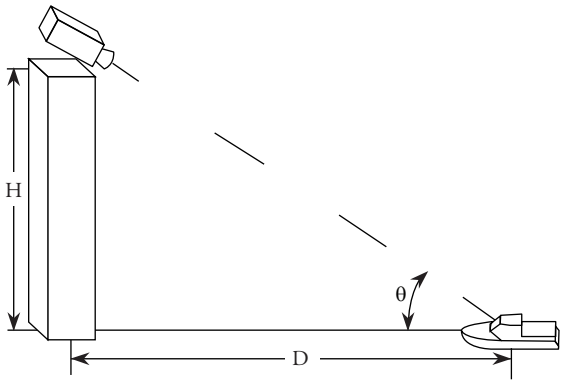

Nomenclature and Reference System

The nomenclature and the reference system described by the IMO in the MSC/Circ.1053, Appendix 1 were used in this research. The mathematical models of vessel dynamics consider the forces acting along the vessel, separated by their components in each axis of the fixed-coordinate system on the G body (*XY*). The vessel's six degrees of freedom are defined by the linear velocities (*u,v,w*) and by the angular velocities (*p,q,r*). For this study, it was sufficient to consider three degrees of freedom on the G plane (*XY*), the vessel moved forward in the "*X*" sense, with a u velocity (surge), on the flank in "*Y*" sense, with a v drift velocity (sway) and rotate around the "*Z*" axis with an r yaw velocity. Fig. 10 shows the vessel's six degrees of freedom, highlighting those considered in the present research.

The vessel's turning circle maneuver, as shown by Fig. 9 and Fig. 11, is carried out on the X_0Y_0 plane; the origin of this system coincides over time t=0, with the longitudinal position of the vessel's center of gravity "*G*". The X_0 axis is aimed north, i.e., time zero coincides with the heading (ψ); hence, drift does not exist (β=0) and the course coincides with the vessel's heading (χ = ψ). Once the rudder order is given, the vessel's heading deviates from the vessel's advance direction, with a drift appearing when the vessel describes a circular trajectory. The following are the velocities and angles describing the trajectory and orientation of the vessel:

U : Advance speed
u : Surge in X sense
v : Sway in Y sense
r : Yaw in N sense (angular velocity)
β : Drift angle
ψ : Heading, defines the direction of the vessel's bow
χ: Course, defines the direction of the trajectory of the vessel's Center of Gravity
δ: Rudder angle

The equations that define the kinetics of the turning circle maneuver are as follows:

Ship speed:

$$U = \sqrt[2]{u^2 + v^2} \tag{3}$$

Drift angle:

$$\beta = -\tan^{-1}\left(\frac{v}{u}\right) \tag{4}$$

Course:

$$\chi = \psi - \beta \tag{5}$$

Yaw rate:

$$r = \frac{d}{dt} - \psi \tag{6}$$

Turning diameter:

$$TD = 2x\left(\frac{u}{r}\right) \tag{7}$$

The turning circle is the maneuver conducted on one or another band, starboard and port, with 35° of rudder, or the maximum rudder angle admissible to the trial speed "U", from a straight line approach without heading oscillations. For the case study, It was defined a maximum 20° rudder angle. The main parameters measured in this trial are shown in Fig. 9 and are described next:

1. Advance is the distance covered in the direction of the original course by the midpoint of vessel O, from the position in which the rudder order is given, until the position in which the bow direction has changed 90° from the original heading.

2. Tactical diameter is the distance covered by the midpoint of the vessel from the position in which the rudder order is given, until the bow direction has changed 180° from the original heading.

3. Transference is the distance covered in perpendicular sense to the original course from the position in which the rudder order is given, until the position in which the bow direction has changed 90° from the original heading.

4. Turning diameter in steady state is an important measurement that is verified once the drift, forward speed, and yaw rate become constant and the vessel is describing a circular trajectory.

Fig. 9. Turning test parameters

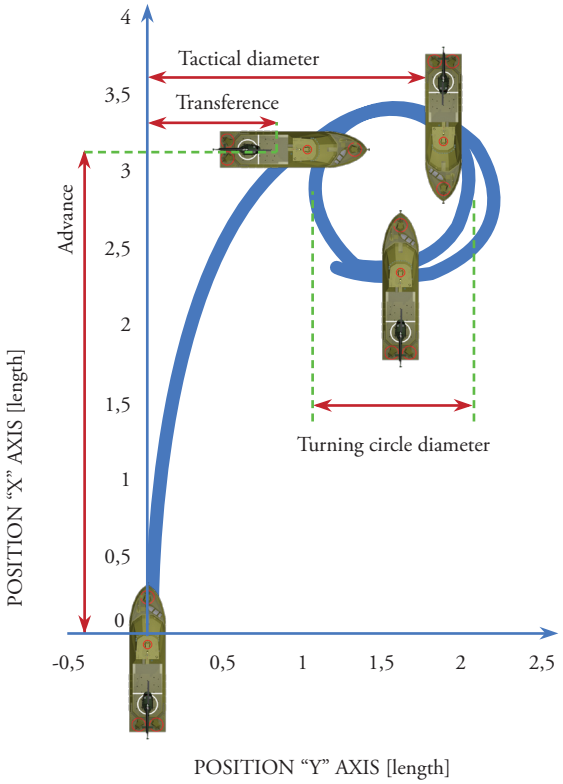

Results of trials

Table 6 presents a summary of the results of the full-scale trials carried out on the "ARC STCIM

Fig. 10. 6 DOF Body-fixed reference frame

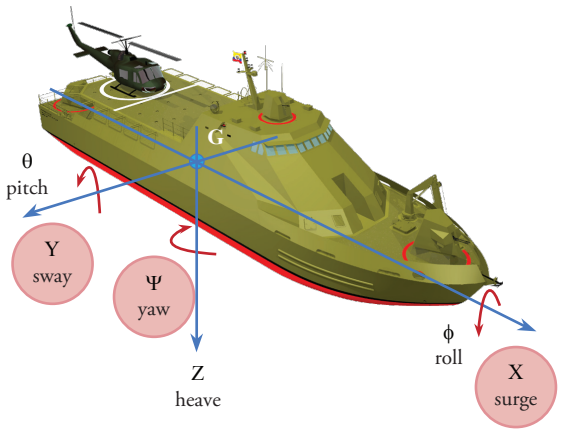

EDIC CRISTIAN REYES HOLGUÍN", after correcting for wind and current; It was considered the average of the results of pairs of maneuvers executed under similar circumstances (equal depth, velocity, and rudder angle) but on different flank, contrasting the results between trials conducted in shallow waters and those conducted in deep waters.

During turning circle trials, It was evaluated the vessel's turning ability, which was considered satisfactory according to IMO if it complied with the following criteria: the values of the results of trials for tactical diameter must be less than 5 L, consider the set of results in Table 6 (2.1 L, 1.1 L, 2.4 L, 1.9 L); additionally, the advance values of the results must be less than 4.5 L, consider the set of results (2.5 L, 1.2 L, 2.4 L, 2.6 L); according to said results, note that the vessel complies with ITTC criteria and, hence, its turning ability is considered satisfactory.

The vessel's turning ability was influenced by the depth of the area of navigation, due to changes in the magnitudes of the hydrodynamic forces and moments acting on the hull and by action of the thrust force and steering generated by the propulsion system. The vessel's turning ability was quantitatively evaluated from the results of the turning diameter, tactical diameter, advance, and transference, whose values, for the case study, diminish as water depth diminishes (Table 6), also the velocity; while values of turn rate increase with diminished depth. In the maneuvers reported at

Fig. 11. Reference axis system

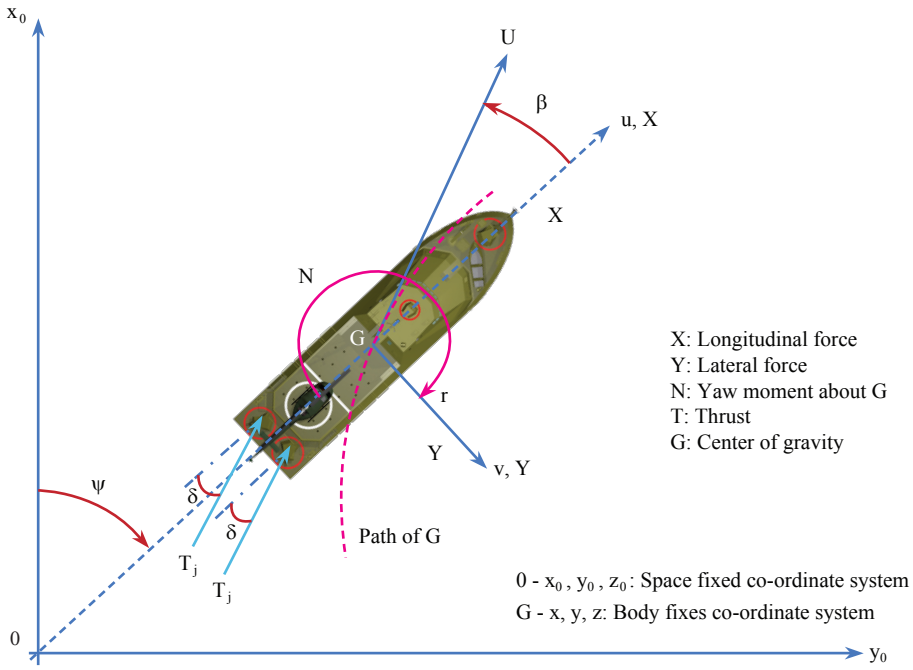

20 degrees of rudder angle no significant change in the drift angle value was observed in the steady state upon varying depth; nevertheless, it was very high.

The contour of the response surface estimated for the turning diameter, processed from the full-scale trials, for advance speed of 9.0 knots, is shown in Fig. 12; evidently, there is improved ease of vessel turn in shallow waters, the effect is even more pronounced than that shown by results simulated with TRIBON M3©, as observed in Fig. 5. Also, Fig. 13 reports the Pareto diagram with the significance of the experimental factors, It is notice that "Water depth" has an effect in the same sense on the "Turning diameter", this effect although in the same sense is much more pronounced than that obtained via simulation with TRIBON M3© (Fig. 4).

The same effect was reported in 1988 by Yasuo Yoshimura and Hitoshi Sakurai, as a result of the study of the maneuverability qualities in shallow waters, conducted with double propeller and double rudder vessels, one wide beam and the other conventional [18].

Similarly, the ITTC – through its 25th committee – reported the same effect due to shallow waters, known as NS type. The results of the study by Yasukawa and Kobayashi in four different models of vessels in shallow and deep waters reported the NS effect, which indicates that the turning diameter for the turning circle trial is smaller as water depth diminishes [10]. This phenomenon is attributed to the increased steering forces generated by the rudder as depth diminishes.

For the case study, given that the RSPV vessel is not equipped with rudders; rather, the steering force is obtained from the direction of the water jet from each of its pumps. It is relevant to assess these forces, as well as their equilibrium with the hull's hydrodynamic forces under different depth conditions. This will be possible in a future investigation, which permits validating a mathematical model based on the time series, trajectories and records taken during full-scale experimenting.

Annex 1 shows the time series of velocity, heading, course, drift, and yaw rate for a maneuver in deep waters (h/T=24) at starboard with 20 degrees of

Table 6. Summary of the Sea Trials turning test

Water Depth	Speed	Rudder Angle	Turning diameter	Tactical diameter	Advance	Transference	Drift	Yaw rate	Advance speed
[m]	[kn]	[°]	[L]	[L]	[L]	[L]	[°]	[°/s]	[U/Uo]
2.2	3	10	1.0	2.1	2.5	1.3	86.8	3.6	0.128
2.2	8.4	20	0.5	1.1	1.2	0.4	70.3	4.1	0.075
24	3	10	2.1	2.4	2.4	1.4	51.5	1.1	0.151
24	9	20	1.0	1.9	2.6	1.1	70.2	3.8	0.098

Fig. 12. Contour of the estimated response surface for Turning Diameter during Sea trials

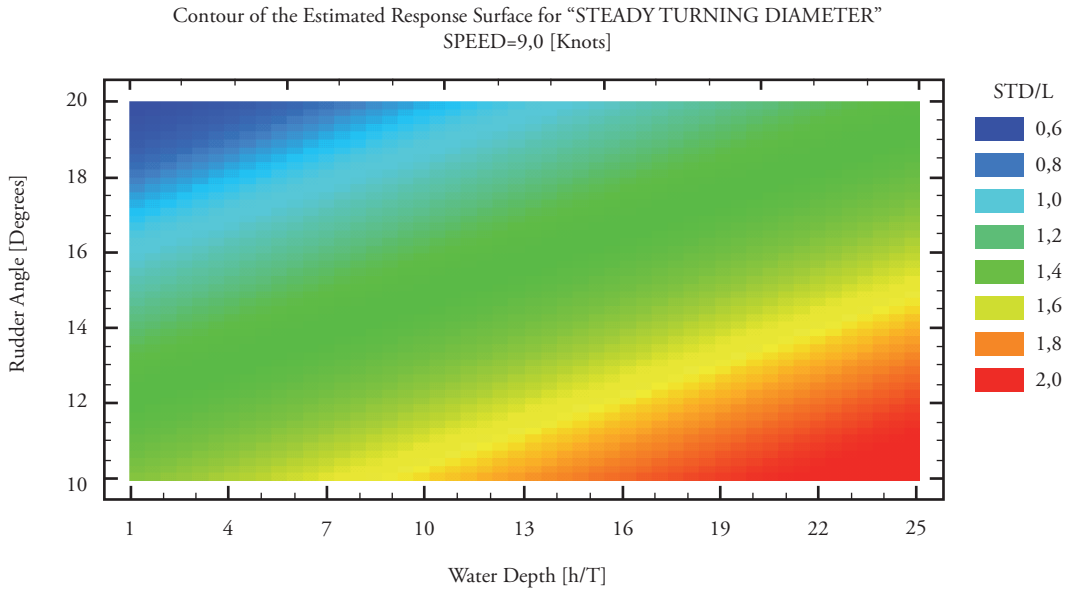

Fig. 13. Pareto Chart for Turning Diameter during Sea trials

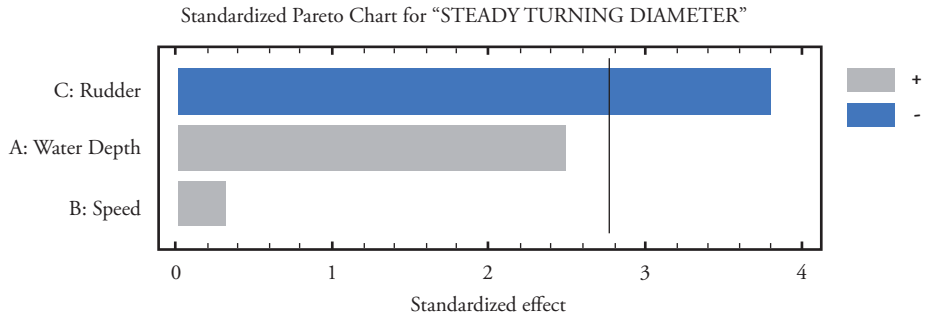

rudder angle and a speed of 9 knots. While Annex 2 shows those corresponding to a maneuver in shallow waters (h/T=2.2) at starboard with 20 degrees of rudder angle and a speed of 8.4 knots.

The time velocity series show the inflection points, indicating the change of maneuver state (vessel entrance to the maneuver, passage to transitory state, and finalization in steady state).

In the time heading and course series, it may be noted that the heading signal responds before than the course signal, because of the rudder action and the external current and wind forces; thereby, the vessel's bow deviates its trajectory with respect to the heading, generating a drift angle.

Annex 1

Time series for turning test in deep water, starboard, 9kn and 20° rudder angle.

Turning test, time series for Advance Speed (U), Deep water, starboard, 9kn and 20° RA

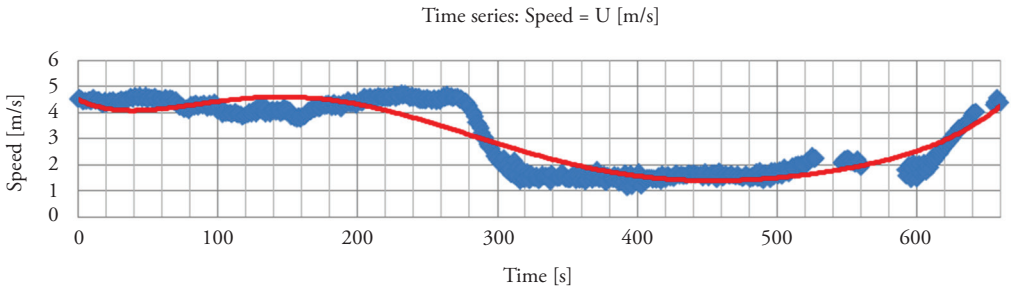

Turning test, time series for Heading (ψ) and Course (χ), deep water, starboard, 9kn and 20° RA

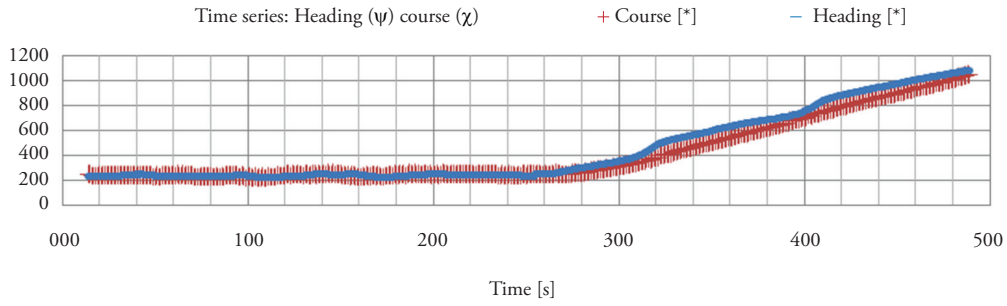

Turning test, time series for drift [deg] (ß), deepwater, starboard, 9kn and 20° RA

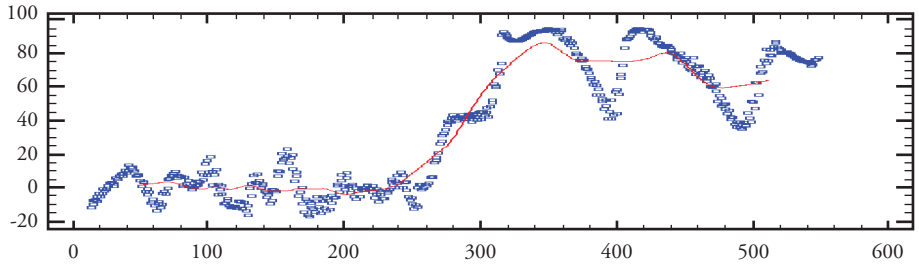

Turning test, time series for Yaw Rate [deg/sec] (r=dψ/dt), deepwater, starboard, 9kn and 20° RA

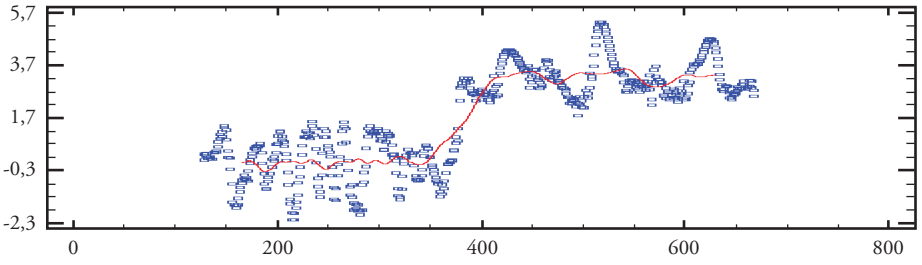

Annex 2

Time series for turning test in shallow water, starboard, 8.4Kn and 20° rudder angle

Turning test, time series for Advance Speed (U), Shallow water, starboard, 8.4kn and 20° RA

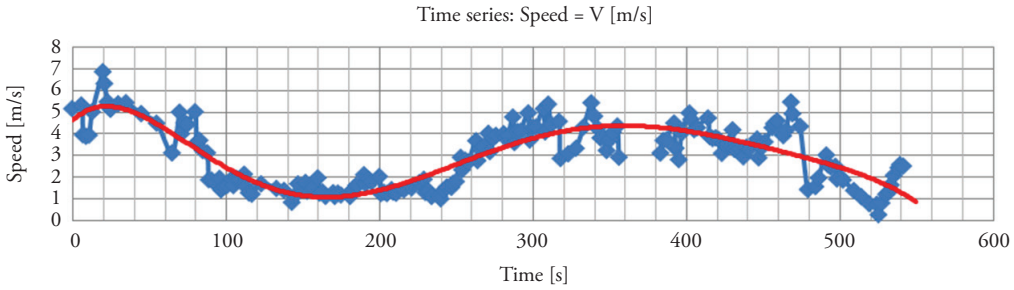

Turning test, time series for Heading (ψ) and Course (χ), shallow water, starboard, 8.4kn and 20° RA

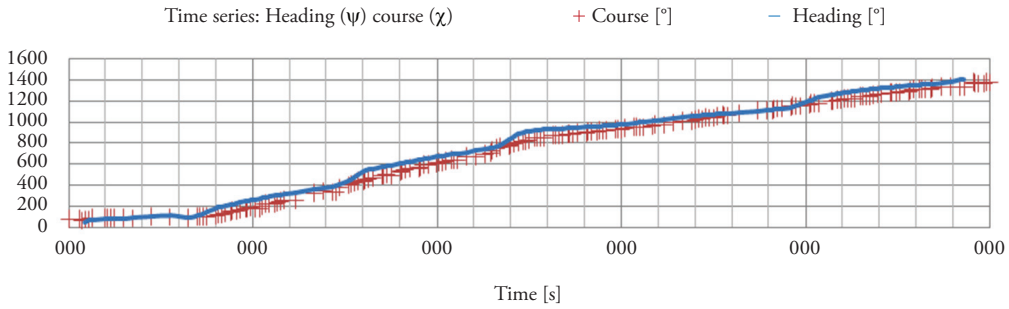

Turning test, time series for drift [deg] (ß), shallow water, starboard, 8.4kn and 20° RA

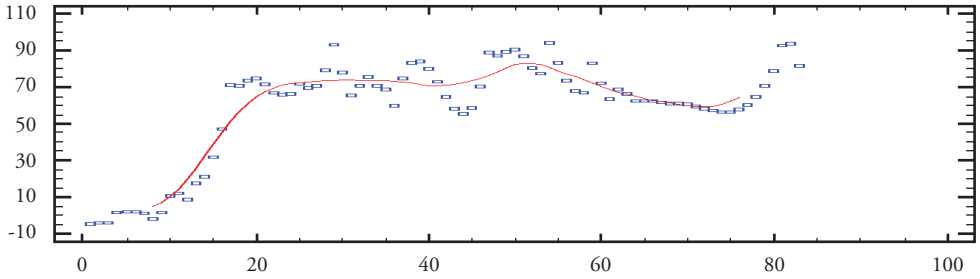

Turning test, time series for Yaw Rate [deg/sec] (r=dψ/dt), shallow water, starboard, 8.4kn and 20° RA

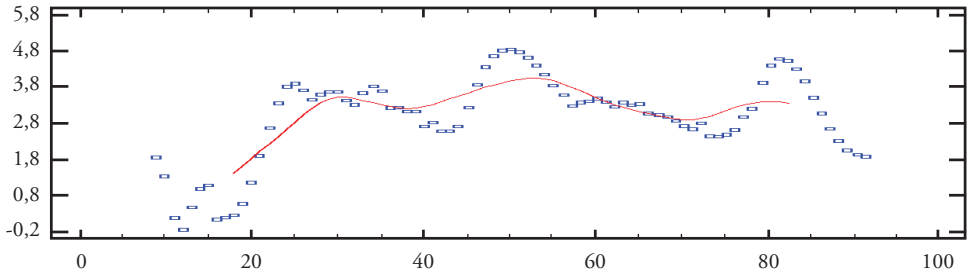

Conclusions

The RSPV vessel fully complies with the IMO standards regarding the ability to changing heading, which was demonstrated by conducting turning circles under conditions of deep waters and 20° rudder angle.

It has been demonstrated that the RSPV vessel's ability to changing heading improves with diminished depth, this is evidenced by diminished turning diameters, advance, and transference when going from depths h/T=24 to shallow waters with h/T=2.2; i.e., it is reported the NS type effect described by Yoshimura and Sakurai in 1984.

It was proved that simulation with mathematical models requires an experimental base that permits adjusting the hydrodynamic forces, as well the interactions among the hull, propulsion systems and steering systems; hence, this work provides elements to validate these models.

Excellent performance is proven regarding the ability to change of heading in vessels equipped with steerable propulsion systems, which provide thrust in any direction; with a 10° angle the RSPV vessel complies with the IMO standards for the turning circle maneuver.

It has been proven the benefit of using experimental design techniques to rationalize resources and obtain quality data covering experimental factors during the previously defined low and high limits, reducing the number of runs from 108 to 18 during full-scale experiments with vessels.

It has been developed and implemented a procedure to validate the vessel's trajectory and the drift angles measured during the trials through digital image analysis.

Acknowledgments

The authors thank the following institutions and individuals for their valuable contributions for the development of this work:

The Colombian National Navy, for making available for the research team the vessel "ARC STCIM EDIC CRISTIAN REYES HOLGUÍN" with its crew and for having provided logistics support required to conduct the trials.

Ship Lieutenant Commander Nicolás Romero and Crew of the "ARC STCIM EDIC CRISTIAN REYES HOLGUÍN" for the enthusiastic participation during March and April of 2009 while conducting maneuverability experiments.

The Colombian National Navy's Center for Oceanographic and Hydrographic Research (CIOH) for technical and human support while conducting the trials, by providing the data processing and measurement system to validate trajectories, as well as selecting the area of operations during March and April of 2009.

Students, Navy Lieutenant Carlos Augusto Estévez Duran and Navy Lieutenant Carlos Enrique Hernández Cruz, who developed in 2008 a "Methodological Guide" within the framework of the present research, thesis required for the degree of Naval Engineer issued by the "Almirante Padilla" Naval School.

Doctor Marcos Sanjuán, professor at Universidad del Norte in Barranquilla, who contributed the necessary knowledge for the authors to carry out the Experimental Design within the framework of cooperation between that University and COTECMAR during the second semester of 2008.

Mr. César Mauricio Quimbaya Sarmiento, who during his industrial practices at COTECMAR as an Electronics Engineering student from Universidad Central in Bogotá during 2008 developed his thesis for the degree of Electrical Engineer, within the framework of the present project, in the conceptualization and preliminary design of the data acquisition system.

Mr. Juan Esteban Villegas, Mechatronics Engineering student from the Antioquia School of Engineering, who during his industrial practices

at COTECMAR during the first semester of 2011 worked in processing the digital images to validate trajectories and drift angles.

References

[1]. CARREÑO, J.E. Proyecto de Tesis Doctoral. 2006. Universidad Politécnica de Madrid, Escuela Técnica Superior de Ingenieros Navales.

[2]. DELEFORTRIE, G. and VANTORRE, M. Modeling the Maneuvering Behavior of Container Carriers in Shallow Water. Journal of Ship Research, No. 4, Vol. 51, December 2007, p. 287–296.

[3]. DIRECTIVA DEL PARLAMENTO EUROPEO Y DEL CONSEJO. Directiva Nº 2006 C/166-E/0. 2006.

[4]. GUEDES, C. FRANCISCO, R.A. MOREIRA, L and LARANJINHA, M. Full-Scale Measurements of the Maneuvering Capabilities of Fast Patrol Vessels, Argos Class. Marine technology, No 1, Vol 41, January 2004, p.7-16.

[5]. IMO. Interim Standards for Ship Maneuverability, Resolution A.751 (18), Nov 1993.

[6]. IMO. Explanatory Notes to the Interim Standards for Ship Maneuverability. Resolution MSC/Circ.644, June 1994.

[7]. IMO. Standard for Ship Maneuverability. Resolution MSC. 137(76), 2002.

[8]. ISLAM, M. Combined use of dimensional analysis and modern experimental design methodologies in hydrodynamics experiments. Ocean Engineering 36, (2009), p. 237–247.

[9]. ITTC MANOEUVRING COMMITTEE. Recommended Procedures. Full Scale Measurements Maneuverability, Full scale Maneuvering Trials Procedure. 2002.

[10]. ITTC MANOEUVRING COMMITTEE. Final Report and Recommendations to the 25th ITTC. 2008.

[11]. KHATTAB, Omar. Multiple regression analysis of the hydrodynamic drifttives for manoeuvring equations. British Ship Research Association, December 1984.

[12]. KIJIMA, K. LEE, S. FURUKAWA, Y and NAKIRI, Y. Ship Manoeuvring Characteristics as Function of Ship Form in Shallow Water. In: Maritime Institute. International Conference on Marine Simulation and Ship Maneuverability MARSIM. June 2006.

[13]. MONTGOMERY, D. C. Diseño y análisis de experimentos, Segunda Edición, Limusa Wiley. 2004.

[14]. SIERRA, E.Y. Diseño y construcción de un equipo portátil que integre los elementos utilizados para las pruebas de mar y estudio de incertidumbre de las medidas, basado en normas y estándares internacionales. Cartagena de indias D.T. y C.2008. Trabajo de grado (Ingeniera Electrónica). UTB. Facultad de ingeniería eléctrica y electrónica.

[15]. SNAME. Guide for Sea Trials. Technical and Research Bulletin N° 3-47, 1989.

[16]. THE SPECIAL COMMITTEE ON TRIALS AND MONITORING. Final report and recommendations to the 22nd ITTC. 2005.

[17]. VILLEGAS, J.E. Herramienta de análisis de videos para apoyar los procesos de recopilación de datos en pruebas de mar. Cartagena de Indias, Julio de 2011.

[18]. YOSHIMURA, Y and SAKURAI, H. Mathematical Model for the Manoeuvring Ship Motion in Shallow Water (3rd Report: Manoeuvrability of a Twin-propeller Twin-rudder ship). KSNAJ, Vol 211, March 1988, p.115-126.

Application-optimised propulsion systems for energy-efficient operation

Sistemas de propulsión de aplicación optimizada para operación energéticamente eficiente

Stefan Kaul [1]
Paul Mertes [2]
Lutz Müller [3]

Abstract

Today, optimal propellers are designed by using advanced numerical methods. Major revolutionary improvements cannot be expected. More essential are the design conditions and the optimal adaptation of the propulsion system according to the operational requirements. The selection and optimisation of the propulsion system based on a systematic analysis of the ship's requirements and the operation profile are the prerequisites for reliable and energy-efficient propulsion. Solutions are presented, which accommodate these issues with a focus on steerable rudderpropellers. Considerations include the efficiency potential of the propulsor itself, optimisation of the engine propeller interaction, and optimisation of a demand-responsive energy supply. The propeller-thruster interaction is complex, but offers some potential for optimisation. Results of examinations show this. The power distribution between multiple propellers at high loads of limited propeller diameters increases the efficiency. This can be done by double-propeller systems like the SCHOTTEL TwinPropeller or by distributing the power on several thrusters. This distributed propulsion offers economic operation and an increased lifetime by means of the demand-responsive use of energy. An efficiency-optimized electric motor instead of the upper gear box reduces the mechanical losses in the case of diesel-electric propulsion. An example: the SCHOTTEL CombiDrive.
Key words: propulsion, efficiency, azimuth steering, cavitation, load distribution.

Resumen

En la actualidad, las hélices óptimas son diseñadas mediante el uso de métodos numéricos avanzados. No se pueden esperar grandes mejoras revolucionarias. Más esenciales son las condiciones de diseño y la adaptación óptima del sistema de propulsión de acuerdo a los requerimientos operacionales. La selección y optimización del sistema de propulsión basado en un análisis sistémico de los requerimientos del buque y el perfil de operación son los prerrequisitos para propulsión confiable y energéticamente eficiente. Se presentan soluciones, que acomodan estos asuntos con un enfoque sobre hélices de timón dirigibles (*steerable rudderpropellers*). Las consideraciones incluyen el potencial de eficiencia del propulsor en sí, la optimización de la interacción entre la hélice y el motor y la optimización de un suministro de energía que responda a la demanda. La interacción de hélice y el propulsor es compleja, pero ofrece algún potencial para optimización; los resultados de las pruebas lo demuestran. La distribución de potencia entre múltiples hélices con altas cargas de diámetros de hélice limitados aumenta la eficiencia. Esto se puede lograr por sistemas de doble hélice como el Doble Hélice de SCHOTTEL o mediante la distribución de potencia en varios propulsores. Esta propulsión distribuida ofrece operación económica y ampliación de vida útil mediante el uso de energía que responda a la demanda. Un motor eléctrico de eficiencia óptima, en vez de la caja de engranajes superior reduce las pérdidas mecánicas en el caso de propulsión diesel-eléctrica. Un ejemplo: El SCHOTTEL *CombiDrive*.
Palabras claves: propulsión, eficiencia, gobierno azimutal, cavitación, distribución de la carga.

Date Received: October 22th, 2010 - *Fecha de recepción: 22 de Octubre de 2010*
Date Accepted: January 27th, 2011 - *Fecha de aceptación: 27 de Enero de 2011*

[1] SCHOTTEL GmbH, Spay/Rhine, Germany. e-mail: skaul@schottel.de
[2] SCHOTTEL GmbH, Spay/Rhine, Germany. e-mail: pmertes@schottel.de
[3] SCHOTTEL GmbH, Spay/Rhine, Germany. e-mail: lmueller@schottel.de

Introduction

Ideal propeller efficiency is derived from the ratio of thrust-to-propeller power, which gives the following relationship as a function of the thrust load coefficient C_{TH}.

$$\eta_{ideal} = \frac{2}{1 + \sqrt{1 + c_{TH}}} \quad (1)$$

$$C_{TH} = \frac{T}{\rho/2 \cdot v_a^2 \cdot D_P^2 \cdot \pi/4} \quad (2)$$

T = thrust
D_p = propeller diameter
v_a = inflow velocity
ρ = water density

These equations clearly show that increasing thrust load coefficient correlates with decreasing potential efficiency of the propeller. This is the case if the thrust requirement is high and/or the propeller diameter is small and/or the inflow velocity is low.

This is basic information and nothing new. It clearly shows, however, that the choice of development parameters significantly influences efficiency.

Fig. 1 shows the efficiency curve of propulsion systems as a function of the thrust load coefficient.

Fig. 1. Efficiency as Function of Load Coefficient

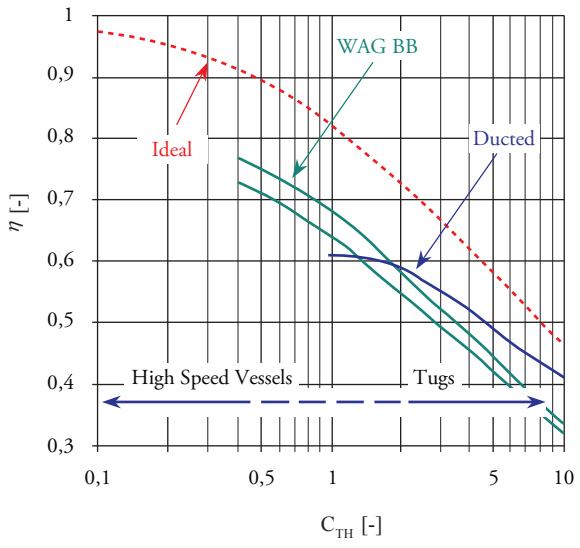

Three approaches are indicated below:

1. Improvement of efficiency by means of double-propeller systems, e.g. STP.
2. Use of multiple-propulsion systems on a vessel.
3. Dosed, load-dependent power distribution, e.g. double-ended ferries.

These measures to increase the efficiency result in further challenges for development engineers, such as calculation of the steering forces, optimisation of the housing with regard to cavitation properties, and interaction of the hull and propeller. Due to the increased power density of the propulsion systems combined with the restricted space for installation and the demands for higher velocities, it is precisely these issues that necessitate great numerical and experimental effort in the development work during design and optimisation.

Propulsion Technology: STP, SCD, Thruster Interaction

STP technology - Interest in improved-efficiency Rudderpropellers began to grow during the early 1990s. The particular reason for this was increasing thrust load and the demand for greater power input in relation to the propeller cross-section, which generally goes hand in hand with efficiency losses.

With multi-propeller systems, on the other hand, in which power is distributed between two or more propellers, it is possible to significantly reduce this disadvantage. Solutions with two contra-rotating propellers have been known for a long time. However, this technology entails a complex mechanical design with twin gear trains and a shaft running within a hollow shaft, involving an elaborate sealing arrangement.

For this reason, SCHOTTEL looked for a simpler solution and developed the principle of the STP based on an analogy with pump and turbine technology. The propellers are mounted here on a single shaft and, thus, rotate in the same direction; in addition, a guide system is installed between the propellers.

Fig. 2. SCHOTTEL Twin Propeller

Fig. 3. Pressure Distribution on an STP Propeller

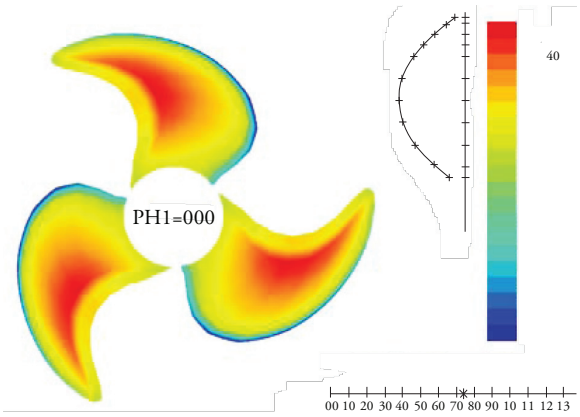

Essentially, two principles are implemented here:

- The distribution of the power between two propellers instead of a single heavily loaded propeller.
- The re-use of the swirl energy generated by the front propeller, which would otherwise be lost.

If a propeller with a limited cross-section must transmit a large amount of power, this presents the designer with a difficult task. The pressure distribution on the blade must satisfy certain criteria. At the blade edges and especially at the tips, it is necessary to reduce the load to avoid losses due to flow around the blade edges. One possibility is to increase the number of blades, although beyond a certain point this increases the grid induction losses, as the losses due to blade interaction are known. It is also necessary to avoid high-pressure gradients in the distribution, otherwise cavitation may result.

The distribution of power between two propellers permits a much more homogeneous distribution of the pressure and ultimately significantly improved blade geometry with greater efficiency. As a result of the load distribution, global cavittion is no longer a critical factor.

Depending on the thrust load and the design-related pitch, the propeller outflow contains tangential velocity components, which do not contribute to thrust generation and which are generally termed rotational or swirl losses. Fig. 4 shows the proportion of swirl energy as a function of the thrust load coefficient and the pitch.

Fig. 4. Rotational losses $\eta_{Rotational}$ as function of pitch ratio P/D and thrust load coefficient C_{TH}

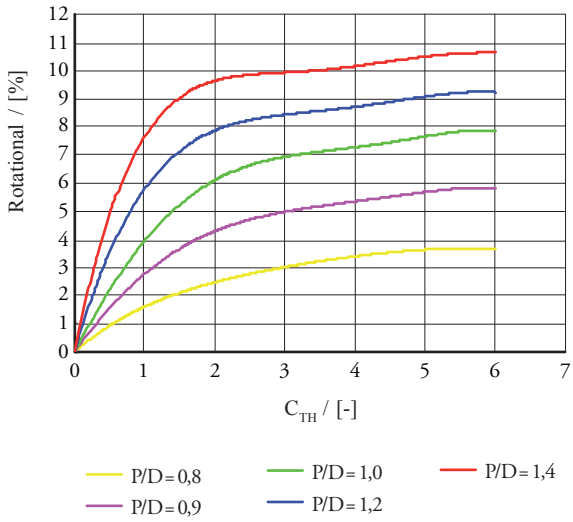

The guide system between the propellers consists of guide fins and the vertical stem of the underwater housing. This interposed guide system deflects the tangential components in the outflow from the front

propeller and redirects them in an axial direction. The lift effect on these guide components gives rise to forces, which reduce the housing resistance and boost forward thrust. As already mentioned, the mechanical components, especially the underwater gear train with its bearing arrangement, require a housing of a certain size. Of particular importance here is the symbiosis of hydrodynamic contour and mechanical expedience.

In general, the mechanical design of the STP does not differ fundamentally from that of the SRP. The propeller shaft extends out of the underwater housing on both sides, allowing a propeller to be mounted at each end. A second shaft seal and two additional exchangeable fins are required. The twin-propeller principle is also implemented in the so-called pod drives. Pod drives have an electric motor integrated in the underwater pod; the propellers are directly mounted on and, thus, driven by the drive shaft of this motor. Both modes of operation are illustrated in Fig. 5.

Fig. 5. TWIN Propeller Principle e.g. STP and SEP

Hence, STP is an integrated total solution, which takes account of all the relevant hydrodynamic aspects.

SCD - The SCD (Fig. 6) is a new form of propulsion system. Instead of an above-water gearbox, it has an electric motor compactly integrated into the support cone of the Z-drive that drives the vertical shaft. In the underwater gearbox, speed is stepped down to the propeller speed in the conventional manner by using a bevel gear stage. This design is highly space saving and combines the advantages of an electric propulsion system with the service-proven reliability of a mechanical Z-drive. The gear losses are reduced by about half due to the absence of an above-water stage.

Fig. 6. TWIN Propeller Principle e.g. STP and SEP

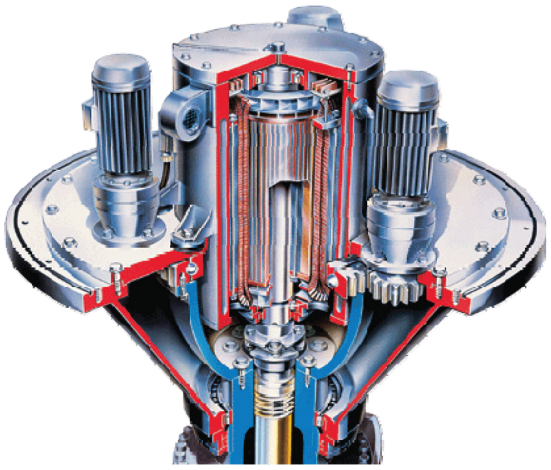

Influence of housing in Z-drives - One extremely important aspect is the design of the underwater gearbox housing. The fineness coefficient of the housing and the ratio of the pod diameter to the propeller diameter have a decisive influence on the overall efficiency of the system. In the design as *push propeller*, the housing disturbs the propeller inflow. Steering the system results in greater irregularity of the inflow, particularly for larger steering angles. This goes hand in hand with the increase in load fluctuations that are transferred via the outer shell and the point of integration into the vessel and have a negative effect on the noise level. This design has the advantage, however, that the housing is not located in the accelerated propeller outflow and can be better counter-balanced, which generally results in significantly reduced steering forces. In the design as pull propeller, the propeller inflow is disturbed less. The housing is located in the accelerated propeller outflow, resulting, on the one hand, in increased housing resistance. On the other hand, the pod and stem act like a rudder with a Costa propulsion bulb. The goal here is to create housings with very low resistance, but which also achieve a high degree of de-swirling. Consequently, a pod shape was chosen for the STP, which not only provides the maximum

diameter at the requisite point, but which also has a remarkably low resistance coefficient (Fig. 7).

Fig. 7. STP Housing

Systematic investigations show the importance of good housing design.

Systems that are not heavily loaded require as slender a housing as possible and a good propeller-to-housing diameter ratio. Fig. 8 shows model test results with four different housing forms. The resistance K_{TZ} of the underwater housing of the rudderpropeller is plotted as ratio of the total unit thrust, K_{Ttotal}, as a function of the thrust load coefficient, C_{TH}. Further influential factors are the propeller pitch and the propeller advance ratio.

Application-adapted Thrusters

The following example is intended to illustrate the possibilities and significance of application-specific selection and design of the propulsion system. SCHOTTEL GmbH fitted five double-ended ferries of the Norwegian shipping company FJORD 1 with four steerable Z-type drives each. The ferries are of identical design; the only difference is in the size of their propulsion systems. The three ferries with the larger propulsion systems can reach speeds of 22 knots, while the two ferries with the smaller propulsion systems achieve speeds of 18 knots. The ferries have been in operation on coastal and fjord routes in southern Norway since the end of 2006.

The propulsion systems in question are gas-electric-driven with high demands on availability, redundancy, and stopping, acceleration and manoeuvring characteristics, particularly in highly confined cruising areas. For this reason, a comfortable power reserve was planned into the four propulsion systems fitted.

Fig. 8. $K_{TZ}/K_{Ttotal} = f(C_{TH})$ for different housings

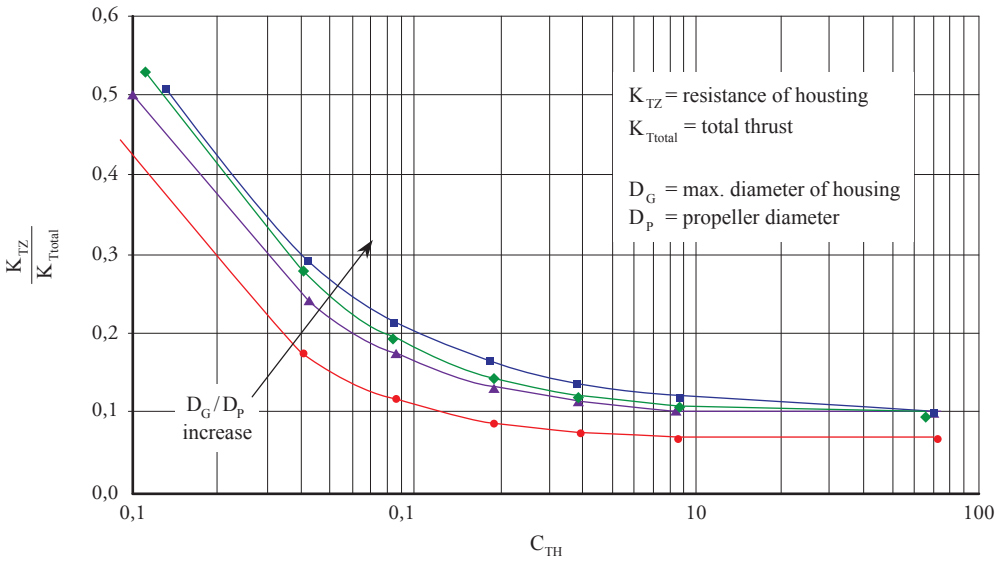

Fig. 9. Double Ended Ferry Fjord 1 FANAFJORD

Principal dimensions and propulsion units:
L_{OA} = 129.80 m
L_{PP} = 122.40 m
LWL = 128.87 m
BOA = 18.70 m
T_{Max} = 4.10 m
Disp. = 3899 t

Thruster SCD 2020
P_{Input} = 2750 kW
n_{Input} = 800 min-1
i = 3.154:1
D_p = 2650 mm
η_{Mech} = 0.975

Thruster STP 1515
P_{Input} = 1800 kW
n_{Input} = 1000 min-1
i = 4.470:1
D_p = 2400 mm
η_{Mech} = 0.950

Problem description - It is no exaggeration to describe the operation of the ferries as "extreme". Speeds in excess of 20 knots (here 21 – 24 knots) remain the exception with conventional, mechanical Z-drives and require special measures in terms of design and housing geometry. Furthermore, the ferries and the propulsion systems are subjected to massive deceleration on every crossing to keep idle times as short as possible. This is achieved by reversing the Z-drives at full speed before entering the harbour; thereby, reducing the speed of the vessel to approximately 10 knots. The loads generated correspond to a crash stop manoeuvre, with the difference that this is not a one-off or rare emergency occurrence, but a frequently recurring standard manoeuvre.

Fig. 10. SCD Functional Principle

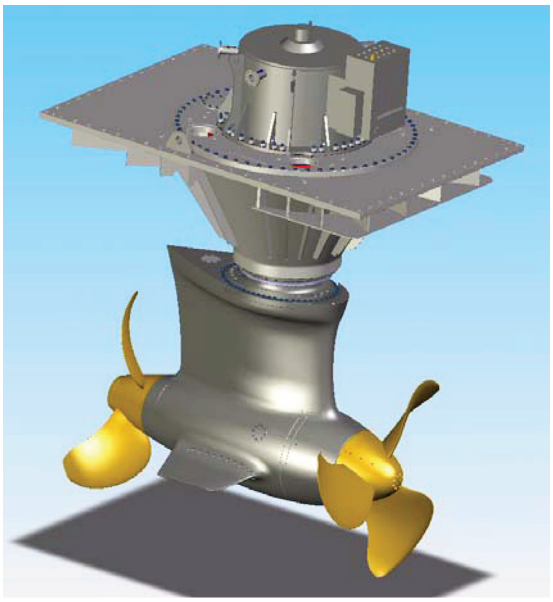

The highly narrow design of the vessels with extremely V-shaped frames generally requires the use of a head box. Major design effort is required to achieve a configuration that generates as little resistance as possible. CFD provides a good means of implementing an effective draft process. The vessel shape described still results in a large distance between the hull and the housing, leading to a large lever arm. The mechanical structure has to meet these high demands, while the design has to improve the housing geometry with a view to flow separation, housing resistance and cavitation.

The two measures necessary here, in the fields of mechanical engineering and fluid dynamics, mutually hinder one another:

- The propeller torque that can be transferred determines the necessary diameter of the force-transferring crown wheel in the underwater gearbox. This defines the smallest possible pod diameter.
- The dimension of the lower vertical shaft bearing at the transition from stem to pod defines the smallest possible profile thickness of the stem at this point.

- The connecting flange of the underwater gearbox to the support cone with its foundation in the vessel must be dimensioned to absorb the lateral forces, steering and bending moments generated and must, therefore, not be smaller than a certain minimum necessary dimension.
- The housing structure must be subjected to a thorough FEM analysis to achieve sufficient stiffness with the smallest possible wall thickness and size by means of suitable ribbing and wall geometry.

The fluid dynamics formula is simple: "as slender as possible" or "as small a thickness: length ratio as possible" for the housing profiles. It must also be considered that it is a steerable drive and, thus, permanently subjected to moderately oblique inflow during corrections to the course, e.g. by the autopilot.

The pitch of the propellers at high speed is high; so too, as a result, are the tangential velocity components towards the housing. Already in the case of small steering manoeuvres, the superposition with the flow around the vessel leads to a considerable change in the angle of attack on the stem. In a steering angle range of +/- 10°, erosive cavitation should be avoided under all circumstances.

This problem is alleviated, to a certain extent, by the use of TwinPropellers with corresponding power distribution, as the load and pitch of the front propeller acting on the housing stem are considerably lower than with a single, highly loaded pull propeller. To check the cavitation properties, a cavitation test was carried out for the existing standard housing (Fig. 7). For design reasons, the crown wheel is located to the rear; this explains the unusual shape which has, however, proven its worth for normal velocity ranges. The cavitation test revealed that the current standard form is not suitable for high velocity. Fig. 11 shows the suction side of the stem with massive, highly erosive cavitation, which increases still further with oblique inflow. The development process for a new housing was based on these findings. During this process, all necessary disciplines repeatedly passed through several stages:

Fig. 11. Cavitation Observation

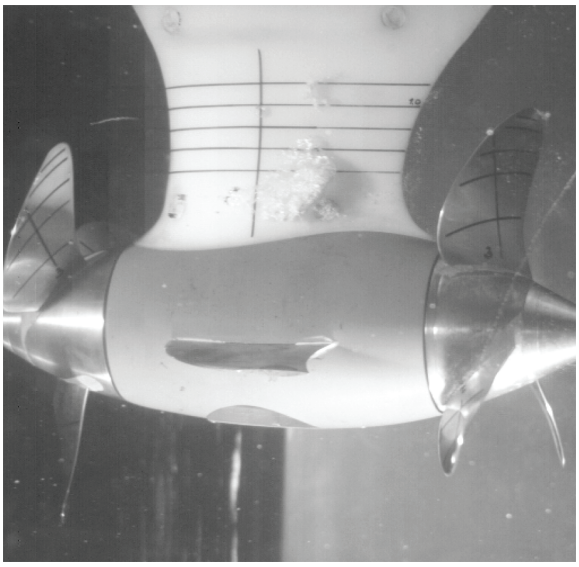

Housing draft – determination of the hydrodynamic loads in the open-water test with different swivel angles – testing of all mechanical components by means of FEM (strength, weight, availability of parts, mountability…) – strengthening or streamlining as required – revision of the housing contour.

Only this time-consuming procedure could ensure that all limits were exploited to the fullest and that an optimal compromise between mechanical and hydrodynamic demands was achieved. To this end, it is necessary to know the hydrodynamic loads and their dynamic amplitudes with a very high degree of accuracy. For this purpose, a special model drive was developed at the Potsdam Shipbuilding Research Establishment (SVA) that is able to measure separately not only the global forces on the Z-drive, but also the forces and torques on the propellers, the stem, the nozzle, and the mounting and bearing points. Fig. 12 illustrates the principle of this drive and Fig. 13 shows an example of the curve for the torque coefficient with dynamic components during a steering manoeuvre from 0° to 180°.

Fig. 14 shows a draft of the new housing shape as a 3D model. Care was taken to ensure that the length

Fig. 12. New Model Drive

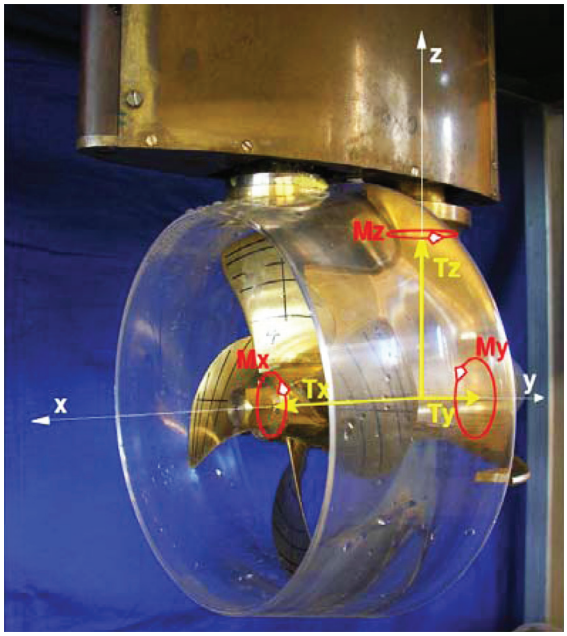

of the drive only needs to be increased slightly. Limiting factors here include the need to be able to uninstall the unit upwards with the vessel afloat. It was only possible to reduce the thickness of the stem profiles slightly, so streamlining of the profiles had to consist essentially of stretching the profiles. It was possible to reduce the thickness:length ratio in the central sections by approx. 30% from t/CL = 0.35 – 0.45 to t/CL = 0.26 – 0.30. The design was modified to move the crown wheel from the rear to the front, resulting in a number of positive effects:

Fig. 14. New Design

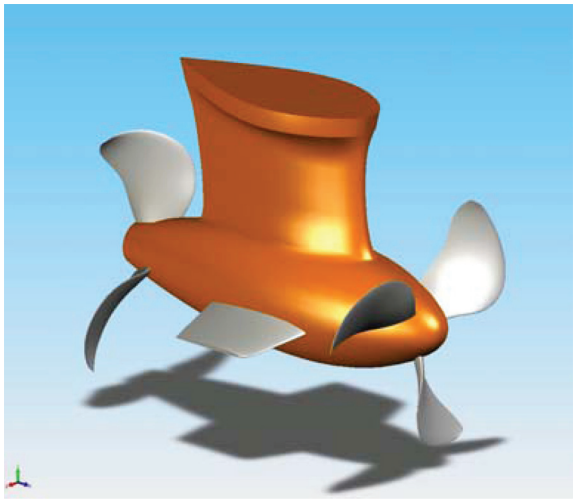

- The vertical shaft bearing partially disappears into the pod itself.
- The stem profile in the connection area becomes more slender.
- The installation cover on the underwater pod, which also demonstrated massively erosive cavitation, can disappear almost completely.

The steering axis of the drive can be moved further towards the leading edge; this means that due to the return torque caused by the larger area behind the rotational axis, the steering torque itself is reduced, despite the enlargement of the surface. The pressure characteristic along the pod and the stem profiles is more harmonious and aligned in

Fig. 13. K_Q Characteristic During Steering

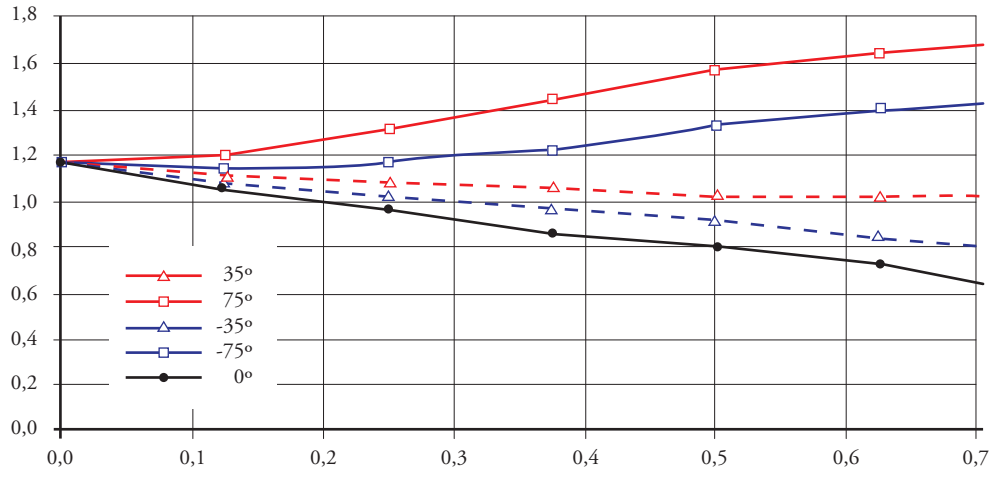

the same direction. In the standard housing, the thickness of the stem profiles decreased in the outlet, while that of the pod increased, resulting in an inverse pressure characteristic.

The propeller blades were designed to be positioned on the hub as far away as possible from the stem and systematically adapted to the housing. The front propeller was optimally drafted first, and then the wake field at the location of the rear propeller was measured by laser (LDA) with the front propellers running. The wake field consists of the outflow of the front propeller and the influence of the housing combined. The rear propeller was then adapted and the overall system was tested in open-water, steering and cavitation tests at the Potsdam Shipbuilding Research Establishment.

Results: With an angle of attack of 0° and +/- 10°, the housing is absolutely free from cavitation (Fig. 15). With the exception of a slight tip vortex, the intensity of which depends on the angle of attack, the propellers are also free from cavitation. It was possible to reduce the housing resistance compared with the previous variant, resulting in 68% efficiency at the operating point of the overall system. This excellent value was also confirmed in final tests at *MARINTEK* in Trondheim.
High velocities of vessels...

- place demanding new requirements on the flow shape of a Z-drive
- lead to high hydrodynamic loads as a result of high inflow velocity and large profile lengths
- require high-strength mechanical components of low weight and with compact installation space
- demand the best possible compromise of hydrodynamic and mechanical requirements.

Fig. 15. New Design – Cavitation Test

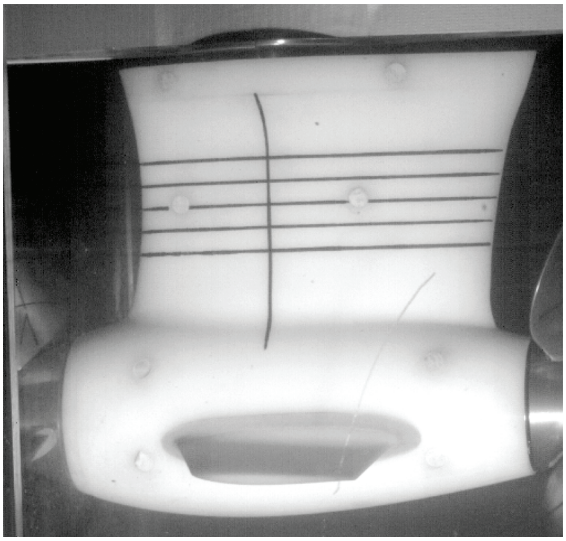

It is, nonetheless, possible to avoid housing cavitation with relatively little, but intelligent modification work. Comprehensive, all-encompassing tests are required, however. Complex simulations help to reduce the highly time-consuming and costly model tests. The key to success is thorough analysis and coordination of all technical disciplines in the design process.

Distributed Propulsion

An even more systematic step is the use of multi-propeller systems. For river cruisers, which must cope with widely varying operating conditions, one goes a step further and installs four double-propeller systems instead of two large propulsion systems. These vessels operate in both deep and shallow waters, and both with and against the current. The power requirements and the operating point of the propeller vary greatly. Velocity ranges from 22-23 km/h in deep water to maximum 15 km/h for typical operation in shallow water. Particularly, for this type of operation, considerable power reserves are required. Draught is limited and the need to minimise pressure variation requires sufficient propeller tip clearance. These demands lead to a very small-diameter, but highly loaded propeller and a flexible, requirement-controlled energy management system. The following Figs. 16 and 17 show the installation of four electrically driven STP 200s with a propeller diameter of 1050 mm and a power rating of 4 x 330 kW. Comparable vessels have tow directly powered diesel STP 440s, for example, with a propeller diameter of 1400 mm and a power rating of 2 x 740 kW.

Summary of the principal advantages:

- Approx. 20% lower thrust load coefficient
- 16% lower power requirement in deep water

Fig. 16. Viking River Cruises

Fig. 17. Installation Proposal

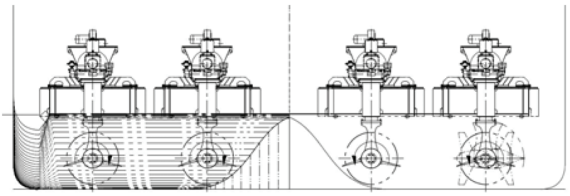

- 12.5% lower power requirement in shallow water
- Reduced wear of the main engine, which is always operated at the optimal operating point, avoiding harmful part load
- Longer service life with low load and/or rolling maintenance
- Significantly greater distance between propeller tips and hull (factor 2)
- First-order pressure variations reduced to 60%
- Reduced extent of the suction side cavitation combined with lower pressure variations for the higher orders
- According to on-board measurements, the significant reduction of the overall pressure variation level resulted in a considerable improvement of the noise level
- Small propulsion systems allow more efficient, resilient mounting with improved damping as a result of the low natural frequency
- Redundancy in the case of failure of a unit
- Lower procurement costs of the smaller propulsion units; use of standard units.
- Reduced risk of grounding in shallow-water operation; yet if grounding does occur, removal and exchange can be carried out anywhere (using a crane) thanks to the low weight, without the need for docking.

Another example is double-ended ferries, which often have high power reserves and multi-propeller systems for reasons of redundancy due to the high wind loads during mooring and casting-off. Load-dependent power distribution fore and aft is highly significant and should be an obligatory part of propulsion tests. Depending on the form of the vessel, active bow propulsion results in very high losses, because the units direct the flow against the hull, destroying thrust. On the other hand, the bow units should not be shut down completely, but generate at least enough thrust to compensate for their intrinsic resistance. If the bow unit only provides little thrust, it is necessarily working with a high propeller advance ratio and, thus, below optimum efficiency. It is therefore useful to have the bow unit generate a certain proportion of the required overall thrust, as this reduces the load on the stern unit, making it more efficient. A sensible compromise is required, which depends both on the operating conditions and on the design of the vessel. A vessel design that takes the thrust losses of the front unit into consideration can significantly improve propulsion efficiency.

Such concepts are also being considered for special vessels in the offshore industry. The aforementioned aspects apply here; also, although the investment costs for larger systems require different consideration. Nevertheless, reliability, service life and high availability resulting from intelligent maintenance logistics play a decisive role. Diesel-electric propulsion systems are well-established in this area. Here, a combination of three propulsion systems is also advantageous. Example of a supply vessel that can be fitted with two or three propulsion units (Fig. 18)

- 8% lower power consumption at operating speed of 15 kn
- 30% thrust reserves for bad weather
- Maximum speed that can be reached is 16.2 kt instead of 15 kt
- Longer service life with low load and/or rolling maintenance
- Redundancy in the case of failure of a unit
- Improved manoeuvrability and lower load in DP

Fig. 18. PX 105

Fig. 19. Propulsion Diagram for SCD application

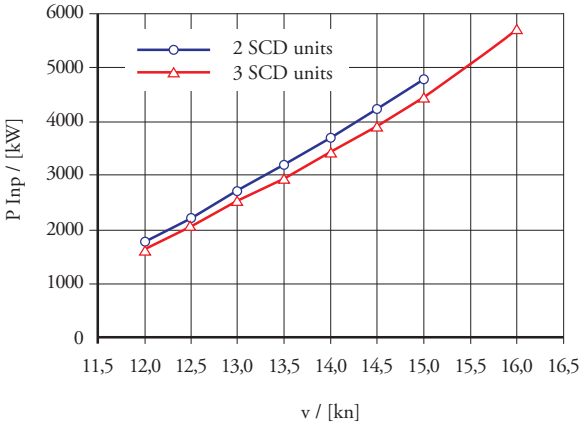

In this connection, a combination of different propulsion systems is also conceivable. The third drive could be a centrally positioned conventional propeller. In this concept, the advantage of high manoeuvrability is coupled with high thrust. One drive configuration that has already been implemented, particularly for fast vessels with high requirements in terms of manoeuvrability, is the installation of an azimuthing propulsion unit as a booster (Fig.20). These vessels have 2 shaft installations (mainly CP propellers) and an additional unit amidships. This offers the following principal advantages:

- The load on the outer units is reduced; this has a positive effect, particularly on noise levels, in the case of fast vessels where comfort is a high priority.

Fig. 20. View of Stern Model Scale and Full-Scale*

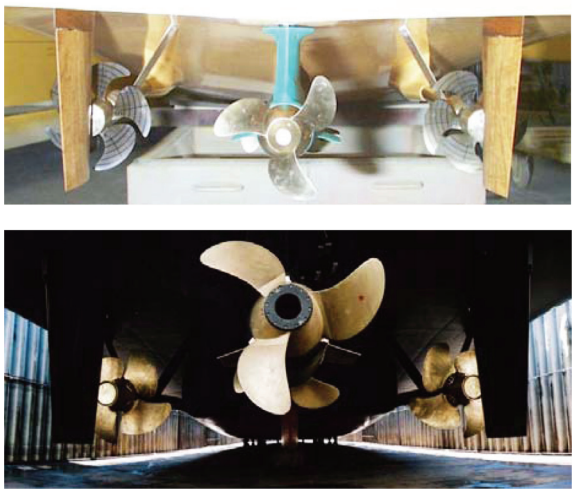

- The maximum velocity of the vessel is increased.
- There are also clear advantages during manoeuvring at low velocity and during positioning.
- Improved crash stop manoeuvrability due to the central unit, as the rudder effect of the main propulsion units is reduced.

Acknowledgement

The author would like to thank Kusch Yacht Projekte GmbH, Germany, for the productive cooperation during the sea trials of the yacht and the enabling of the model test results, including the view from stern of the model.

References

HANDBUCH DER WERFTEN, Band XIII, Schifffahrts-Verlag “Hansa“, Hamburg, 1976, ISBN 3-87700-017-7

J.P.BRESLIN AND P. ANDERSEN. Hydrodynamics Of Ship Propellers, Cambridge Ocean Technology Series 3, Cambridge University Press 1994.

SVA-Report 3093, Freifahrtversuche mit dem SCD2020, Potsdam 2005, unpublished.

SVA-Report 19/3160, Kavitationsversuche mit dem SCD2020, Potsdam 2005, unpublished.

CFD modeling of 2D asymmetric entry impact along with horizontal velocity

Modelado del impacto en dos dimensiones de secciones típicas de botes de planeo con entrada asimétrica y velocidad horizontal

Roberto Algarín [1]
Antonio Bula [2]
Oscar Tascón [3]

Abstract

The 2D impact phenomenon in calm water, considering asymmetric entry and asymmetric entry with horizontal velocity is studied. The analysis was performed by using a commercial CFD software (STAR-CCM+ ©). The results obtained from the simulations are: pressure distribution, force and roll moment. The study was carried out for typical planing boat sections. Furthermore, the critical conditions required for flow separation from the keel are also determined. The results are compared with models and results obtained from some authors and they present very good agreement.

Key words: 2D Impact, CFD modeling, asymmetric entry, keel flow separation.

Resumen

En este trabajo se modela la entrada asimétrica de secciones con ángulo de astilla muerta variable y velocidad horizontal con la ayuda del software CFD Star-CCM+, con el cual se determinan la distribución de presión, la variación de fuerza y momento de rolido durante impacto. Los resultados obtenidos son comparados con los modelos de otros autores para entrada asimétrica logrando gran similitud. Se introduce el efecto de la velocidad horizontal y se analiza el comportamiento de este tipo de secciones, y también se evalúan las condiciones críticas que dan origen a la separación del flujo de la quilla para diferentes cuñas.

Palabras claves: Impacto 2D, entrada asimétrica, superficie libre, modelado CFD.

Date Received: August 20th, 2011 - *Fecha de recepción: 20 de Agosto de 2010*
Date Accepted: January 17th, 2011 - *Fecha de aceptación: 17 de Enero de 2011*

[1] Department of Mechanical Engineering. Universidad del Norte. Barranquilla, Colombia. e-mail: algarinr@uninorte.edu.co, ingmec_83@yahoo.com.mx
[2] Department of Mechanical Engineering. Universidad del Norte, Barranquilla, Colombia. e-mail: abula@uninorte.edu.co
[3] Research, Development and Innovation Direction. Science and Technology Corporation for the Development of the Naval, Maritime and Riverine Industry in Colombia. Km 9, Via Mamonal. Cartagena D. T., Colombia. e-mail: otascon@cotecmar.com

Symbols

B	Beam length.
C_{fy}	Horizontal force coefficient.
C_{fz}	Vertical force coefficient.
C_{mv}	Rolling moment coefficient.
C_p	Pressure coefficient.
f_y	Horizontal Force per unit length.
f_z	Vertical Force per unit length.
m_x	Rolling Moment per unit length.
p	Pressure.
t	Time.
w	Vertical velocity.
v	Horizontal velocity.

Greek Symbols

τ	Time coefficient.
β	dead rise angle.
ρ	Fluid density.

Introduction

The 2D impact phenomenon has been studied through the application of added mass theory, boundary valued problems, and CFD applications. Wagner (1932) applied added mass theory to obtain the lift force in a wedge section, as presented in Fig.1. He also evaluated the pressure distribution assuming potential flow and applying energy conservation. Tveitnes (2001) also studied the impact applying added mass theory. He also calculated the lift force and concluded that the hydrodynamic force experienced by a wedge section under symmetric entry and constant velocity entry, is generated by the variation of mass and flow moment. Moreover, the force exerted during the impact linearly increases as the section submerges and reaches the flow separation at the knuckle. This separation occurs when $z/d = 2/\pi$. From that point, the moment decreases. The behavior in this zone was empirically obtained, showing that the force remains constant after a certain time. The added mass and flow moment coefficients were empirically determined as functions of the dead rise angle. Caponnetto *et al*., (2003) generalized the impact for symmetric entry for sections with variable dead rise angle. He also evaluated the flow separation for section including knuckles. Vorus (1996) studied the 2D impact with symmetric entry for a section with variable dead rise angle, solving the problem as a boundary value problem, assuming potential flow. Based on Vorus (1996), Xu *et al*., (1998) analyzed the 2D impact with asymmetric entry, calculating the pressure, force and roll moment in the section. Seif et al., (2005) simulated the impact by using CFD tools for circular and wedge sections, considering symmetric and asymmetric entry over calm waters with vertical velocity. The results obtained are very close to Wagner (1932) and Toyama (1993). According to results, the surface tension and viscosity effects can be neglected, but the gravity effect must be considered.

Fig. 1. Geometric characteristics of a wedge

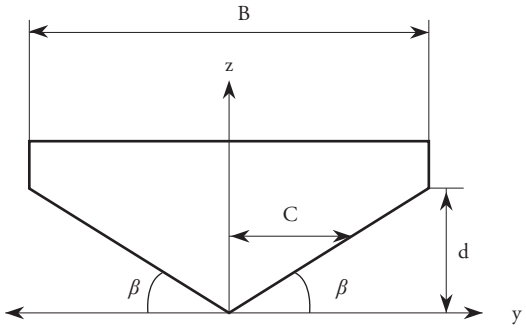

Mathematical Model

To present the results, some variables were defined according to the following equations:

Vertical force Coefficient

$$C_{fz} = \frac{f_z}{\frac{1}{2}\rho w^2 B} \quad (1)$$

Horizontal force Coefficient

$$C_{fy} = \frac{f_z}{\frac{1}{2}\rho w^2 B} \quad (2)$$

Rolling moment Coefficient

$$C_{mx} = \frac{m_x}{\frac{1}{2}\rho w^2 B^2} \quad (3)$$

Pressure coefficient

$$C_p = \frac{p}{\frac{1}{2}\rho w^2} \quad (4)$$

Time coefficient

$$\tau = \frac{wt}{\frac{1}{2}B} \quad (5)$$

Numerical Computation

The conservation of mass and momentum equations were numerically solved. The commercial CFD software (STAR-CCM+) was used as a tool to solve the differential equations that govern the phenomenon. The software uses finite volume approximation, and the equations obtained from the discretization procedure are solved by using an Algebraic Multi-Grid (AMG) solver. The models used to simulate the phenomenon are: multiphase mixture (water-air), inviscid flow, segregated flow, and unsteady (implicit method). For the fluids, water was modeled as an incompressible liquid, while air was considered an ideal gas. To confirm that the viscosity and the surface tension could be neglected, some simulations were carried. The conclusions attained are similar to Seif *et al.*, (2005), where the effects of these two variables were discarded.

The size of the computational domain was developed changing the width and the height to model the impact in calm waters over an infinite canal. The peak force during impact was monitored, and the grid size was selected when the variation of the peak force was less than 1%. The final width and height of the domain were 9B to 10B, and 5B to 12.5B, respectively. The time step was also varied considering the impact velocity and it ranged from 0.008 to 0.016 *d/w*.

The mesh was developed by using polyhedral elements and it was divided in three regions, as shown in Fig. 2a. Region 1 is mainly water; region 2 is a phase mixture, where the hull gets in contact with the water and the air and the free surface is generated. This area is very important for the study and because of this the mesh was refined, as shown in Fig. 2b. Region 3 is mainly air.

Figure 2a. Wedge Section with symmetric entry. Computational domain mesh

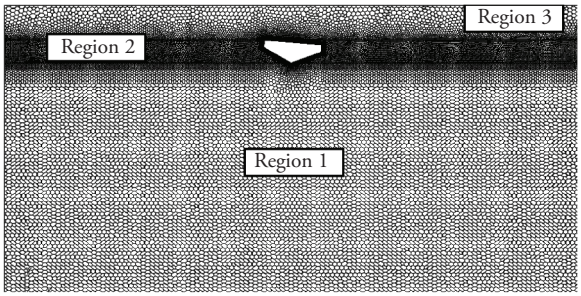

Fig. 2b. Wedge Section with symmetric entry. Mesh in the hull

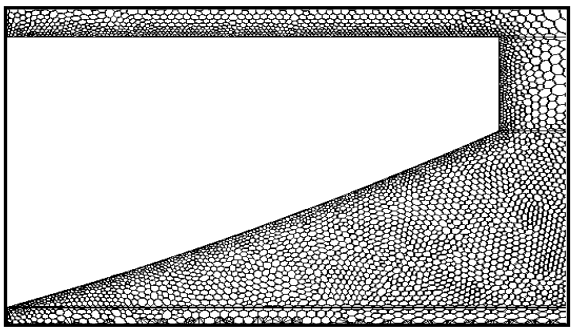

Figs. 2a and 2b show the mesh after a refinement process for a section. The base size of the polyhedral element took values ranging between 0.15B and 0.25B. For Regions 1 and 3, the values ranged between 0.045B and 0.100B. For Region 2, the values ranged from 0.0075B to 0.020B. The residuals values for the impact force, keel pressure, and roll moment were used as the stop criteria, and the magnitude of the global residual was limited to10^{-8}, while the maximum number of inner iterations in each time step was limited to 30.

Results and Discussion

The boundary conditions considered for modeling the asymmetric entry are: constant atmospheric pressure at the top boundary, velocity entry on the base and vertical boundaries, and wall at the hull. The geometries simulated are presented in Fig. 3, and the results are compared with Xu *et al*., (1998).

Fig. 3. Sections evaluated by Xu et al. (1998)

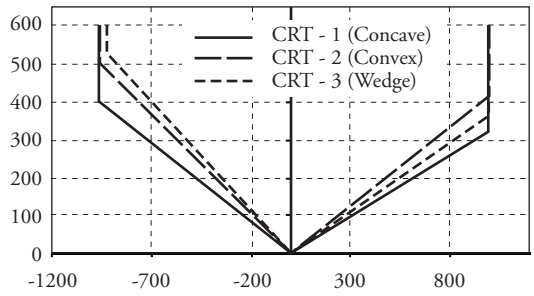

Asymmetric Entrance – No horizontal velocity

Fig. 4, 5 and 6 show the results of vertical force coefficient variation with time for sections CTR-1, CTR-2 and CTR-3.

Fig. 4. C_{fz} vs τ, CRT-1 (Concave section)

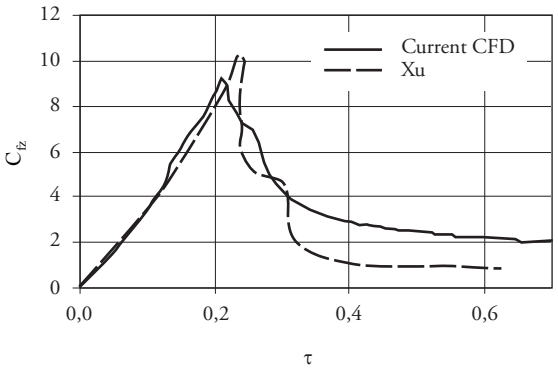

The force on the impact increases while the section immerses until the point where flow separation begins from the knuckle in side 1; after that, the force decreases. There is a second force peak, which appears when the flow separates on side 2; after that, the force decreases. The results show good agreement with the results by Xu L. (1998) before the flow separation of the knuckle. The maximum error in the peak force is 15% respect to the models by Xu L. (1998).

Fig. 5. C_{fz} vs τ, CRT-2 (Convex section)

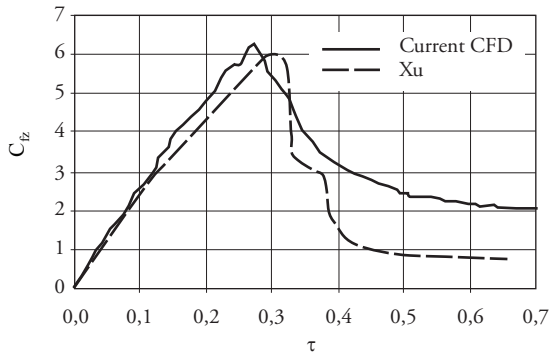

Fig. 6. C_{fz} vs τ, CRT-3 (Wedge section)

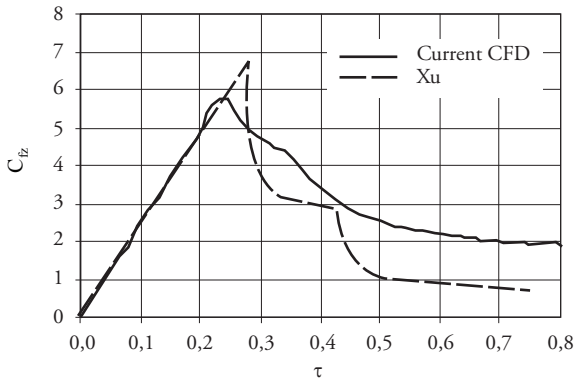

Figs. 7, 8, and 9 show the results of the variation of roll moment coefficient with respect to time for sections CRT- 1, CRT-2, and CRT-3. As the section enters the water, the pressure distribution is asymmetric, generating a restoring moment (roll moment). The figures show that the moment increases up to the point where the flow separates from side 1. At this point, the pressures in this side are higher. When the flow separates from the knuckle, the pressure on side 1 and the moment decrease. On the other hand, the pressure on side 2 reaches a higher value than side 1, reversing the direction of the roll moment. This reversing is presented until the flow separates from side 2.

Figs. 7, 8, and 9 show great similarity with the results reported by Xu L. (1998). The maximum error in the peak moment is 29%, comparing

with that reported by Xu L. (1998). Also, the time required for flow separation is shorter, meaning that the jet velocity of the simulation is higher than that found by Xu L. (1998).

Fig. 7. C_{mx} vs τ, CRT-1 (Concave section)

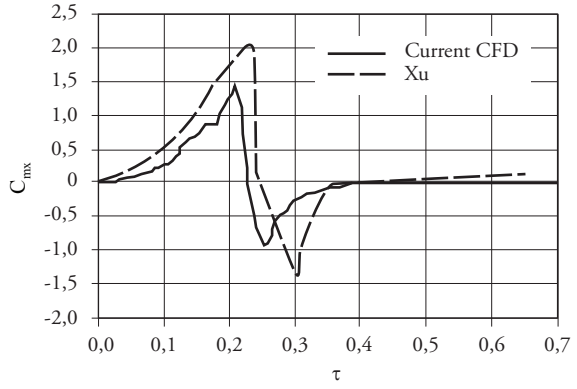

Fig. 8. C_{mx} vs τ, CRT-2 (Convex section)

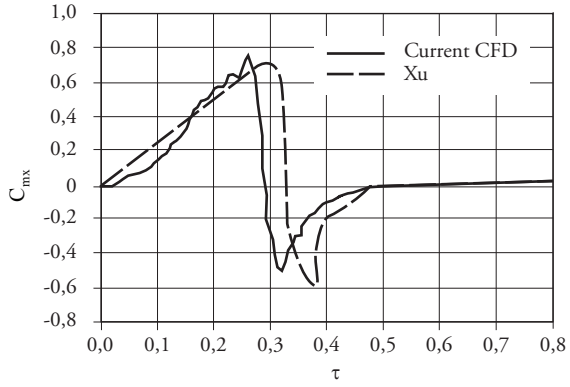

Fig. 9. C_{mx} vs τ, CRT-3 (Wedge section)

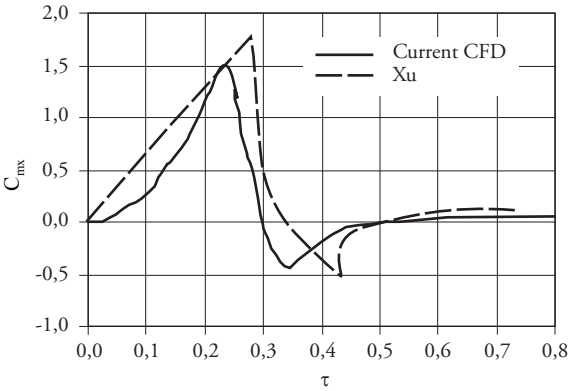

Asymmetric Entrance – Horizontal velocity

The results attained are shown for vertical force and roll moment, and the sections considered are CRT-1, CRT- 2, and CRT-3. The velocity ratios considered for the simulation were v/w= -1.0, 0.0, and 1.0. Figures 10, 11, and 12 show the vertical force coefficient variation with time for sections CRT-1, CRT-2, and CRT-3. Similar behavior is noticed when comparing with asymmetric entrance with no horizontal velocity. The force reaches peaks at the points where the flow separates from the knuckles in both sides. Furthermore, the time required for flow separation is independent from the velocity ratio. The main effect of the velocity ratio is noticed for the peak on side 2; the value obtained increases as the velocity ratio increases. Also, after the flow separation is attained, the force decreases faster when the velocity ratio is increased.

Fig. 10. C_{fz} vs τ, CRT-1, asymmetric entry with horizontal velocity (Concave section)

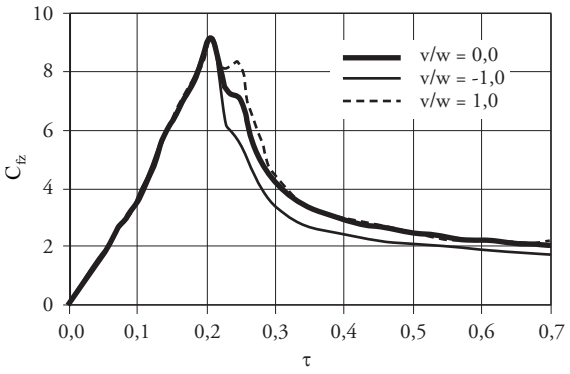

Fig. 11. C_{fz} vs τ, CRT-2, asymmetric entry with horizontal velocity (Convex section)

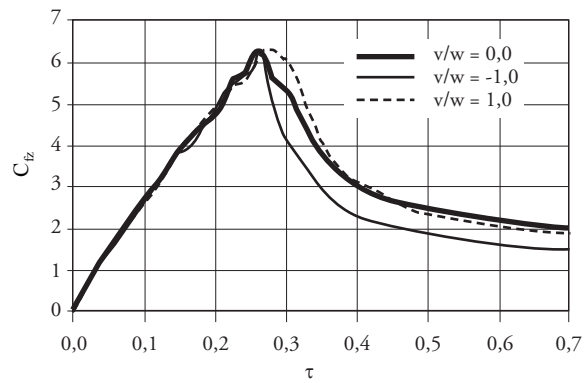

Fig. 12. C_{fz} vs τ, CRT-3, asymmetric entry with horizontal velocity (Wedge section)

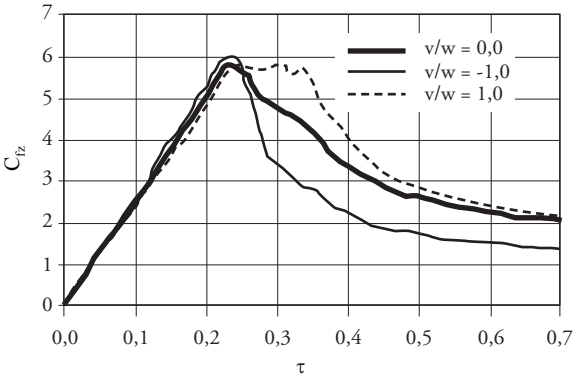

Figs. 13, 14, and 15 show the variation of the roll moment with time for sections CRT-1, CRT-2, and CRT-3. It is noticed that the behavior is different from that observed for asymmetric entry without horizontal velocity. There are two force peaks corresponding to flow separation from the knuckles. The velocity ratio has an important effect over the pressure distribution, generating instability over the section. In Figures 13, 14 and 15, for a velocity ratio of 1.0, instability is noted due to side 2 apparent impact velocity higher than apparent impact velocity on side 1.

Fig. 13. C_{mx} vs τ, CRT-1, asymmetric entry with horizontal velocity (Concave section)

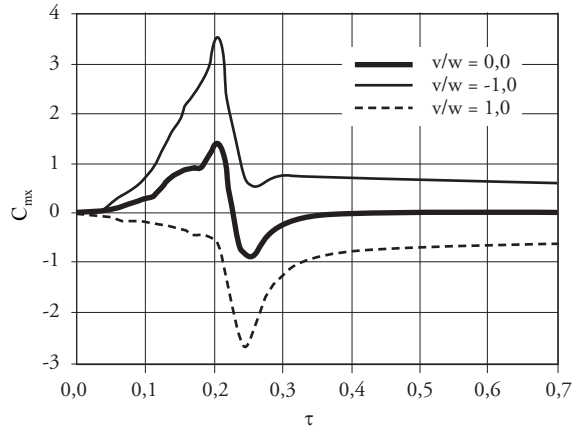

Transition from Type A to Type B Flow

As a section enters in the water under the appropriate conditions of asymmetric angle, φ, and

Fig. 14. C_{mx} vs τ, CRT-2, asymmetric entry with horizontal velocity (Convex section)

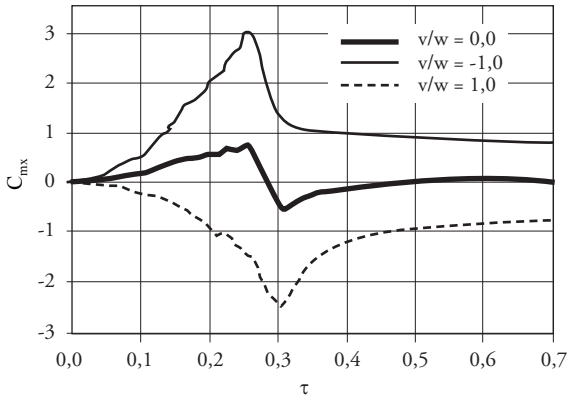

Fig. 15. C_{mx} vs τ, CRT-1, asymmetric entry with horizontal velocity (Wedge section)

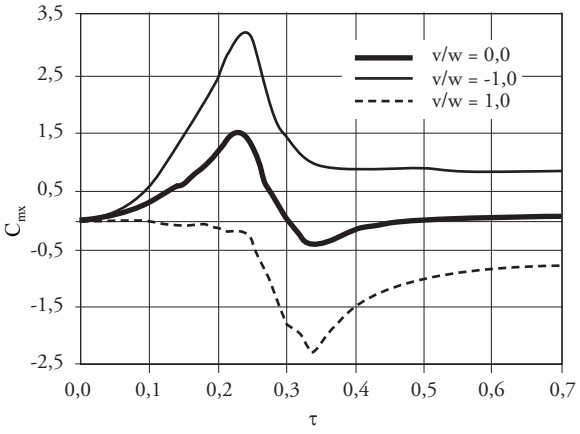

Fig. 16. v/ w vs. ß critical for the flow separation of the keel for symmetric entry

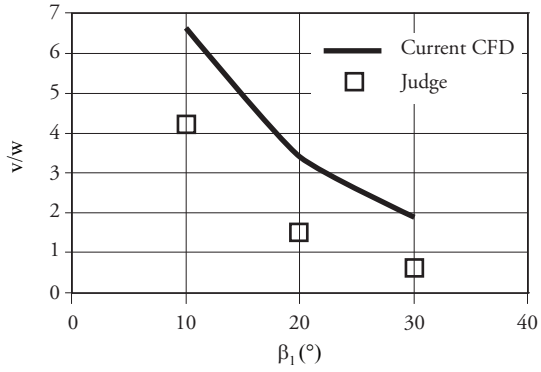

velocity ratio, v/w, it is possible that flow separation occurs from the keel. To determine the zone where the transition occurs, a slamming wedge

section with horizontal and vertical velocities was simulated. To find the critical condition, the water volume fraction in the hull was monitored from the beginning of the impact. The results are shown in the Figs. 16 and 17.

Fig. 16 presents the critical velocity ratio, which creates flow separation from the keel for asymmetric entry of a wedge section. The graphic shows that a lower horizontal velocity component is required as the dead rise angle of the section increases.

Fig. 17. ß 2 vs. ß1 critical for the flow separation of the keel for asymmetric entry

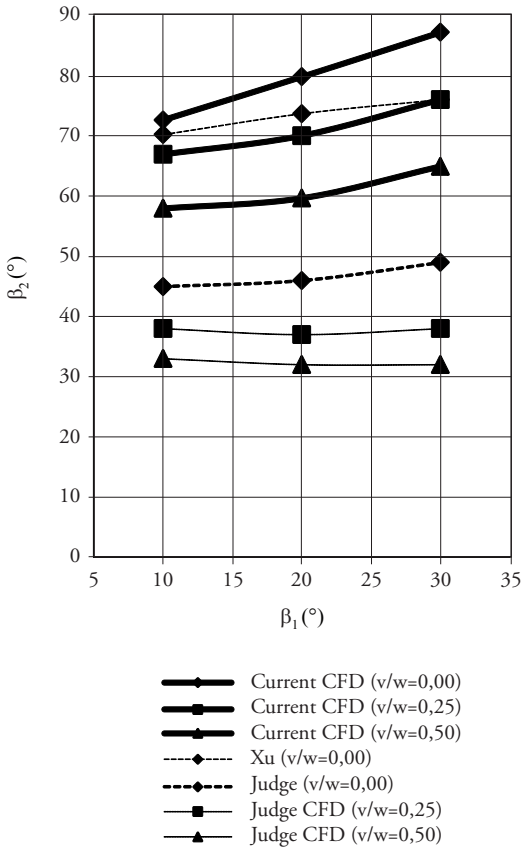

Fig. 17 shows the critical β_2 angle, which creates flow separation from the keel for asymmetric entry of a wedge section. A higher angle β_2 is required as the β_1 angle increases. Furthermore, as the velocity ratio increases, the flow separation from the keel occurs at a smaller β_2 angle.

Conclusions

The 2D impact was modeled for asymmetric entry of different sections by using STAR –CCM+ ©. The pressure distribution was obtained, as well as the force and roll moment variation with time. The results present great similarity with those reported by Vorus (1996) and Xu L. (1998). The effect of the horizontal velocity was also analyzed for wedge sections with variable dead rise angle, determining the influence of this parameter in the force and roll moment.

The critical condition for flow separation from the keel was evaluated. The results obtained are similar, but the values are higher than the results reached by Xu L. (1998) and Judge (2000).

References

ALGARIN, R. "*Modelamiento del impacto en dos dimensiones de secciones asimétricas con velocidad horizontal con aplicaciones en el diseño de botes de Planeo*". [M.Sc. thesis]. Barranquilla: Universidad del Norte. Programa de ingeniería Mecánica, 2010. 120p.

SEIF, M., MOUSAVIRAAD, S., SADDATHOSSEINI, S., AND BERTRAM, V. *"Numerical Modeling of 2-D Water Impact in One degree of Freedom"*. Síntesis Tecnológica. No. 2, Vol. 2, November 2005, p. 79-83.

CAPONNETTO, M., SÖDING, H., AND AZCUETA, R. *"Motion Simulations for Planing Boats in Waves"*. Ship Technology Research, Vol. 50, 2003, pp. 182-196.

TVEITNES, T. *"Application of Added Mass theory in planing [Ph.D. Thesis]"*. Glasgow: University of Glasgow. Department of Naval Architecture and Ocean Engineering, 2001, 339p.

VORUS, W. S. *"A flat cylinder theory for vessel impact and steady planing resistance"*. Journal of Ship Research. No. 2, Vol. 40, June 1996, p. 89-106.

WAGNER, H. *"Über stoss – und Gleitvorgänge an der Oberfläshe von Flüssigkeiten. eitschrift für Angewandte Mathematik und Mechanik"*. No. 4, Vol. 12, August 1932, p. 193-215.

XU, L., TROESCH, A., AND VORUS, W. *"Asymmetric Vessel Impact and Planing Hydrodynamics"*. Journal of Ship Research, No. 3, Vol. 42, September 1998, p. 187-198.

CD-ADAPCO. 'Star-CCM+ Version 3.06.006 User Guide', 2008.

JUDGE C. AND TROESCH A. *"Asymmetry and horizontal velocity during water impact"*, [on-line]. Available at: http://www.eng.tau.ac.il/~greg/ABST.pdf/judge.pdf/judgeWWWFB2.pdf, 2000.

TOYAMA Y. *"Two-dimensional water impact of unsymmetrical bodies"*. Journal of Soc. Naval Arch. Japan. Vol. 173, 1993, p. 285-291.

XU, G.D. *"Numerical simulation of oblique water entry of an asymmetrical wedge"*. Journal of Ocean Engineering. Vol. 35, August 2008, p. 1597-1603.

YOON, B.S. Flow Separation At The Initial Stage Of The Oblique Water Entry Of a [on- line]. Available at: http://www.iwwwfb.org/Abstracts/iwwwfb24/iwwwfb24_53.pdf, 2009.

Generating fuzzy autopilot for ship maneuvering

Generación de piloto automático difuso para maniobras de embarcaciones

Juan A. Contreras Montes [1]
Fernando J. Durán Martínez [2]
Alejandro Castro Celis [3]

Abstract

This paper introduces a method to generate autopilots for ship headings by using issues from the observation of control actions performed by human operators. The controller is designed based on fuzzy logic and uses triangular membership functions for the antecedent and consequent functions for Singleton type. For an automatic adjustment of the consequential, the recursive least squares method was used. This method is used to generate and validate the course driver of a 350-m tanker, at different load conditions.

Key words: ship maneuvering, heading control, fuzzy identification, intelligent control.

Resumen

Este documento presenta un método para generar pilotos automáticos para rumbo de embarcación mediante el uso de asuntos provenientes de la observación de acciones de control realizadas por operadores humanos. El controlador está diseñado basado en lógica difusa (*fuzzy logic*) y utiliza funciones de pertenencia triangular para las funciones antecedentes y consecuentes para tipo Singleton. Para un ajuste automático de la consecuente, se utilizó el método de mínimos cuadrados recursivos. Este método es utilizado para generar y validar el conductor de curso de un buque cisterna de 350 m, en diferentes condiciones de carga.

Palabras claves: maniobra de buques, control de rumbo, identificación difusa, control inteligente.

Date Received: January 19th, 2011 - *Fecha de recepción: 19 de Enero de 2011*
Date Accepted: January 28th, 2011 - *Fecha de aceptación: 28 de Enero de 2011*

[1] Escuela Naval Almirante Padilla - Facultad de Ingeniería Naval. Cartagena, Bolívar. Colombia. e-mail: epcontrerasj@ieee.org
[2] Escuela Naval Almirante Padilla - Facultad de Ingeniería Naval. Cartagena, Bolívar. Colombia. e-mail: almnando@gmail.com
[3] Escuela Naval Almirante Padilla - Facultad de Ingeniería Naval. Cartagena, Bolívar. Colombia. e-mail: cblackman3@hotmail.com

Introduction

On ships, the autopilot is used to control the direction of the rudder to reduce the error between the desired heading and the actual angles. Problems in maneuvering of vessels by the action of the rudder are related to the relatively high mass of the vessel with respect to the limited size of the rudder, which should be significantly deflected to obtain the required change in the ship's heading. *(Fosse, 2002; Witkowska et al., 2007)*.

These autopilots are designed to help improve efficiency in fuel consumption and reduce wear on components. *(Witkowska and Smierzchalski, 2008)*. Often, autopilots use classical control systems, such as Proportional Integral Derivative (PID) control. However, to compensate disturbances, like wind and currents, acting on the ship, as well as the characteristic nonlinear dynamics, permanent adjustments of the PID parameters are required.

The PID controller, once its parameters have been adjusted, performs well but only for small variations under operation conditions. Ship dynamics are constantly changing due to various reasons, such as variations in speed, trim, load, wind, currents, depth, among others, requiring continuous adjustment of the PID controller parameters. In many boats, this parameter setting is done manually, which becomes an additional burden on the crew and does not guarantee optimal performance of the controller at each operating point.

The methodology used in this section to obtain the fuzzy controller based on input and output data is presented in three phases: in the first, we present the nonlinear mathematical models that describe the dynamics in the course of the vessel; the second describes the fuzzy identification method used to generate fuzzy controller from experimental data; and in the third, we present an application to obtain the fuzzy controller in the direction of a cargo-type vessel.

Nonlinear model of the dynamics of a ship's course

Fig. 1. Variables defining the course of the vessel

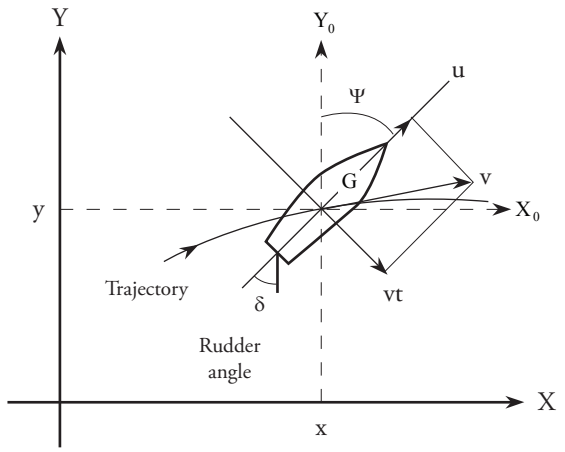

The Nomoto linear model *(Tzeng, and Chen, 1999)* has been widely accepted to design ship heading controllers *(Du, and Guo, 2004)*.

$$T\ddot{\psi}(t) + \dot{\psi}(t) = K\delta(t) \quad (1)$$

Where ψ(t) is the yaw angle, δ is the rudder angle, T is the time constant, and K is the rudder gain. Nonetheless, the Nomoto linear model is only valid for small deflections of rudder angle (δ < 5°) and low frequency of the action itself. For a better representation of the dynamic behavior of the ship's course, also valid at large and rapid movements of the rudder, the nonlinear equation proposed by Wenger and Bench has been proposed (*Fossen, 2002; Casado and Ferreiro, 2005)*:

$$\dddot{\psi}(t)+\left(\frac{1}{T_1}+\frac{1}{T_2}\right)\ddot{\psi}(t)+\frac{1}{T_1T_2}H_N\left(\dot{\psi}(t)\right)=\frac{K}{T_1T_2}\left(T_3\dot{\delta}(t)+\delta(t)\right) \quad (2)$$

Where $H_N(\dot{\psi}(t))$ is a nonlinear function of the angular velocity $(t)^{\dot{\psi}(t)}$. The function $H_N(\dot{\psi}(t))$ expresses the relationship between steady state $\delta(t)$ and $\dot{\psi}(t)$, when $\dddot{\psi}(t) = \ddot{\psi}(t) = \dot{\delta}(t) = 0$. To determine the shape of the curve $H((t))\ N\bullet\psi$, a "spiral test" experiment was conducted on the tanker, the object analyzed in this article, which was approximated by the following function:

$$H_N\left(\dot{\psi}|(t)\right) = \alpha\,\dot{\psi}^3(t) + \beta\,\dot{\psi}(t) \quad (3)$$

Parameters α and β are real constants obtained from the "spiral test"; also, α is always taken as a positive value. Herein, we assigned to these parameters the values of 1: α = β = 1 *(Witkowska et al., 2007)*. Parameters K, T1, T2, T3 are defined by:

$$K = K_0\left(\frac{u}{L}\right) \quad (4)$$

Where u is the longitudinal speed of the vessel [m/s] and L is the length in [m]. The mathematical model of the vessel's dynamic characteristics was taken from a tanker model described by *(Åström and Wittenmark, 1989)* and modeled by a Bech and Wenger third-order equation, nonlinear model. For the simulation, the following parameters were considered *(Passino and Yurkovich, 1998)*:

$$K_0 = -3{,}86,\ T_{10} = 5{,}66,\ T_{20} = 0{,}38,\ T_{30} = 0{,}89 \quad (5)$$

These parameters were determined for a velocity u = 5 m/s and a length of L = 161 m.

The model of the vessel's dynamic characteristics was complemented by the steering system model (Fig. 2). The input signal to the rudder system is Autopilot. In most vessels, speed and rudder angle should be kept within limits *(Amerongen, 1982)*, where,

$$\delta_{max} = 35[\text{deg}],\ 2{,}3 \le \dot{\delta}\ \text{max}\ \le 7[\text{deg/s}] \quad (6)$$

It has been estimated that the rudder blade moves from a limit position to another during a time period not greater than 30 seconds. This article assumes a maximum speed of movement of the rudder of δ_{max} = 6 - °/s. The maximum angle the rubber blade can reach is δ_{max} = 35 degrees. In summary, the dynamic of the rudder is expressed as:

$$\delta(t) = \frac{K_R}{T_R}\delta_z(t) - \frac{1}{T_R}\delta(t) \quad (7)$$

Where T_R = 156 seconds and K_R = 96 degrees.

Fuzzy modeling algorithms

The algorithm to generate fuzzy operators uses the weighted average rate *(Babuska, 2001)* for the combination, rather than T-norm type operators. The user should only introduce the data from the input and output variables. The algorithm determines the ranges of each variable, distributes the membership functions in the universes of each input variable, locates the Singleton-type consequents (*Chae et al., 1999*) in the output space, determines the rules, and adjusts the location of the consequents, using least squares to minimize the approximation error.

The algorithm stops when reaches a metric error lower than that required by the user or when the number of fuzzy sets for the input variable is greater than nine. The distribution of membership functions in each input universe is uniform to ensure that the resulting partition sum is 1, i.e., the sum of the degrees of membership of an entry in an input variable is always equal to 1 *(Contreras, et al., 2007, 2008)*.

Given a collection of input and output experimental data $\{(x^k_i, y^k)\}$, with i = 1...N; k = 1,..., p , where x^k_i is the input vector p-dimensional x^k_1, x^k_2, x^k_3... x^k_p, and y^i is the one-dimensional output vector.

Fig. 2. Block diagram of the rudder system

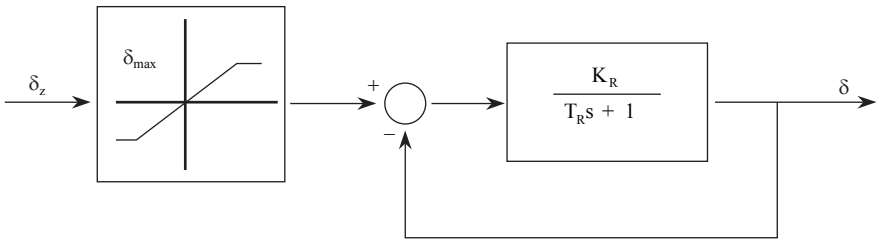

1. Scheduling of all N pairs of input - output $\{(x_i, y_i) \mid i=1,2,..., N\}$where $p\ i\ x \in \Re$ are input vectors and are scalar output.
2. Determination of the range of universes for each variable according to the maximum values of the associated data $[x^-_i, x^+_i]$, $[y^-, y^+]$.
3. Distribution of triangular membership functions (*Pedriycz, 1994*) on each universe. There is a general condition that the vertex with a membership value (modal value) falls in the center of the region covered by the membership function, while the other two vertices, with membership value equal to zero, fall in the centers of two neighboring regions. To efficiently approximate the upper and lower extremes of a function, it is necessary that in the triangular partition of the membership functions covering the start and end of the universe its vertices coincide with the membership value, with its left and right vertices, respectively, as noted in Fig. 3.

Fig. 3. Distribution of the triangular membership functions

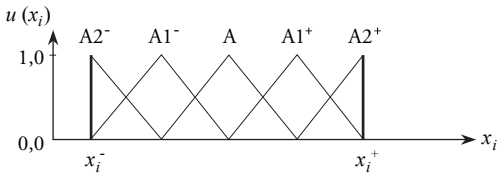

4. Calculation of the position of the modal values of the entry variable, according to

$$\text{if} \quad u_{A_k^{(n)}}(x_k^{(i)}) = 1 \qquad \text{End} \quad ys_k^{(n)} = y[i] \tag{8}$$

where $ys_k^{(n)}$ corresponds to the projection on the outlet space of the assessment of data $x^{(i)}$ de la k-th input variable in the n-th corresponding partition set. The value of the output that corresponds to the said projection is given by the value of the i-th position of the output vector y.

5. Determination of the rules. The number of rules initially obtained is equal to the number of sets from each input variable multiplied by the number of variables, that is, equal to $n\ x\ k$. The membership functions associated to each consequent will form the antecedents of the rules. An algorithm to reduce the number of rules is shown ahead.

Fig. 4. Consistent determination

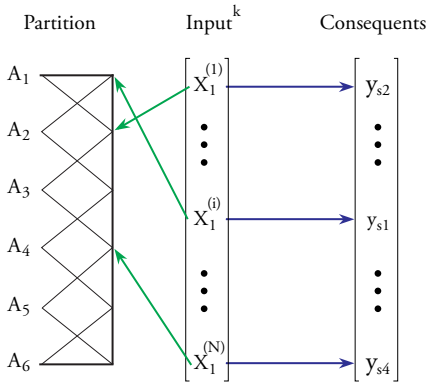

6. Validation of the model, or calculation of the approximation, by using the inference method described by

$$f(x^{(i)}) = \frac{1}{N}\sum_{j=1}^{L} \bar{y}^{j} m_j\left(x^{(i)}\right) \tag{9}$$

where $\bar{y}^{j}$ is the solitary value that corresponds to rule j.

7. Parameter adjustment, relocating the solitary output, using the least squares method. To do this, we proceeded to represent equation (2) in the form

$$f\left(x^{(i)}\right) = \sum_{j=1}^{L} \bar{y}^{j} w_j(x^{(i)}) \tag{10}$$

where

$$w_j\left(x^{(i)}\right) = \frac{m_j\left(x^{(i)}\right)}{\sum_{j=1}^{L} m_j\left(x^{(i)}\right)} = w_j^i \tag{11}$$

According to the process of inference, the n output values can be represented as Y =Wθ + E, which in matrix form is given by

Fig. 5. Determining the rules.

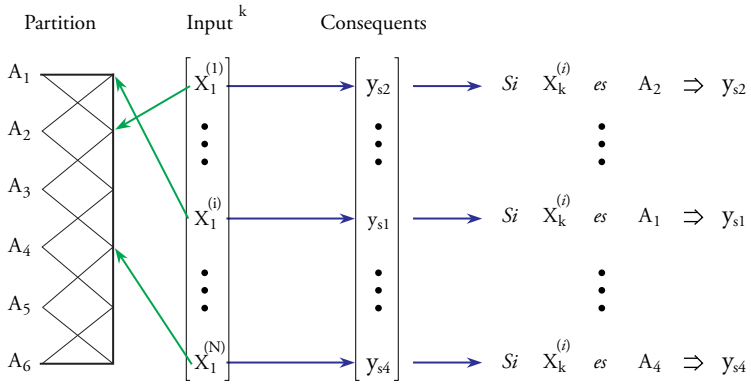

$$\begin{bmatrix} y^1 \\ y^2 \\ \vdots \\ y^n \end{bmatrix}_{Y} = \begin{bmatrix} w_1^1 & w_2^1 & \dots & w_L^1 \\ w_1^2 & w_2^2 & \dots & w_L^2 \\ \vdots & \vdots & \ddots & \vdots \\ w_1^n & w_2^n & \dots & w_L^n \end{bmatrix}_{W} \begin{bmatrix} \bar{y}^1 \\ \bar{y}^2 \\ \vdots \\ \bar{y}^L \end{bmatrix}_{\theta} + \begin{bmatrix} e_1 \\ e_2 \\ \vdots \\ e_n \end{bmatrix}_{E} \quad (6)$$

Where E is the approximation error, which must be minimized, and θ is the consequent vector. Using the least squares method

$$E^2 = (Y - W\theta)^2 = (Y^2 - 2YW\theta + (W\theta)^2) \quad (12)$$

The solution to this least squares problem by adjusting the consequent is given by

$$\frac{\partial E^2}{\partial \theta} \quad 0 = -2Y^T W + 2W^T W\theta \quad (13)$$

$$\theta = \frac{Y^T W}{W^T W} = (W^T W)^{-1} Y^T W \quad (14)$$

This solution is valid if $(W^T W)$ is not singular, which means that all the rules should receive sufficient excitation (persistent excitation) during the training. In practice, this is not always possible, so it is advisable to resort to the application of recursive least squares, seeking to ensure that the adjustment only affects the excited rules (*Contreras, 2006; Espinosa and Vandewalle, 2000, 2005*).

$$\theta(k+1) = \theta(k) + \gamma(k)[y(k+1) - W_{k+1}\theta(k)] \quad (15)$$

Where,

$$W_k = \{w_1^k, w_1^k, \dots w_L^k\}$$

$$\gamma(k) = \frac{P(k)\, W_{k+1}}{W_{k+1} P(k) W_{k+1}^T + 1} \quad (16)$$

$$P(k+1) = [1 - \gamma(k)\, W_{k+1}]\, P(k)$$

The initial value P(0) was obtained in step (4) of the algorithm.

8. Determine whether the measure of mean square error MSN is less than one, as previously established. Otherwise, increase n by 1 set of variable input and return to step 3.

It is possible to accomplish a greater approximation ("fine adjustment") if upon ending the process mentioned we apply the gradient descent method to only adjust the location of the modal values of the triangular sets of the antecedent, retaining the partition sum 1 and, hence, the interpretability of the system.

Results

Fig. 6 shows the result of a simulation by using Matlab/Simulink, which shows a comparison between the desired yaw angle (solid line) and the actual yaw angle for the implementation of the steering angle variation shown in Fig 7. The difference between these two signals is called the signal error.

Fig. 6. Desired yaw angle (continous) vs real yaw angle (--)

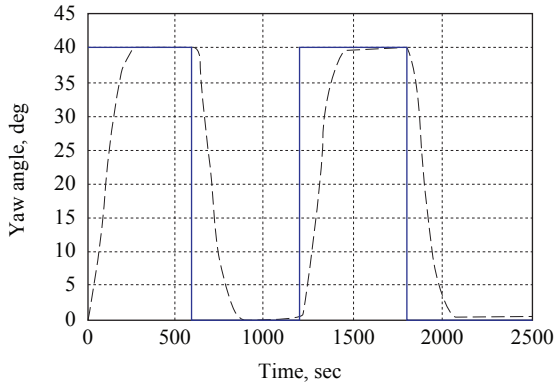

Fig. 7. Input applied to nonlinear system: rudder angle

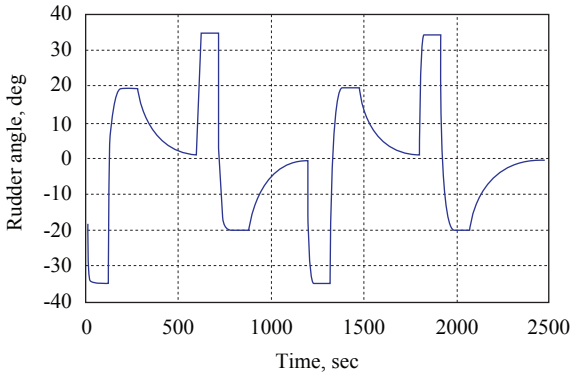

Rudder angle δz (k-2), error ψe (k-1), and variation in error ψc (k-1) were used for the training process as inputs to the past values of the fuzzy controller. The controller output is the current value, and the rudder angle δ (k) is necessary to achieve the desired course.

The structure of fuzzy controller or autopilot obtained is shown in Fig. 8. The labels "S" and "L" denote the linguistic terms "small" and "Large", respectively. The mean square error MSE of 0.0175 is reached. With three variables and two input triangular membership functions for each input variable, we generated six Consequences (6 rules), according to step 5 of the fuzzy identification algorithm.

Fig. 8. Partitions of δz (k-2), ψe (k-1), and ψc (k-1) with two triangular membership functions

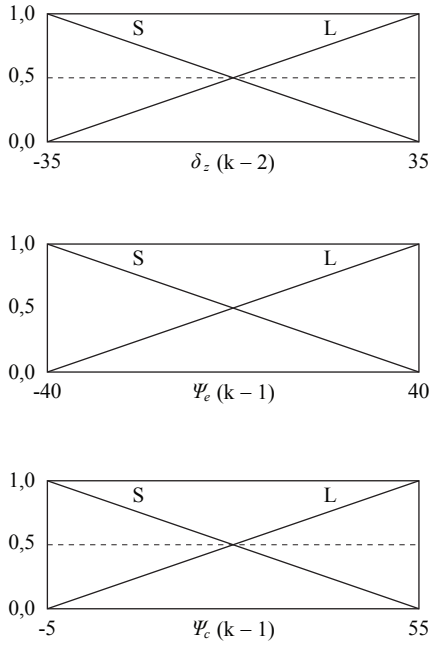

The consequent arrangement is given by:

$$\theta(k) = \begin{bmatrix} -\ 34{,}375 \\ +\ 34{,}375 \\ +\ \ 0{,}229 \\ -\ \ 0{,}226 \\ -\ \ 0{,}127 \\ +\ \ 0{,}128 \end{bmatrix} \tag{17}$$

The output of fuzzy controller (autopilot) is calculated by using equation (9). Fig. 9 shows a comparison between the rudder angle commanded by the autopilot and the rudder angle used in training.

Fig. 9. Required output for rudder angle (solid line) vs. rudder position ordered by the fuzzy autopilot (dashed line).

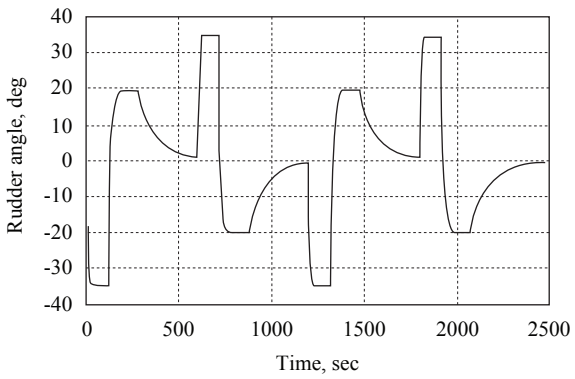

Conclusions

A new method is presented for the generation of vessel auto pilots. The pilot or automatic control generated is a fuzzy controller with triangular membership functions, normal and with overlap at 0.5, for input variables. The membership functions of the consequents are singleton type and are obtained by using the recursive least squares method. The method does not require the use of any other artificial intelligence techniques.

The results show that the method accurately captures the high dynamics of maneuvering the vessel when it is implemented in the generated fuzzy autopilot. In addition, the system is easily adaptable to new states of the vessel by adjusting the consequent.

References

AMERONGEN J., Adaptive steering of ship. A model reference approach to improved manoeuvering and economical course keeping. Ph.D. thesis, Delft University of Technology, the Netherlands. 1982.

ÅSTRÖM K.J. AND WITTENMARK B. Adaptive Control. Reading, MA: Addison Wesley. 1989.

BABUSKA, R. Fuzzy and Neural Control. Disc Course Lecture Notes. Delft University of Technology. Delft, the Netherlands. 2001.

CHAE, Y., OH, K., LEE, W. AND KANG, G.. *"Transformation of TSK fuzzy system into fuzzy system with singleton consequents and its application"*. IEEE International Conference on Fuzzy Systems. IEEE Computational Intelligence Society, Vol. 2,. pp.: 969-973. 1999.

CONTRERAS, J., MISA, R., MURILLO, L. *"Obtención de Modelos Borrosos Interpretables de Procesos Dinámicos"*. RIAI: Revista Iberoamericana de Automática e Informática Industrial, vol. 5, No. 3, pp. 70-77. Jul. 2008.

CONTRERAS, J., MISA, R., MURILLO, L. *"Interpretable Fuzzy Models from Data and Adaptive Fuzzy Control: A New Approach"*. IEEE International Conference on Fuzzy Systems. IEEE Computational Intelligence Society. pp.: 1591-1596. Jul. 2007.

DU, J., GUO, CH. *"Nonlinear Adaptive Ship Course Tracking Control Based on Backstepping and Nussbaum Gain"*. Proceeding of the 2004 American Control Conference Boston, Massachusetts, pp. 3845-3850, July, 2004.

ESPINOSA, J. VANDEWALLE, J. Constructing Fuzzy Models with Linguistic Integrity from Numerical Data-Afreli Algorithm, IEEE Trans. Fuzzy Systems, Vol. 8, No. 5, pp. 591 – 600. Oct. 2000.

ESPINOSA, J., VANDEWALLE, J., WERTZ, V., Fuzzy Logic, Identification and Predictive Control. Springer. USA. 2005.

FOSSEN, T. I. *"Marine Control Systems. Guidance, Navigation, and Control of Ships, Rigs and Underwater Vehicles"*. Marine Cybernetics. Trondheim, Norway. 2002.

TZENG, CH-Y., CHEN, J.F. *"Fundamental Properties of Linear Ship Steering Dynamic Models"*, Journal of Marine Science and Technology, Vol. 7, No. 2, pp. 79-88. 1999.

WITKOWSKA, A., SMIERZCHALSKI, R., *"Nonlinear Bacsteeping Ship Course Controller"*, R&RATA, vol, 1, No. 2, pp. 147-155. Jun. 2008.

WITKOWSKA, A., TOMERA, M., SMIERZCHALSKI, R., *"A Bacsteeping Approach to Ship Course Control"*, Int. Journal Appl. Math. Comput. Sci., Vol. 17, No. 1, pp. 73–85, 2007.

PASSINO, K, Y YURKOVICH, S. Fuzzy Control. Addison-Wesley. California. (pp. 301-390). 1998.

PEDRIYCZ, W. Why Triangular Membership Functions?", IEEE Trans. Fuzzy Sets and System, vol. 64, pp.21-30, 1994.

Vol. 5 - n.° 9
July 2011

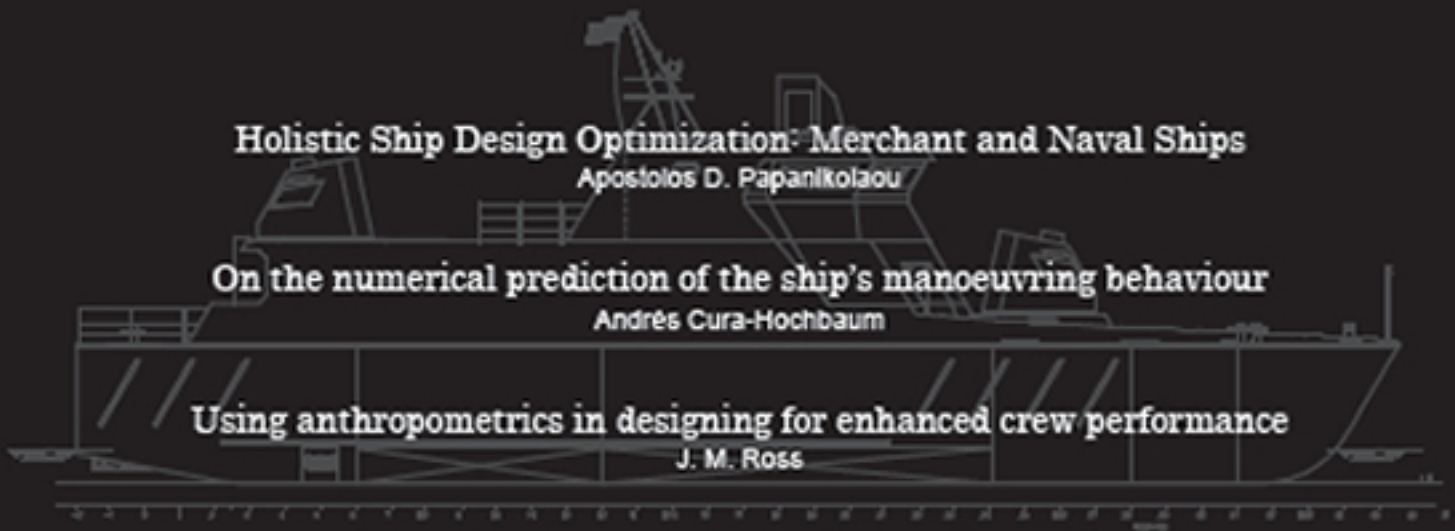

COTECMAR

www.shipjournal.co